CHEMICAL WEATHERING OF SULFIDE MINERALIZATION ON MARS

by

DUNCAN SOUTHAM FISHER

B. Sc., University of Toronto
(1987)

Submitted to the Department of
Earth, Atmospheric and Planetary Sciences
in Partial Fulfillment
of the Requirements for the Degree of

MASTER OF SCIENCE
in Earth Sciences

at the

Massachusetts Institute of Technology
February 1990

Signature of Author _____
Department of Earth, Atmospheric and Planetary Sciences
19 January 1990

Certified by _____
Roger G. Burns, Professor of Geochemistry
Thesis Supervisor

Accepted by _____
Tom H. Jordan, Chairman
Departmental Committee on Graduate Studies

CHEMICAL WEATHERING OF SULFIDE MINERALIZATION ON MARS

by

DUNCAN SOUTHAM FISHER

Submitted to the Department of Earth, Atmospheric and Planetary Sciences on 19 January 1990, in partial fulfillment of the requirements for the Degree of Master of Science in Earth Sciences

ABSTRACT

Pathways of chemical weathering of sulfide minerals on Mars are proposed based on Viking geochemical data, SNC meteorites and remote-sensed reflectance spectra. An oxidative weathering scheme is suggested, similar to that found occurring in terrestrial pyrrhotite-pentlandite ore deposits associated with Archean komatiites. To test this weathering model, pyrrhotite and troilite were reacted in heated sulfuric acid solutions (pH 2 and 4, at either 60 or 80°C), with or without aqueous Fe(III) cations (10^{-2}M) added to simulate deep-weathering reactions. Reaction products were characterized by Mössbauer spectroscopy using computer-fitted spectra obtained at 298K and 4.2K. Results indicate that acidic groundwater on Mars induces the following oxidative reaction pathway: pyrrhotite to FeS_2 (pyrite or marcasite) to nanophase FeOOH ± jarosite and lepidocrocite, leading to the production of gossaniferous materials in the martian regolith. The reactions seem to be promoted by the presence of the Fe(III) cations in solution. Dehydration of the lepidocrocite, possibly during eolian processes, along with remnant pyrrhotite, is thought to account for the martian fines magnetic fraction discovered by the Viking landers. Pyrrhotite was also found to form from oxidation of troilite in sulfuric acid solutions.

Thesis Supervisor: Dr. Roger G. Burns
Title: Professor of Mineralogy and Geochemistry

TABLE OF CONTENTS

SONNET — TO SCIENCE

Science! true daughter of old Time thou art!
Who alterest all things with thy peering eyes.
Why preyest thou thus upon the poet's heart,
Vulture, whose wings are dull realities?
How should he love thee? or how deem thee wise,
Who wouldst not leave him in his wandering
To seek for treasure in the jeweled skies,
Albeit he soared with an undaunted wing?
Hast thou not dragged Diana from her car,
And driven the hamadryad from the wood
To seek a shelter in some happier star?
Hast thou not torn the naiad from her flood,
The elfin from the green grass, and from me
The summer dream beneath the tamarind tree?

— Edgar Allan Poe

INTRODUCTION

The two Viking landers have provided, since 1976, a wealth of data about Mars. Unfortunately, the onboard experiments were designed principally for the detection of life and for planetary surface imaging. The Viking X-ray fluorescence (XRF) spectrometer gave quantitative analyses only for elements heavier than sodium. As such, no direct mineralogical data exists to characterize Mars' surface mineralogy. Furthermore, the indirect evidence that is available, in the form of reflectance spectroscopy, is also inconclusive in specifying a unique assemblage. One approach to investigating the nature and evolution of the martian regolith is by the studying of a (hopefully) analogous terrestrial process deduced from the limited chemical data available for Mars. This, then, allows Earth-based experimental measurements to be carried out leading to a refined martian petrogenetic model which, in turn, leads to a proposed mineralogical composition for the martian fines.

Plausible candidates put forward for the bulk of the martian fines must account for: one, the high iron and sulfur concentrations discovered by the Viking XRF experiment [*Toulmin et al.* 1977]; and two, the reflectance spectra of Mars, especially those of the bright regions, which are known to be controlled by a varying ferric iron component mixed with a more spectrally neutral component [*Singer* 1982]. Thus, the traditional view of iron being present as ferric-bearing phases has lead to the following proposed minerals: iron-rich montmorillonite [*Banin et al.* 1985], clay silicates [*Clark et al.* 1982], palagonites [*Gooding and Keil* 1978; *Singer* 1982] and poorly crystalline ferric

oxides [*Morris et al.* 1989; *Sherman et al.* 1982]. The sulfur is thought to occur mainly as magnesium and calcium sulfate minerals [*Clark and Van Hart* 1981; *Gooding et al.* 1988]. The occurrence of these ferric- and sulfate-bearing phases in the martian regolith suggests that oxidative weathering of iron-rich ultramafic rocks containing significant sulfide mineralization (pyrrhotite –pentlandite ± accessory chalcopyrite, pyrite) analogous to that of terrestrial komatiites has produced gossaniferous goethite–jarosite–opal–clay silicate type deposits on Mars [*Burns* 1987; *Burns* 1988; *Burns and Fisher* 1990a].

The purpose of this thesis is the investigation of the above proposed chemical weathering model. Previous studies have examined sulfur reaction pathways in the martian lithosphere [*Clark and Baird* 1979] and the thermodynamic stabilities of primary minerals and alteration products in the present day weathering environment on Mars [*Gooding* 1978]. This investigation examines oxidation-reduction reactions between primary iron sulfides and their oxidative weathering products. Studies of chemical weathering reactions of iron sulfides in aqueous sulfuric acid were undertaken in an attempt to: one, identify phases forming (or formed) in the martian regolith and relate them to primary komatiitic pyrrhotite-pentlandite mineralization; two, investigate the role of ferric ions as an oxidizing and leaching agent of primary sulfide ores; and three, determine whether or not secondary FeS_2 phases are produced.

Mössbauer spectroscopy was the principle tool used for characterizing the chemically weathered phases. Because this technique can easily distinguish between ferric and ferrous bearing phases it readily provides a qualitative and quantitative measure of the oxidation process for any given reaction. Due to the nature of the experiments undertaken, Mössbauer spectroscopy also proved

invaluable because of its ability to characterize the small quantities of X-ray amorphous product obtained from the reactions without destroying the sample as some methods require. With a theoretical energy resolution on the order of a part per trillion, Mössbauer spectroscopy is a powerful tool in the identification of iron-bearing phases. Though for more practical purposes, a sample has to have about 1–2% of the product of interest before any useful data can be obtained. Furthermore, through the use of low temperature (4.2K) Mössbauer studies, additional information about the reaction products may be obtained by the ability to distinguish between low-spin ferrous cations in pyrite from high-spin ferric cations in octahedral coordination in paramagnetic iron oxyhydroxides [*Murad and Johnston* 1987] and by the ability to identify X-ray amorphous phases having different magnetic interaction parameters.

For a brief but detailed account of the Mössbauer effect, its use in Mössbauer spectroscopy and the data obtained from its application in characterizing iron-bearing phases, refer to the appendix.

BACKGROUND

A brief review of existing data on Mars and earlier interpretations of the source and mineralogical compositions of the martian fines is given in order to justify the model that is under investigation in this thesis. These data, as indicated in the Introduction, are drawn from several different sources: (1) from *in situ* analyses of martian surface materials, (2) from modelling of partial melts of the martian mantle derived mostly from the studies of SNC meteorites, (3) from remote sensing observations of surface materials and (4) from investigations of weathering reactions under martian conditions.

Direct Evidence — The Viking Landers: The Viking landers provide the only direct chemical data on Mars through the use of an *in situ* analysis of inorganic chemical composition of martian regolith by XRF spectrometers [*Clark et al.* 1982]. Table 1 lists the average analyses for the two Viking lander sites. At both sites, which exhibit similar compositions, the samples contain abundant Fe (12–14% or 18-20% expressed as Fe_2O_3 – any FeO is included) with significant concentrations of S (3–4% or 7–10% expressed as SO_3). The sulfur concentration is one to two orders of magnitude higher than the average for the Earth's crust[*Clark et al.* 1976], and low trace element, alkali and aluminum abundances were observed [*Baird et al.* 1976; *Toulmin et al.* 1977]. About 1% bound water was deduced from Earth-based observations and by detection by the gas chromatograph mass spectrometer when soil samples were heated [*Biemann et al.* 1977]. Strong and weak magnets mounted on the sample scoop indicate 3–7% of the soil is magnetic [*Hargraves et al.* 1977].

Adherence of the material to the weak magnet restricts the possible magnetic materials to metallic iron, pyrrhotite, magnetite and maghemite [*Arvidson et al.* 1980].

The measured soil described above probably represents the weathering product of an "average" martian rock. The similarity of the two landing sites is attributed to an aeolian homogenization process [*Clark et al.* 1982; *Toulmin et al.* 1977]. Taking into account the higher Fe/(Fe + Mg) ratio for the mantle of Mars when compared to Earth [*Goettel* 1981; *McGetchin and Smyth* 1978], this average parent rock is concluded to be of mafic to ultramafic composition rather than a highly-differentiated silica-rich rock [*Baird et al.* 1976; *Clark et al.* 1982; *Toulmin et al.* 1977]. Suggested terrestrial analogs of these martian rocks are Fe-bearing picrites and komatiites [*Baird and Clark* 1981; *Burns and Fisher* 1990b; *Bussod and McGetchin* 1979].

Indirect Evidence, Part I — SNC Meteorites: SNC meteorites (Shergottite-Nakhlite-Chassignite) are unusual meteorites. They have an average age of formation of 1.3 b.y., compared with the usual age of 4.4 to 4.6 b.y. for most other meteorites, indicating their non-primordial nature. Mars has been suggested as an appropriate parent body for their origin [*Wood and Ashwal* 1981]. Their igneous textures, rare earth fractionation patterns and chemical composition, all indicate a large parent body, roughly the size of Mars [*Bunch and Reid* 1975; *Reid and Bunch* 1975]. The presence of trapped gases in shocked-produced glasses in EETA79001, which resembles the martian atmosphere in their elemental and isotopic compositions [*Becker and Pepin* 1984; *Bogard and Johnson* 1983; *Carr et al.* 1985], also points to a martian origin. And, the volatile nature of the SNC meteorites [*Driebus and Wanke* 1987],

and therefore Mars, has been shown to greatly decrease the strength of the impact event needed to eject material from the planet [*O'Keefe and Ahrens* 1986].

The above evidence, which suggests a martian origin for the SNC meteorites, has lead researchers to examine them for any signs of preterrestrial weathering products that may give clues to weathering processes occurring on Mars. Also, studies of their primary phases have been carried out in order to further classify the nature of the martian mantle and magma processes. Given below, is a brief summary of these studies.

A number a sulfide minerals have been identified as possible primary phases in SNC meteorites, including, pyrrhotite, Ni-bearing troilite, pentlandite, chalcopyrite, marcasite and pyrite [*Bunch and Reid* 1975; *Floran et al.* 1978; *McSween and Jarosewich* 1983; *Smith et al.* 1983; *Steele and Smith* 1982]. Studies of the oxidation states of these meteorites have indicated that they vary between the FMQ and the WM buffers [*Delano and Arculus* 1980; *Stolper and McSween* 1979]. It has been suggested that as a result of this and their volatile-rich nature, the SNCs indicate that the sulfur dissolved in parent basaltic melts on Mars probably existed as S^{2-} and HS^{-} but not as SO_4^{2-} [*Burns and Fisher* 1990b]. Textural features suggest that martian igneous rocks underwent magmatic differentiation [*Treiman* 1986; *Treiman* 1988] with attendant fractional crystallization of sulfides leading to localized concentrations of pyrrhotite-pentlandite ores in an analogous fashion to terrestrial sulfide-bearing komatiites [*Burns and Fisher* 1990b]. Attempts have been made to identify preterrestrial weathering products in the SNCs in the form of oxidized iron sulfides (jarosite, for example) [*Gooding and Muenow* 1986; *Solberg and Burns* 1989], but even though such ferric bearing phases do exist, the evidence is not

conclusive that they are preterrestrial in origin.

Indirect Evidence, Part II — Reflectance Spectroscopy/Remote Sensing: Many attempts have been made to estimate the composition of the surface material by comparing the reflectance spectra of different planetary areas with the spectra of known rocks, minerals and mixtures used as standards, from both Earth-based studies in the visible and infrared regions and multichannel colorimetric data provided by the Viking orbiters and landers [*Singer* 1985]. Mars' surface, to a general approximation, can be divided into two discontinuous areas distinguishable by their different albedos: the bright-regions and the dark-regions. Figure 1 shows typical spectra for these two regions. The features of bright-region spectra, including the broad band at 0.86 - 0.87 μm and slope changes near 0.5 μm and 0.6 μm, are all indicative of crystal field transitions in ferric ions [*Burns* 1989], suggesting various ferric-bearing oxidative weathering products are present on the surface of Mars. The dark-region spectra, in addition to showing the characteristic ferric ion absorptions, also show diagnostic ferrous iron absorptions in the 1 μm region [*Singer* 1985]. This is more indicative of the presence of mafic silicates, namely, pyroxenes and possibly olivines in an iron-rich basalt [*Adams and McCord* 1969; *Burns* 1989]. Because the dark regions may be relatively dust free, these spectra might be identifying primary rock minerals.

Plausible mineral phases of the martian fines giving rise to these spectra can generally be divided into three types: (1) ferric oxides, (2) clay minerals and (3) carbonates, sulfates and nitrates. Pure crystalline ferric oxides, such as hematite and goethite, exhibit quite distinct diagnostic spectral features due to crystal-field effects. None of this detail is exhibited by the martian spectra, indicating

the virtual lack of crystalline ferric oxides as a major ferric-bearing phase of the martian soils [*Singer* 1985]. Even as little as 1 wt.% hematite or goethite mixed with a spectrally neutral material still exhibits discernible band structure. The suggestion that the smectite clay nontronite is a major iron-bearing component of martian soils [*Baird et al.* 1976; *Toulmin et al.* 1977] is also dispelled for similar reasons because its octahedrally coordinated ferric ion exhibits analogous spectra characteristics as the ferric oxides [*Singer* 1982]. This leaves the possibility that the ferric ion in the martian soil exists in an amorphous or poorly crystalline form. Studies of Hawaiian palagonites have yielded approximate spectral analogs to the martian soils, suggesting that these might be a more attractive candidate for a terrestrial analog of the soil [*Singer* 1982]. More recent work, however, done during the 1988 Mars opposition, showed absorption peaks at 0.62-0.72 μm and 0.81-0.94 μm, which were interpreted as Fe^{3+} electronic transitions due to the presence of crystalline ferric oxide or hydroxide [*Bell et al.* 1990]. This is in agreement with recent work, which attributes the ferric iron features of the martian spectra to hematite of varying particle sizes, from bulk crystalline size to a superparamagnetic nanocrystalline phase, in a spectrally neutral material [*Morris et al.* 1989].

Clay minerals have also been popular as likely soil components because of their ubiquity as terrestrial weathering products and because the best simulations to the soil chemical analyses conducted by the Viking landers contained abundant clay minerals [*Toulmin et al.* 1977]. Due to their hydrated and/or hydroxylated nature, clays have diagnostic spectral features at wavelengths greater than 1 μm attributable to the vibrational modes of H_2O and OH^- and their overtones. While well-crystallized clays as a bulk component have been

found to be poor models for the bright region martian soil spectra, either a combination of clays as a minor phase mixed with other materials [*Singer* 1982] or a combination of montmorillonite clay having iron as a major absorbed ion [*Banin et al.* 1988; *Banin et al.* 1985] have the necessary spectral characteristics so as not to preclude the presence of clays in martian soils.

Non-silicate minerals, such as nitrates, carbonates and sulfates [*Clark and Van Hart* 1981], ferric sulfates [*Burns* 1987] and carbonates [*Gooding et al.* 1988], have been suggested as possible secondary soil phases. Unfortunately there is little or no spectral evidence for these phases on Mars. This is due to the difficulty of obtaining spectra, from Earth, in the range (3-5 μm) where nitrates, carbonates and sulfates are most spectrally active [*Singer* 1985]. Therefore their presence is not precluded but not confirmed either.

Theoretical Modelling — What This Is All About: From the observational data discussed above it becomes apparent that a unique interpretation for the origin and composition of the martian soil is not yet possible and its solution will probably depend upon direct mineralogical analysis of some future sample returned from Mars. And yet theoretical modelling based on the available data can still help in constraining the possible makeup of the martian soils. It is with this end in mind that this thesis investigates the merits of one of those theoretical models. The proposed existence of gossans on Mars derived from weathering of martian analogs of terrestrial komatiites suggests that pyrrhotite-pentlandite deposits will be the dominant sulfide mineralization on Mars [*Burns and Fisher* 1990a; *Burns and Fisher* 1990b]. A weathering model based on known terrestrial processes is investigated to validate the inferences about martian surface mineralogy that can be drawn from it.

Terrestrial komatiites originated by the partial melting of the Earth's mantle during the Archean, induced by a high radiogenic heat production, causing the extrusion of high temperature ultramafic lavas. Experimental measurements show that sulfur solubility increases in silicate melts with rising temperature, pressure, FeO content and sulfur fugacity and decreases with increased silica content, oxygen fugacity and oxidation of ferrous iron to ferric iron in the melt [*Caroll and Rutherford* 1985; *Haughton et al.* 1974]. Thus, iron-rich komatiitic magmas extruded at temperatures of 1350-1700 °C [*Green* 1975; *Green* 1981; *Green et al.* 1975] could transport several percent dissolved sulfur to the surface [*Burns and Fisher* 1990b], where, upon cooling, an immiscible FeS melt segregates due to sulfur-saturation and undergoes gravitational settling to form massive and disseminated sulfide mineralization.

By analogy and based on the evidence cited above from studies of SNC meteorites and Viking lander results, Mars is thought to have undergone a similar magma generation process. The higher Fe/(Fe + Mg) ratio of 0.23 to 0.33 for Mars compared to 0.15 for Earth suggests that very low viscosity iron-rich basaltic magmas were extruded upon partial melting of the martian mantle [*Bussod and McGetchin* 1979]. These magmas would be extruded at a slightly lower temperature, 1400 °C [*Bertka and Holloway* 1988], than their earthly counterparts. Still, the sulfur solubility of such iron-rich magmas would be more than adequate to transport significant amounts of the estimated 4.5% S content of the martian mantle to the surface of Mars [*Burns and Fisher* 1990a; *Burns and Fisher* 1990b] to become segregated as Fe (±Ni) sulfide mineralization. This sulfide mineralization could occur either as massive ore deposits or be thinly disseminated within ultramafic lavas, both of which might be expected to occur

near or on the surface and be vulnerable to oxidative chemical weathering by aerated aqueous acidic solutions, by analogy to chemical weathering of sulfide mineralization associated with terrestrial komatiites, to produce a gossaniferous martian regolith [*Burns* 1988; *Burns and Fisher* 1990b].

OXIDATIVE WEATHERING MODEL OF IRON SULFIDES

The composition of magmas on Mars, proposed as being similar to terrestrial komatiites, suggests a weathering process applicable to Mars that is similar to that for the formation of gossans overlying a komatiitic pyrrhotite-pentlandite assemblage [*Burns and Fisher* 1990a]. The mineralogy of gossans is dominated by the presence of "limonite" and silica (mainly jasper) where limonite refers to amorphous iron oxides or finely crystalline goethite with secondary admixed silica, hematite, jarosite and lepidocrocite in various proportions [*Blain and Andrew* 1977]. It is this assemblage that is of interest as a model for the martian soils.

Terrestrial Weathering Processes: In a near-surface environment such sulfide mineralization is unstable in the presence of oxygenated aqueous solutions and oxidative weathering is thought to proceed by electrochemical processes involving coupled half-cell reactions [*Blain and Andrew* 1977; *Burns* 1988; *Thornber* 1975]. As the oxygenated water percolates down through the sulfide mineralization, the chemical weathering reactions oxidize the primary massive sulfides (mainly pyrrhotite and pentlandite) to secondary sulfides and then further to gossaniferous oxide mineral assemblages, producing a vertically zoned weathering profile. This weathering process depends upon the presence of dissolved oxygen, but below the water table dissolved oxygen is usually absent. Thus, the above weathering process can occur to a depth no greater than the depth of the water table. Below the water table so called deep-weathering reactions may take place based on the oxidative powers of dissolved

ferric iron rather than oxygen. This gives us the two following half-cell reactions that provide the driving force behind the weathering of sulfide mineralization. In the near-surface environment we have,

$$O_{2(aq)} + 2H_2O + 4e^- = 4OH^- \quad (1)$$

and below the water table, where the dissolved oxygen concentration may be very low, we have,

$$Fe^{3+} + e^- = Fe^{2+} \quad (2).$$

These then couple with a variety of reduction half-cell reactions depending upon the sulfide mineral and oxidation environment present.

Also of utmost importance in sulfide chemical weathering is the role of pyrite. It may be present either as a primary sulfide phase or be formed during deep-weathering reactions in which pyrrhotite is oxidized by dissolved ferric ions (reaction (2) above),

$$Fe_7S_{8(s)} + 6Fe^{3+} = 4FeS_{2(s)} + 9Fe^{2+} \quad (3).$$

More importantly, the pyrite itself is oxidized at or near the water table by the oxygenated groundwater generating acidic and sulfate-rich solutions,

$$2FeS_{2(s)} + 2H_2O + 7O_{2(aq)} = 2Fe^{2+} + 4SO_4^{2-} + 4H^+ \quad (4)$$

and,

$$4FeS_{2(s)} + 2H_2O + 15O_{2(aq)} = 4Fe^{3+} + 8SO_4^{2-} + 4H^+ \quad (5).$$

The production of ferric ion in reaction (5) not only further promotes the dissolution of pyrite below the water table,

$$FeS_{2(s)} + 14Fe^{3+} + 8H_2O = 15Fe^{2+} + 2SO_4^{2-} + 16H^+ \quad (6)$$

but also that of the initial pyrrhotite (reaction (1)) and pentlandite in the absence of dissolved oxygen,

$$(Fe,Ni)_9S_{8(s)} + 2Fe^{3+} = 3Fe^{2+} + 2(Fe,Ni)Ni_2S_{4(s)} \quad (7).$$

Other supergene reactions not examined in this thesis, involving primary pentlandite, secondary violarite ($FeNi_2S_4$) and chalcopyrite cause further supergene enrichment of nickel and copper leading to economically important ores.

Reactions (4) through (7) indicate that strongly acidic (ph 2 - 5) and sulfate-rich solutions (approx. 10^{-2}M) are generated in the presence of sulfide mineralization, even under the low oxygen partial pressure of Mars (10^{-5} atm) [*Burns* 1988]. These acidic solutions form potent weathering reagents, being able to dissolve primary and secondary sulfides and silicates. Similarly, when extremely low concentrations of dissolved oxygen are encountered, ferric iron is also a potent weathering reagent. In this acidic aqueous environment dissolved ferrous and ferric ions may be stabilized and mobilized as simple and complex iron-bearing compounds, such as, $FeSO4^0$, $FeSO_4^+$, $Fe(SO_4)_2^-$, $FeOH^{2+}$, $Fe(OH)^-$, Fe^{2+} and Fe^{3+} [*Dousma et al.* 1979; *Sapieszko et al.* 1977]. Of note is that the ferric and sulfate ions necessary for the formation of these complexes are continuously being replenished by the oxidation of pyrite (reactions (4) - (6)) and that secondary pyrite is continually being formed from primary pyrrhotite by oxidation by ferric ions (reaction (3)). These dissolved ferric and ferrous sulfato and hydroxo complex ions may lead to the formation of hydroxo ferric sulfate minerals [*Burns* 1987],

$$2FeSO_4^+ + FeOH^{2+} + 6H_2O = (H_3O)Fe_3(SO_4)_2(OH)_{6(s)} + 6H^+ \quad (8)$$

or

$$Fe(SO_4)_2^- + 2FeOH^{2+} + 5H_2O = (H_3O)Fe_3(SO_4)_2(OH)_{6(s)} + 3H^+ \quad (9)$$

both of which form the hydronium jarosite, carphosiderite. Jarosites may also form by direct oxidation of pyrite or dissolved ferrous ions [*Burns* 1988],

$$12FeS_{2(s)} + 45O_{2(aq)} + 30H_2O + 4K^+ =$$
$$4KFe_3(SO_4)_2(OH)_{6(s)} + 16SO_4^{2-} + 36H^+ \quad (10)$$

and

$$6Fe^{2+} + 4SO_4^{2-} + 9H_2O + 3/2O_{2(aq)} + 2(K^+,Na^+) =$$
$$2(K,Na)Fe_3(SO_4)_2(OH)_{6(s)} + 6H^+ \quad (11).$$

Mono-dispersed hydronium jarosite sols are stabilized in low pH solutions (reactions (8) and (9)). However, in the presence of alkali metal cations, released from the chemical weathering of feldspars found in the host igneous rocks [*Siever and Woodford* 1979], extremely insoluble jarosite minerals precipitate out (reaction (10) and (11)) giving rise to the ferric sulfates that are often found in gossans in arid regions. The presence of dissolved nickel and magnesium in solution may inhibit the formation of these carphosiderite-jarosite phases [*Matijevic et al.* 1975]. Both of these cations may be present due to supergene oxidation of violarite [*Thornber* 1975] and to chemical weathering of ferromagnesian silicates respectively.

Above the water table, in less acidic environments, the dissolved ferric ions and mono-dispersed ferric sulfate sols are hydrolysed to poorly crystalline ferric hydroxyoxide phases, namely, ferrihydrite, goethite and lepidocrocite,

$$Fe^{3+} + 2H_2O = FeOOH_{(s)} + 3H^+ \quad (12)$$

$$FeOH^{2+} + H_2O = FeOOH_{(s)} + 2H^+ \quad (13)$$

and

$$FeSO_4^+ + 2H_2O = FeOOH_{(s)} + SO_4^{2-} + 3H^+ \quad (14).$$

Dissolved ferrous ions are also oxidized to form goethite,

$$4Fe^{2+} + 6H_2O + O_{2(aq)} = 4FeOOH_{(s)} + 8H^+ \quad (15)$$

and hydronium jarosite decomposes in the following reaction, which is kinetically

very slow,

$$(H_3O)Fe_3(SO_4)_2(OH)_{6(s)} = 3FeOOH_{(s)} + 2SO_4^{2-} + 4H^+ + H_2O \quad (16).$$

These reactions account for the presence of both goethite and jarosite in the oxidized zones of some gossans [*Blain and Andrew* 1977; *Burns* 1988]. Further dehydration of the FeOOH polymorphs, lepidocrocite and goethite, leads to the formation of ferromagnetic maghemite and antiferromagnetic hematite (both Fe_2O_3 polymorphs) respectively. It is probably the presence of maghemite or unoxidized remnant pyrrhotite that is responsible for the magnetic component of the martian soil that the Viking landers detected [*Burns* 1987; *Burns* 1988].

The acidic solutions generated in sulfide deposits also promotes the chemical weathering of silicates associated with the host igneous rocks to ferric oxide and hydroxyoxide phases and clay silicates (kaolinite and montmorillonite, for example),

$$2KAlSi_3O_{8(s)} + 2H^+ + H_2O = Al_2Si_2O_5(OH)_{4(s)} + SiO_{2(s)} + 2K^+ \quad (17).$$

It is these hydrolysis reactions of silicates that account for the release of silica and the presence of alkali and alkaline-earth elements in solution. The silica is then precipitated in gossans due to its decreased solubility in acidic environments. It is important to note that these reactions are acid-buffering in nature but kinetically quite slow [*Blain and Andrew* 1977]. Thus there is a balance between acid-producing sulphide decomposition reactions and acid-neutralizing silicate hydrolysis reactions which controls the overall pH of the aqueous environment which in turn affects the various stabilities of the weathering products and the ultimate mineral composition of the gossan.

Of primary importance from the above review is the role of the ferric ion

in the weathering model. Even in the absence of oxygen, dissolved ferric ions in an acidic aqueous solution have the ability to initiate deep-weathering reactions of the primary sulfide mineralization (pyrrhotite-pentlandite) to produce secondary sulfide minerals (pyrite/marcasite). The role of oxygen is in the production of ferric and sulfate ions in the near-surface environment leading to the formation of ferric sulfate and hydroxyoxide phases. In either case, the critical role in the formation of gossans is the decomposition of sulfides at or near the water table. On Earth where the partial pressure of oxygen is relatively high, atmospheric oxygen is, in general, the driving force behind chemical weathering of terrestrial sulfides. But in situations where the concentration of oxygen is low, the role of dissolved ferric ions becomes crucial. Peroxides may also form during the weathering process when the concentration of oxygen drops and the water supply becomes limited, as might happen when the water table drops and the atmospheric partial pressure of oxygen is low [*Sato* 1960],

$$O_{2(aq)} + 2H_2O + 2e^- = H_2O_{2(aq)} + 2OH^- \qquad (18)$$

and

$$O_{2(aq)} + 2H^+ + 2e^- = H_2O_{2(aq)} \qquad (19).$$

These reactions then become the driving force of weathering instead of reaction (1). Such conditions, which indicate incomplete oxidation of sulfide minerals, may be significant in the arid martian soils [*Burns* 1988].

Application to Mars: The inevitable question arises as to how applicable this is to Mars. It's all very well to postulate that Earth-like oxidative weathering has taken place on Mars in komatiitic hosted sulfide mineralization, but Mars isn't Earth. A certain amount of justification is needed before proceeding onwards with testing the model experimentally, which is the final goal of this thesis.

Present day conditions on Mars influencing the weathering reactions outlined above that differ from those on Earth, include, temperature, atmospheric oxygen partial pressure, source and state of water, and the nature (composition and permeability) of the parent rocks.

As mentioned above, the partial pressure of oxygen on Mars is 10^{-5} atm compared with 0.2 atm for Earth. This is a combination of both a low absolute oxygen concentration (0.13% for Mars, 21.0% for Earth) and a much smaller atmospheric pressure (0.00642 atm for Mars, 1 atm for Earth). This reduction leads to dissolved oxygen concentration in an aqueous solution that is four orders of magnitude less for Mars than for Earth [*Gooding* 1978]. However, large as this difference is, its effects on the stability of the weathering minerals and their oxidation products has been shown to be minimal [*Burns* 1988]. Thus, one would expect the nature of the weathering of iron sulfides to be similar on both Mars and Earth based only on their differences in dissolved oxygen concentrations.

Of greater concern is the local temperature and its effects on the nature of water on Mars. All the above reactions that describe the theoretical weathering model need an aqueous environment. The oxidation process is carried out by ***dissolved*** oxygen and ferric cations. Unfortunately, under present day martian conditions (6 mbar atmospheric pressure, mean diurnal temperatures ranging from 150K to 220K), liquid water is unstable everywhere on the surface [*Carr* 1987]. What water that is present, is stable either as ice at the poles or as permafrost ranging in thickness from several hundred meters at the equator to kilometers at the poles. Two possibilities exist that allow for oxidative weathering. First, that in the past, Mars had a wetter, warmer climate and that

water flowed freely on the surface [*Carr* 1987]. This is based upon atmospheric arguments and on the morphology of Mars, which includes water erosion features. Further evidence suggests that unbound water may still be present at depths. This indicates that the martian soils are probably products of a weathering regime that no longer exists today and that any oxidative weathering and gossan formation took place in Mars' earlier history. The second possibility is that weathering is still taking place under present day conditions within the permafrost region. Seasonal high temperatures on Mars may cause some melting of the permafrost near the equator providing an aqueous solution for continuing weathering processes. Evidence given elsewhere (*Gibson et al.* (1983), for example) also suggests that oxidation of igneous materials can take place within the permafrost zone, albeit the kinetics will be very slow. Thus, there seems to be little stopping an oxidative weathering process from occurring on Mars.

Beside the role that temperature plays in the nature of water, it also affects the stability fields of the weathering reactants and products. Jarosite's predominance field is thought to increase to higher pHs with decreasing temperature [*Burns* 1988] and the complex iron sulfate and iron hydroxyl ions are also stabilized at the low temperatures and in the acidic solutions found within the martian permafrost [*Burns* 1987]. Furthermore, the permafrost is thought to be still acidic in nature. Without the tectonic activity encountered on Earth, the groundwater on Mars wouldn't be buffered to nearly the same extent as it would be in a terrestrial seawater-basalt hydrothermal system. Thus the groundwater on Mars, now permafrost, could still be acidic, unlike present day terrestrial oceans which have a slight alkaline nature (pH 8.2) [*Burns and Fisher* 1988]. Of course without the level of tectonic activity on Earth, other processes on Mars

have to be invoked, to increase the permeability of the rocks to allow for aqueous solution transport. The increased permeability needed to facilitate deep-weathering reactions is achieved through fracturing associated with volcanism and impact cratering.

Finally, there are the results of the Viking lander biology experiments which indicated the presence of superoxide and peroxide phases in the martian soils [*Huguenin* 1982]. These could be explained by reactions (17) and (18) above and by the low concentrations of oxygen and limited water supply proposed for Mars. All of the above evidence, the indirect evidence obtained from SNC meteorites and remote sensing spectra, the discussion of compositional differences in the parent bodies between Earth and Mars and the direct evidence from the Viking lander experiments, gives credence to the weathering model under investigation and does not present any inconsistent and/or incompatible theories. All of which suggests that oxidative chemical weathering of iron sulfide mineralization associated with komatiitic host rocks lead to the formation of a gossaniferous martian regolith.

EXPERIMENTAL PROCEDURES

The formation of gossans on Earth depends upon a humid warm climate, one which does not exist on Mars at present. The experiments performed for this thesis involved conditions (oxygen-rich, 1 atm pressure and 60–80°C acidic aqueous solutions) that more closely resemble an Earth-like environment than a present day Mars. This was done for two main reasons: one, the cold and frozen nature of Mars, which inhibits the oxidative weathering process outlined above, has not, in all probability, prevailed throughout martian history; and two, due to time constraints, a higher reaction temperature was required in order to "speed up" the process to a more practical time length.

The possibility of a higher density and temperature for the martian atmosphere in the past, as evidenced by the erosion channels, suggests that our chemical weathering model based on heated acidic aqueous conditions is quite plausible. Studies of SNC meteorites suggest that the global inventory of volatiles on Mars was proportionately larger than on Earth [*Driebus and Wanke* 1987]. Assuming outgassing of these volatiles, upwards of 10 bars CO_2 and 500 m of H_2O are proposed to have been released [*Carr* 1987]. This is sufficient enough to think that Mars experienced warm, moist climatic conditions in its early history, similar to the experimental conditions used in this study. The acidity of the solutions used in the experiments is in keeping with studies of terrestrial iron-sulfide ore deposits and mine waters [*Blain and Andrew* 1977; *Thornber* 1975] both of which can produce highly acidic solutions with pHs ranging from 2 upwards.

Sample Preparation and Reactions: Table 2 lists the various experimental conditions of the reactions carried out for this investigation. Samples of pyrrhotite (Fe_7S_8, from Elizabethtown, Ont.) and troilite (stoichiometric FeS, from Del Norte County, Cal.) were obtained from the Harvard Mineralogical Museum. These samples were whole samples and were stored under normal room conditions. The use of troilite as a starting material for these experiments was chosen because of its less complicated Mössbauer spectrum when compared with pyrrhotite. Even though troilite is, at best, a minor phase in sulfide deposits, it was thought that any reaction products would be easier to identify against the single sextet of a troilite spectrum rather than the complicated 3 or 4 sextets of the pyrrhotite spectrum. Yet at the same time, since troilite is just stoichiometric pyrrhotite, its reaction behavior should be similar to that of the more common non-stoichiometric pyrrhotite.

For the reactions, rock chips were obtained and powdered using an agate mortar and pestle. Powdered samples were used to provide more surface area for reaction in order to decrease reaction time. 250 mg quantities were then reacted under various conditions (see Table 2) in stoppered flasks with 25 ml of the appropriate solution. Reaction products were filtered, washed with distilled water and air-dried. For Mössbauer analysis, from 80–100 mg of these products were further powdered with mortar and pestle with the addition of approximately 300 mg of sucrose. The addition of sucrose serves a two-fold purpose. First, if the density of iron (both ferric and/or ferrous) is too high in the sample then too much of the incident radiation is absorbed and decent statistics are not acquired. By mixing the sample with a neutral bulking material like sucrose, a more efficient iron density is obtained which ultimately yields a

better spectrum (a density of 5–7 mg Fe/cm^2 was found to be optimal [*Dyar* 1984]). Second, mixing of the sample with sucrose reduces preferred orientation of the sample in the plexiglass holder, which might affect the spectrum-fitting process. Note that this last grinding was done "dry" without the use of acetone as might usually be done. It was thought that the desiccation properties of acetone might degrade some of the less stable hydrated reaction products that were expected to form under the experimental conditions. Not using acetone reduces the effectiveness of the sucrose in reducing whatever preferred orientation the samples exhibit, but the trade-off was considered acceptable.

The ferric sulfate solutions used in the reactions detailed above have a tendency to hydrolyze themselves [*Music et al.* 1982]. Studies were made of these hydrolysis reactions in an attempt to differentiate between reaction products due to the weathering of the sulfides from hydrolysis products of the solution itself. These reactions were carried out in a similar fashion to those above.

Data Collection: Each reaction product was analysed at room temperature (298K) using a constant acceleration Austin Science Associates Mössbauer Spectrometer model S3K3 with a 1024-channel multi-channel analyzer. Because of the setup of this spectrometer, data for two samples may be collected simultaneously in each of half (512) of the 1024 channels (as opposed to the more usual procedure of collecting date from one sample in both of the 512 "halves" and then folding the data to obtain one spectra). The source used was ^{57}Co (whose half-life is 270 days) in a rhodium matrix with a radiation level that decreased after three half-lives from 100 mCi to approximately 12 mCi.

Results were calibrated against the mid-point and peak positions of a metallic iron foil standard with current reference values supplied by the Mössbauer Effect Data Center. The cryogenic facilities at the Bitter National Magnet Laboratory at M.I.T. were also used to acquire low-temperature (4.2K) Mössbauer spectra of the same reaction products in order to aid in the identification of the X-ray amorphous ferric oxide and sulfate phases formed in the reactions. Correlative Mössbauer spectra, for use as "in-house" standards, were also obtained for pyrite, marcasite, hematite, goethite, jarosite and lepidocrocite (see Table 6).

The ambient room temperature spectrum were collected in two velocity ranges, ±2.5 mm/s and ±10 mm/s. The expanded (±10 mm/s) range allowed identification of magnetic sextets originating from the iron sulfide reactants, troilite and pyrrhotite, and from any ferric iron phases formed as products. The ±2.5 mm/s range was of greater interest due to its ability to better resolve the quadrupole doublets associated with low-spin ferrous-bearing phases (pyrite and marcasite) and nanophase (< 10 nm) ferric oxides/sulfates that do not yet exhibit magnetic hyperfine splitting due to extremely small particle size. The 4.2K spectra were all acquired in a ±10 mm/s range to allow identification of the sextets associated with the nanophases which at this temperature now exhibit diagnostic magnetic hyperfine splitting parameters.

Data Fitting: After being downloaded, acquired spectra were transferred to a PDP 11/73 computer where interactive curve fitting was executed. Lorentzian distribution functions were used throughout the fitting process to resolve the separate peaks as no justification for the addition of a Gaussian component to the curve shapes existed. Spectra were fit using a Gaussian non-linear regression procedure [*Stone et al.* 1984] that allows for constraining of

any set of parameters or any linear combination of parameters (peaks widths, peak heights, baseline count, etc.). A "best fit" is obtained when the fitting procedure converges (reaches an arbitrary pre-determined minimum deviation between the calculated fit and the actual data) and the statistical parameters, χ^2 and MISFIT, are acceptable. The peak parameters, once an acceptable fit is achieved, are converted to mm/s units by the use of the iron foil standard.

Additional peaks may be added to the fitting procedure to see if the statistical parameters are improved, indicating the presence of another iron-bearing phase. Use of the two statistical parameters to test for goodness-of-fit is tempered by the expected mineralogy of the sample and by a visual inspection of the curve fitting based on the outputted plot. Thus fitting an extra doublet or sextet to a spectrum that improves the χ^2 value but indicates the presence of a phase that is known *not* to exist is generally discarded. The parameter χ^2 is most useful only for deciding which of a number of converged fits is best for a given spectrum. For comparisons between different samples, χ^2 is not useful as it depends upon the number of baseline counts of a spectrum. Instead the MISFIT parameter provides a comparative goodness-of-fit criterion that can be used to compare different spectra with different baseline counts [*Ruby* 1973].

The precision of the M.I.T. Mössbauer spectrometer and the fitting program is, at best, approximately ±0.02 mm/s for isomer shifts, ±0.06 mm/s for quadrupole splitting and ±1.5% for peak area data for spectra with well-resolved, distinct peaks [*Dyar* 1984]. However, for spectra with overlapping peaks, as is the case with this thesis, one can expect the standard deviations for these parameters to be poorer. Errors for the magnetic splitting parameter, H_{int}, derived from 4.2K spectra, are estimated at ±0.5 T.

In all the fitting procedures done on the 4.2K spectra, the areas and halfwidths of each of the component peaks of quadrupole doublets were constrained to be equal. For magnetic sextets in general, all halfwidths of the six peaks were constrained to be equal but the peaks were only constrained to have equal areas as couples (i.e. peak areas 1 = 6, 2 = 5 and 3 = 4, but no constraints were made relating peak 1's area to peak 2's for instance). The equal area constraint is justified because care was taken during sample preparation to minimize orientation effects. Thus, one would expect doublet peaks to have equal areas and for magnetic sextets to have areas in the ratio 3:2:1:1:2:3. This ratio can be used as a double-check on the acceptability of the fits where magnetic sextets are present (from either troilite or ferric oxides, for example). In the ±2.5 mm/s velocity range spectra only the inner peaks of any sextets present would be visible. Thus, all peaks were fit as doublets with halfwidths and areas constrained to be equal for pairs of peaks. Figures 4 and 5, the ±2.5 mm/s velocity range spectra, show a lone peak of a doublet (or the second peak of a sextet) at a position ranging from -2.0 to -1.5 mm/s, whose companion peak is cut off on the positive side of the range. These single peaks were ignored in the fitting procedure and given "zero-weight" as allowed for by the STONE fitting program.

Unfortunately, in many of the spectra, the low-spin ferrous doublet peaks of interest, overlapped with the inner peaks of the magnetic sextet of either pyrrhotite or troilite. In order to fit these doublets it was sometimes necessary to constrain peak positions. In each case where this was necessary, the peaks constrained (usually just one peak position held was all that was necessary for convergence of the fit) were those with well known parameters. These

parameters were based upon spectra of standards carried out before hand. Below is given a more detailed account of the separate fitting procedures.

For the expanded scale (±10.0 mm/s) troilite runs carried out at 4.2K, the six peaks constituting the magnetic sextet of troilite occur at approximately -4.53, -2.03, +0.10, +1.88, +3.99 and +6.20 mm/s (Figures 2a-f); they are designated as peaks T1 through T6, respectively, and should have the area ratios 3:2:1:1:2:3 expected for powdered samples. Two problems were encountered in the fitting procedure of these spectra. First, the low velocity peak of a quadrupole doublet (labelled F2 and F2', due to ferrous iron, as at this low a temperature all ferric doublets should have resolved themselves into magnetic sextets) was found to coincide, within the limits of the resolution of the spectra, with the third peak of troilite's sextet (peak T3). Thus, the two peaks were fitted as one peak only (attempts at fitting two peaks, with peak positions held, failed to work). This enabled the fitting procedure to converge to an acceptable fit.

The second problem was encountered when a magnetic sextet was fitted to the spectra. It is obvious from the spectra (Figures 2a-f) that a ferric-bearing phase is present from the presence and position of the two outlying peaks beyond troilite's peaks T1 and T6. A sextet was fitted to account for these and their associated inner peaks (designated G1 through G6 in the figures). Unfortunately, the associated inner peaks of this sextet have very small areas (≤1.0% of the area) and it was very hard to resolve them. In order to obtain a convergent fit, the fourth peak (peak G4) of this sextet generally had to have its position held constant and to allow its area to vary independently of any other peak. Thus, for the expanded scale troilite spectra, a total of 13 peaks were fitted with 32 to 34 constraints (Figures 2a-f). Other peaks present were too weak to

be resolved in these Mössbauer spectra and were ignored in the fitting process.

For the expanded scale pyrrhotite spectra, no attempt was made to fit the magnetic sextets associated with this non-stoichiometric iron sulfide. The 3 or 4 sextets that make up the pyrrhotite spectra cannot be resolved with the procedures at hand. In addition, the multiple sextets overlap any weak inner peaks associated with any ferric oxide/oxyhydroxide/sulfate weathering product. Instead, in an attempt to obtain useful data from the spectrum, only the outermost peaks of a ferric sextet, the inner two peaks of pyrrhotite and a ferrous doublet were fitted. Thus, the data from channels 140-230 and from 305-400 were given zero weight and ignored. The two peaks constituting the pyrrhotite occur at approximately +0.04 and +1.66 mm/s and are labelled P3 and P4 respectively (Figures 3a-f).

In addition to the complex nature of the pyrrhotite spectra, there existed a problem similar to that encountered in the troilite spectra fitting procedure. The low-velocity fitted pyrrhotite peak (P3) overlapped with the low-velocity peak of the ferrous doublet (labelled F2 and F2'). In order to obtain a convergent fit, peak P3's position was held constant based on the position obtained from a standard pyrrhotite spectrum. Also, an additional peak needed to be added to the fit at a lower velocity than peak P3. This was necessary as a weak peak existed in that region, presumably due to a magnetic sextet, and the low-velocity ferrous doublet peak tended to converge to that point if no extra peak was present. This choice of fitting parameters was validated by better statistical parameters and by the more "normal" mineralogy of the sample eventually derived. All five of these peaks were constrained to have equal halfwidths and their areas were constrained to be equal as pairs (except for the

lone peak which had its area unconstrained).

The outermost peaks, due to the presence of a ferric-bearing magnetic phase, were fit as either one or two doublets (labelled G1 and G6, and L1 and L6 if present) with their widths all constrained to be equal and their areas constrained to be equal in pairs. The need for two sets of doublets was indicated by the asymmetrical nature of these peaks. In all cases where an extra doublet was able to be fitted to the spectra, the χ^2 statistical parameter was improved by a significant amount. This extra doublet was not always able to be resolved by the fitting program due to very weak peak intensities and therefore is not always present. In general, for the expanded scale pyrrhotite spectra, 7 or 9 peaks were fitted with 18 or 23 constraints, respectively (Figures 3a-f).

The room temperature Mössbauer spectra in the ±2.5 mm/s velocity range were fit using only doublets with areas and widths constrained to be equal (Figures 4a-f and 5a-f). In all cases, two doublets were initially fit. One represented the inner two peaks of the sextet of either troilite or pyrrhotite (labelled either T3 and T4 or P3 and P4, respectively), and the second represented a reaction product of a mixture of a superparamagnetic ferric oxide/oxyhydroxide and a low spin ferrous phase (labelled "s.p. Fe^{3+} & l.s. Fe^{2+}" and "s.p. $Fe^{3+'}$ & l.s. $Fe^{2+'}$"). After an initial failed attempt to fit the inner peaks of the pyrrhotite sextet as three separate doublets, as expected from previous pyrrhotite fits [*Vaughan and Craig* 1978], it was decided that fitting the inner peaks as a single doublet was adequate for the purposes at hand. After the initial fit had converged, a second doublet was added to the fit. In some cases this was successful, in others it was not. In order to achieve a converged fit (for either the four peak or six peak fits), the center of the low-velocity troilite or

pyrrhotite peak was held constant (due again to the overlapping nature of the fitted doublets). The value used being based on fits of unreacted standards (peak positions of -0.05 and -0.02 mm/s were used for pyrrhotite and troilite respectively). The usefulness of these fits was guided by the expected mineralogy of the sample based on its 4.2K spectra and by the statistical parameter, χ^2. The first 120 channels of each spectra were given zero-weight so as to ignore the effects of a low-velocity peak that was present but whose high-velocity mate wasn't present in this velocity range.

The ±2.5 mm/s velocity range spectra were disappointing as tools for investigating the mineralogy of the reaction products. Due to the multiple overlapping doublets involved and to the, apparently, less then adequate statistics acquired, it was impossible to fit the number of doublets one would have thought were present based on the 4.2K spectra. As such, the data (isomer shifts and quadrupole splittings) obtained from these spectra probably have proportionally quite large errors and should be viewed with caution. Nonetheless, some trends were observed which are discussed below and which provide insight on the reactions carried out.

DATA AND RESULTS

The results of the curve fitting procedures are presented in Tables 3 through 5 and the fitted spectra themselves can be seen in Figures 2 through 7. The spectra are grouped according to their starting material (whether pyrrhotite or troilite) and to the temperature at which the statistics were acquired. Below is given a more detailed description of the fitting results.

4.2K Spectra: The most evident consistencies among the 4.2K spectra (for both troilite and pyrrhotite reactions) are the appearance of: (1) two peaks at approximately 0.1 and 0.7 mm/s (labelled F2 and F2'); and (2) two well developed peaks at approximately -7.9 and 8.6 mm/s (labelled G1 and G6) outlying the peaks associated with either troilite or pyrrhotite.

The first pair of peaks are attributable to an FeS_2 phase containing low-spin ferrous cations. This could be either pyrite or marcasite but a more specific identification was impossible with the statistics at hand. The errors associated with the isomer shifts (IS) and quadrupole splittings (QS) are large enough that to attempt to differentiate between the two FeS_2 phases would be meaningless.

The outermost peaks are attributable to the presence of a magnetic hyperfine sextet. The magnetic hyperfine splitting parameter, H_{int}, for these peaks is ~50.5 T. In the troilite spectra, a sextet was fitted which included these two peaks (labelled G1 through G6 in Figures 2a-f) with the following, approximate, peak positions: -7.9, -4.0, -0.6, 2.8, 5.5 and 8.6 mm/s. This yielded an IS of ~0.65 mm/s. Based on the H_{int} value alone, these peaks would seem to indicate the presence of goethite rather than any other hydrated iron

oxide phase (for example, ferrihydrite (46.5–50.0 T), maghemite (53.0 T) or jarosite (49.7 T); see Table 6 for a list of the literature values of various iron oxide and sulfide phases). Unfortunately, the commonly accepted value for the IS of goethite at 4.2K is 0.50 mm/s. The discrepancy between the expected IS of 0.50 mm/s compared to the one obtained of 0.65 mm/s is too large to be accounted for by errors alone. The explanation for this can be seen in Figures 8a and 8c. Figure 8a shows an expanded scale, unfitted, room temperature spectrum of sample T2F60. By comparison with a room temperature spectra of pyrrhotite (Figure 8c), it becomes apparent that the troilite sample has reacted to produce pyrrhotite as a reaction product (the incoming shoulders attributed to pyrrhotite are labelled P1 through P6). Unfortunately, it is these pyrrhotite peaks that have been fitted as part of the goethite sextets in the 4.2K troilite spectra. Thus, the IS and QS parameters, listed in Table 3, represent something other than the correct values for the supposed magnetic component fitted. Fortunately, the magnetic splitting parameter is still correct since it is only dependent on the two outermost peaks. Thus, based solely on the H_{int} parameter (which is all that is available from the pyrrhotite fits, in any case), the phase represented by the two peaks at -7.9 and 8.6 mm/s is most likely goethite.

The halfwidths (0.40 – 0.80 mm/s) and asymmetry (see Figure 3c or 3f, for example) of these outermost peaks exceed those expected from just a poorly crystalline goethite phase [*Murad* 1982]. This is attributable to two effects: one, a wide range of variable particle sizes of one phase, from nanocrystalline to bulk crystalline; and two, the combining of two or more separate phases with similar magnetic splitting parameters.

Inspection of Figures 8a and 8b show that even at room temperature a

magnetically split hydrated iron oxide phase is present (labelled h.s.Fe^{3+} and h.s. Fe^{3+}'). This indicates a well crystalline phase with particle diameters >10 nm [*Morris et al.* 1989]. When these spectra are compared with their 4.2K counterparts, it can be seen that the relative intensity of the low-spin ferrous doublet is lowered in the 4.2K spectra when compared to the 298K spectra, and this is combined with a proportional increase in the intensity of the peaks at -7.9 and 8.6 mm/s. This indicates the presence of superparamagnetic nanophase goethite, with a particle size <10 nm [*Morris et al.* 1989]. This variation in particle sizes contributes to the wide and asymmetric nature of the ferric sextet peaks.

In certain cases, the wide peaks were able to have more than one doublet fit to them (labelled L1 and L6). In all cases but one (sample P2N80), this additional doublet indicated a phase with a very low H_{int} parameter (~45 T). Two ferric oxyhydroxides have magnetic splitting parameters in this range, ferrihydrite and lepidocrocite. Even though ferrihydrite can approach this value, average values tend more towards a larger value of ~50 T (varies with particle size with smaller values indicating more poorly crystalline samples) [*Murad and Schwertmann* 1980]. On the other hand, lepidocrocite has a magnetic splitting parameter (~46 T) that is lower than that of any other ferric oxide [*Murad and Johnston* 1987]. Thus, this additional doublet is assigned as a superparamagnetic lepidocrocite phase. This also holds true for the very weak peaks that were not fitted for the troilite reactions but were calculated from the spectra nonetheless (see Figures 2a, 2b and 2f). The halfwidths of these outermost peaks are, in some cases, large even when fitted with a pair of doublets (for example, the peak widths for the two doublets for sample P4N60 are both 0.65

mm/s). In addition to particle size effects, this might also be due to the presence of another phase with a similar magnetic splitting parameter to that of goethite. Jarosite has a splitting parameter (49.7 T at 4.2K) that is similar enough to goethite (50.9T at 4.2K) that these peaks, if both present, might not be able to be differentiated by the fitting program and, instead, are fitted as one combined peak. Thus, some hydronium jarosite may be present in the reaction products. This is furthered evidenced by the room temperature spectra discussed below.

The reaction conditions of the experiments, with their aqueous environments, should favour hydrated ferric oxide compounds (lepidocrocite and goethite, for example) over non-hydrated ferric oxides (hematite and maghemite, for example). For the most part, the spectra bear this out. Only in one case, with sample P2N80, did this not hold true. A second doublet was fitted to the outermost peaks (Figure 3c) which indicated a phase with a splitting parameter of ~53.7 T. This most closely resembles the value for hematite (54.4 T) more than any other ferric-bearing phase. Unfortunately, hematite is a non-hydrated ferric oxide (α–Fe_2O_3) and wouldn't be expected to form under the experimental conditions. Its presence is most likely due to the desiccation of goethite after the reaction has ended and the products have been filtered off. Some of these reaction products were stored in an arid environment for up to a year before a spectrum was acquired. It is conceivable that during this time some of the goethite under went dehydration yielding hematite.

Room Temperature Spectra: The 298K spectra, with their small velocity range (±2.5 mm/s) and the overlapping of the fitted peaks (halfwidths varied from 0.30 to 0.46 mm/s) yielded less conclusive results than those of the

4.2K spectra. Nonetheless, some useful information and trends may be drawn from them.

Figures 4a-f show the troilite 298K spectra. Three different sets of doublets (in addition to the troilite peaks themselves) were obtained form the various reactions (Table 4 lists their Mössbauer parameters). The most consistent of these doublets (labelled "s.p. Fe^{3+} & l.s. Fe^{2+}" and "s.p. $Fe^{3+'}$ & l.s. $Fe^{2+'}$") have peak positions at ~0.05 and 0.60 mm/s, yielding IS values of ~0.33 mm/s and QS parameters of ~0.53 mm/s. These parameters match those observed for both low-spin Fe^{2+} cations in pyrite or marcasite and high-spin Fe^{3+} cations in octahedral coordination in superparamagnetic FeOOH phases [*Murad and Johnston* 1987]. Since we have seen that both these phases are present in the 4.2K spectra, these peaks could be assigned to either. Since no further resolving of these doublets into their, presumably, component peaks was possible, we can, therefore, only say that these peaks are a combination of one or more phases, namely, a FeS_2 phase (pyrite or marcasite) or a FeOOH phase(s) (goethite or lepidocrocite from the 4.2K spectra).

Five of the six troilite reactions exhibited a doublet with peak positions of approximately -0.05 and 1.32 mm/s which corresponds to an IS of ~0.64 mm/s and a QS of ~1.38 mm/s. These peaks are attributable to the inner two peaks of pyrrhotite. Even though the pyrrhotite spectrum is composed of three sextets at room temperature [*Vaughan and Craig* 1978], the inner two peaks (labelled P3 and P4 in the figures) of the sextet overlap and tend to produce normal width peaks (see Figure 8c). It is these two peaks that account for the fitted peaks in the troilite spectra. It was the appearance of these doublets in the room temperature spectra that lead to the conclusion that the fitted goethite sextets in

the 4.2K spectra were incorrect, as discussed previously.

The third and final doublet obtained from the fitted spectra occurs at approximately -0.20 and 0.55 mm/s. This yields extremely low IS values of ~0.20 mm/s indicative of tetrahedrally coordinated Fe^{3+} cations [*Burns* 1990]. QS values of ~0.76 mm/s are consistent with Fe^{3+} cations in a tetrahedral environment. For the most part, the reaction products expected to form under the experimental conditions carried out, do not contain Fe^{3+} in tetrahedral sites (goethite and lepidocrocite, for example) but maghemite [*Murad and Johnston* 1987] and ferrihydrite [*Murad et al.* 1988] do have Fe^{3+} cations occupying tetrahedral sites in their structures. Maghemite (γ-Fe_2O_3) is produced by dehydration of lepidocrocite (γ-FeOOH) and by a similar argument to the one used to explain the presence of hematite in the 4.2K spectra of sample P2N80, it is not inconceivable that maghemite is present, forming after the reaction product had been filtered from the aqueous reaction environment. The presence of ferrihydrite, a hydrated iron oxide, would, in fact, be expected to form under the experimental conditions encountered. Ferrihydrite is an amorphous mineral formed during the rapid oxidation of iron-containing solutions and is thought to be a precursor to more crystalline goethite, lepidocrocite and hematite [*Murad and Johnston* 1987]. Its presence in the reaction products is not unreasonable and is, in fact, probably expected. The only inconsistencies in assigning this doublet to a tetrahedrally coordinated Fe^{3+}-bearing mineral (maghemite and/or ferrihydrite) is its lack of presence in the 4.2K spectra. Presumably, these phases would be in small quantity compared to the other phases present and their weak peaks have been masked by the larger goethite peaks.

The pyrrhotite room temperature spectra (Figures 5a-f) show similar

trends to that of the troilite spectra with one important addition. In addition to the doublets assigned to nanophase FeOOH, to FeS_2 and to tetrahedrally co-ordinated ferric-bearing phases are peaks of a doublet occurring at approximately -0.11 and 0.88 mm/s. The IS of this doublet (~0.35 mm/s) is similar to that of the nanophase FeOOH peaks but its large QS parameter (~1.00 mm/s) is highly diagnostic of hydronium jarosite (literature values are δ=0.39 mm/s and Δ=1.01 mm/s; see Table 6). At 4.2K, its sextet would be masked by the goethite peaks as mentioned earlier, while their large, diagnostic QS parameters allow them to be identified in the room temperature spectra.

Hydrolysis Reactions: The hydrolysis of 10^{-2}M ferric sulfate solutions was studied for two reasons: one, to better understand the interference, in the form of unwanted reaction products, that the addition of ferric sulfate to the weathering reactions might produce; and two, to study the eventual hydrolysis products caused by the oxidation of iron sulfides which produces ferric sulfate rich solutions. The introduction of additional ferric sulfate to the reactions was done to investigate ferric cations as an oxidizing and leaching agent of primary sulfide ores; but a need exists to be able to differentiate between ferric sulfate hydrolysis products due to weathering of the primary sulfide ore versus products due to hydrolysis of the initial starting solution.

Figures 6a-d show the 4.2K spectra of these reactions, while the room temperature spectra are shown in Figures 7a-d. The reactions that lasted for two days or less (S2N80, S2K80 and S7K80), all exhibit large QS values (0.99, 1.09 and 0.97 mm/s respectively) that are highly diagnostic of jarosite. Their IS parameters also agree with the literature values of ~0.38 mm/s for jarosites [*Johnston* 1977; *Leclerc* 1980]. The variation in the QS is due to chemical

variation of the jarosites produced. Hydronium jarosites have smaller QS values than their natural, K-rich counterparts [*Leclerc* 1980]. Thus, samples S2N80 and S7N80, both of which have $\Delta<1$ mm/s and did not contain any alkali elements in the starting solution, are deduced to be hydronium jarosites. However, sample S2K80, in which K^+ cations were introduced into the starting solution, has a QS parameter (1.09 mm/s) more in line with natural, K-containing jarosites. This is as expected due to the extremely insoluble nature of K-rich jarosite, which has a solubility product, pK_{sp}, of 98.56 [*Burns* 1987]. The sample S2N60, which was reacted for a longer period of time (35 days) than the other three, has a QS of 0.58 mm/s which is attributed to the presence of superparamagnetic goethite.

The 4.2K spectra of these reactions confirms the above conclusions. Sample S2N60, which was unfitted, yields a hyperfine magnetic splitting value of 49.9 T, which agrees with the assignment of goethite as the product. Sample S2K80 exhibits Mössbauer parameters that are similar to that of the in-house standard that was run (δ=0.49 mm/s, Δ=0.19 mm/s and H_{int}=47.6 T versus δ=0.49 mm/s, Δ=0.09 mm/s and H_{int}=49.7 T). The slight discrepancy between the two might be accounted for if the product was in fact a mixture of jarosite and hydronium jarosite which would explain the large halfwidths (0.42 - 0.82 mm/s) and the asymmetry of the peaks (see Figure 6c). The other two samples have larger QS values (~0.35 mm/s) associated with the sextets, which is accountable by the existence of hydronium jarosite [*Afanasev et al.* 1974]. The only new information obtained from the 4.2K spectra, that was not already deduced from the 298K spectra, was the presence of a second sextet in sample S2N80 (Figure 6a). An IS of 0.43 mm/s, a QS of 0.57 mm/s and a magnetic

splitting parameter of 44.4 T indicates either lepidocrocite or ferrihydrite. But presumably, the lack of two doublets in the room temperature spectra indicates that the two phases have similar Mössbauer parameters and only ferrihydrite exhibits a QS value anywhere near the 0.99 mm/s observed (lepidocrocite is too small at 0.53 mm/s). Thus, this second sextet in the 4.2K spectrum is attributed to a ferrihydrite phase.

Figure 9 shows a plot of isomer shift versus quadrupole splitting for the various reaction products described above (the parameters are based on the values listed in Tables 3 and 4). This plot shows, quite distinctly, the apparent groupings of the phases that were fitted with STONE and the consistency of the products from one fit to the next. It allows for a much easier visual representation of the reaction products, obtained from the different experimental conditions, than the fitted spectra themselves. Note that, as mentioned above, the values for the goethite 4.2K group are suspect and should probably lie closer to the jarosite 4.2K group.

Finally, as mentioned earlier, the ratios of the areas of the troilite peaks should be 3:2:1:1:2:3 (as should be true for any sextet generated by randomly oriented particles). The peak area ratios of the troilite spectra fitted in the 4.2K spectra (Figures 2a-f) have the approximate ratios of 2:1.5:1:1:1.5:2. This are not the expected ratios. This indicates either that the specimens, when run on the Mössbauer spectrometer, had a preferred orientation or that the fitting procedure (in the choice of peaks and peak positions) was not wholly accurate, even though the goodness-of-fit parameters indicated acceptable fits. The latter of these two choices is most likely the cause of this inconsistency. Again, the fitting of pyrrhotite peaks as part of the goethite sextets is probably the main

culprit. This would leave the real goethite sextet peaks (along with those peaks not included in the fit) to be included with the troilite peaks during the fitting procedure, thus destroying the expected peak area ratios for the troilite sextet.

DISCUSSION

The purpose of this thesis was the investigation of oxidative weathering of sulfide mineralization analogous to that found associated with terrestrial komatiites and relate it to Mars. For this investigation, three main areas were outlined: one, the identification of possible phases forming in the martian regolith; two, the role of ferric ions as an oxidizing and leaching agent; and three, to determine whether or not secondary FeS_2 phases were produced. We will now discuss each of these objectives in turn.

FeS_2 Formation: The 4.2K spectra (Figures 2 and 3), which show the results of the acid weathering experiments on troilite and pyrrhotite, clearly and consistently indicate the formation of secondary FeS_2 mineralization (pyrite or marcasite). This supports the proposed oxidative weathering model of Fe-S mineralization, in which supergene alteration of pyrrhotite (or troilite) in groundwater and the formation of secondary FeS_2 phases precedes the deposition of jarosite and FeOOH phases (goethite and lepidocrocite) in gossans above the water table.

Table 5 shows various peak area ratios. The use of ratios instead of the use of absolute peak areas (expressed as a %) was thought to give a more accurate representation of the effects of the different experimental conditions. The ratios take into account the fact that the pyrrhotite or troilite peaks should be decreasing in area, relative to the increase in areas of the reaction products (either a FeS_2 or a FeOOH phase), whereas direct comparison of the peak areas of the products does not.

From the table, it can be seen that the amount of FeS_2 formed is increased when the experimental pH is raised from 2 to 4 (ratios increase from 0.022 to 0.043 for troilite, and from 0.271 to 0.287 for pyrrhotite) for those samples reacted without additional ferric sulfate (no conclusive behavior can be derived for the effects of increasing temperature on the reactions). This must be due to an increased stability of FeS_2 phases at higher pHs under the experimental oxidizing environment (the oxygenated water is in equilibrium with the Earth's atmosphere). Though, since the reaction times for these experiments were not of the same length, it is questionable whether or not any valid conclusions may be drawn from comparisons between the different reactions. Regardless, the formation of a secondary FeS_2 phase is indicated. The room temperature spectra, due to the nature of their fits (i.e. that low spin ferrous doublets and nanophase goethite peaks overlap and could not be separately resolved), do not confirm nor deny the presence of pyrite or marcasite.

The Role of Ferric Cations: The addition of 10^{-2}M ferric sulfate solution to the reactions was done in an attempt to see if the ferric cation promoted the formation of supergene pyrite or marcasite, as indicated by reaction (3). Unfortunately, the ferric cation also promotes the dissolution of any supergene FeS_2 phase thus formed(see reaction (6)). Any supergene FeS_2 phase is, in effect, an intermediate product in the reaction series: $FeS \rightarrow FeS_2 \rightarrow FeOOH$. Presumably, in an reaction series of this type, the FeS_2 phase will reach some sort of equilibrium concentration dependent on the two rates of reaction involved. Thus, the amount of pyrite or marcasite formed in these experiments, as given by the areas associated with their peaks, might not be so much an indication of increased reaction rates, as an indication of a shift in the

equilibrium concentration of the intermediate phase, FeS_2. In addition, the presence of the ferric sulfate solution will affect the concentrations of the various species in solution, which in turn affects the stability fields of any given phase (for a given temperature and pressure), and thus, the relative proportions of their formation.

On the other hand, observation of the peaks attributed to the FeS_2 phases in Figures 2 and 3, and examination of the ratios of the amount of these phases to that of the starting material (the second column in Table 5), indicates an increase in the amount of supergene pyrite or marcasite formed when the ferric sulfate solution was present to when it wasn't (except for a comparison between T4F60 and T4N60 which seems to indicate a decrease in the amount of FeS_2 mineralization formed upon addition of the ferric sulfate solution). Studies have shown that Fe^{3+} ions are more aggressive and faster at oxidizing pyrite (and marcasite, presumably) than dissolved oxygen [*Moses et al.* 1987], and that the increased oxidation potential due to the increased Fe^{3+} concentration also increases pyrite dissolution [*Garrels and Thompson* 1960]. Thus, if the second reaction rate of the above reaction series has been increased by the addition of a ferric sulfate solution and still the amount of supergene pyrite and marcasite has increased, as indicated by the peak areas of the spectra, then it would seem that the presence of the additional ferric cation must also promote the formation of the supergene FeS_2 phases.

Of course, the sulfate ions also play an important role in the rates of reaction. The ferric ion complexes (for example, $FeSO_4^+$, the dominant species at all temperatures [*Sapieszko et al.* 1977]), that form in the presence of sulfate anions, affect the availability and reactivity of the ferric cations for the above

reactions. Besides forming these complexes, the presence of SO_4^{2-} also promotes increased precipitation rates of ferric oxyhydroxides [*Flynn* 1984], and thus, possibly removing ferric cations from solution and thereby decreasing reaction rates. The end result is that these reaction processes are extremely complicated and depend upon a number of factors (including pH, temperature, reaction time, concentration of solutes, particle size and Fe/S ratio) that control rates and precipitation processes, few of which were studied in any rigorous fashion for this thesis and therefore cannot be adequately discussed.

The use of the growth of the ferric oxyhydroxide (goethite) peaks as an indicator of the various rates of reaction is also not applicable. The ferric sulfate added initially to the solution, itself undergoes hydrolysis reactions (as seen in Figures 6 and 7), and thus, adds its reaction products to that formed from the oxidation of the primary Fe-S mineralization. In effect, the areas associated with the ferric oxide phase peaks are "contaminated" by these hydrolysis products, and this invalidates their use as gauges of the effects of ferric cations as oxidation promoters and leaching agents.

Identification of Possible Martian Regolith Phases: Even though the reactions that produce them may be very complex, the final phases formed during this investigation tend to show a number of consistent trends and can be grouped into a number of well-defined categories (see Figure 9). This allows conclusions to be drawn about the mineralogical assemblage of the martian regolith, which is the prime objective of the thesis.

It was initially thought that the addition of a ferric sulfate solution, to half of the reactions studied, might alter the rate of formation of reaction products. In addition though, it was thought that the hydrolysis of the ferric sulfate

solution itself, might be the origin of some of the products rather than the oxidation of the initial Fe-S mineralization. This appears not to be the case, since the oxidation of pyrrhotite or troilite produces (via the intermediary, pyrite) a solution that is itself rich in ferric and sulfate ions. Thus, the addition of supplemental ferric sulfate to the aqueous environment did not add anything new to the weathering regime but rather increased some of the constituents's concentrations (which may or may not affect weathering processes). Also, examination of Tables 3 and 4 and inspection of the corresponding figures, shows that the formation of the individual reaction products (goethite, jarosite, lepidocrocite and pyrite or marcasite) is not dependent on whether or not the additional ferric sulfate was present. A corollary to this, is the observation that ferric cations are not necessarily needed to initiate the "deep-weathering" reactions of the primary sulfide mineralization (pyrrhotite-pentlandite) to produce secondary sulfide minerals (pyrite/marcasite). Those reactions which did not have the initial addition of ferric sulfate to the reaction solution (T4N60, T2N80, T4N60, etc.) still produced the secondary supergene enriched minerals. Apparently, the dissolved oxygen content of the starting solution (normal aerated water in equilibrium with the Earth's atmosphere) was sufficient to start the oxidation process regardless of whether or not ferric cations were also present.

The results, discussed in the *Data and Results* section, and the labelled peaks in Figures 2 through 5, indicate a rather arbitrary division of reaction products into major and minor phases. The major phases are limited to pyrite or marcasite, goethite and lepidocrocite, while the minor phases include hematite, ferrihydrite or maghemite and jarosite. These products correlate with the

expected mineralogy obtained during the formation of gossans as was outlined in the theoretical model discuss above (see pages 17-22) and agree with those mineralogical assemblages found associated with terrestrial gossans [*Blain and Andrew* 1977; *Thornber* 1975].

Formation of the secondary FeS_2 mineralization, one of the major phases obtained in this study, is not something that directly affects the composition of the martian regolith. It is usually associated with processes taking place at or near the water table, and as such, would not likely be a major constituent of martian soils. Rather, it is the formation of ferric sulfate and hydroxyoxide phases in the near-surface environment, caused by oxidation by dissolved oxygen of the products from the decomposition of sulfides at or near the water table, that controls the martian regolith's mineral composition. Thus, the presence of pyrite or marcasite in martian soils would be minor and only exist in any quantity through exposure of the main ore body by erosional activity.

Of greater importance to the nature of the martian regolith are the hydrolysis reactions that form the ferric sulfate and hydroxyoxide phases in the near-surface environment. The hydrolysis of ferric-containing solutions consists of two competing processes: one, formation of reaction products from low-molecular-weight ferric species; and two, formation from a ferric-bearing cationic polymer (which may contain ferric cations in tetrahedral coordination and might be a probable aqueous precursor of ferrihydrite) [*Flynn* 1984; *Schwertmann and Murad* 1983]. Thus, the final mineral assemblage depends on the varying rates of formation and aging of the polymer and of the rates of formation and reaction of the monomeric species. Studies indicate that goethite is the hydrolysis product of aging of the polymer, while lepidocrocite is formed directly

from the monomeric species [*Flynn* 1984]. This seems to be in conflict with other results that suggest that goethite crystals form from dissolved ferric ions in solution [*Schwertmann and Murad* 1983]. In either case, both papers suggest that increasing ionic strength favours the precipitation of goethite over lepidocrocite [*Flynn* 1984] or hematite (which is thought to form from internal dehydration and rearrangement of the ferrihydrite polymers) [*Schwertmann and Murad* 1983]. This is supported by the studies of *Murphy et al.* (1975) who found that lepidocrocite formation is suppressed in high ionic strength solutions while the formation of goethite is increased.

The ionic strength of the solutions used in the present study's experiments, though never measured, would not be expected to ever be greater than 0.1M (since the ferric sulfate solution used was only 10^{-2}M and the weathering of sulfides only produces sulfate solutions on the order of 10^{-2}M). This would indicate a relatively weak solution in terms of ionic strength, one that would favour the precipitation of lepidocrocite. But from the results listed in Table 3, it is obvious that goethite is the preferred hydrolysis product, in all cases, for our reactions. This is due to two effects: one, the presence of sulfate in solution, from the degradation of pyrite, increases the rate of precipitation of goethite [*Flynn* 1984]; and two, in high-temperature hydrolysis reactions (greater than room temperature) in which the sample is reacted for longer periods of time (on the order of days) lepidocrocite is converted to hematite or goethite [*Flynn* 1984]. Also, in the presence of sulfate ions a variety of sulfate-containing products may be formed in addition to goethite [*Flynn* 1984].

This is further evidenced the studies of hydrolysis reactions. The two reactions S2N80 and S7N80 were reacted only for 1 and 2 days, respectively. In

both cases they produced a hydronium jarosite phase (along with ferrihydrite for sample S2N80). But sample S2N60, which was reacted for 35 days under similar conditions (60°C as opposed to 80°C for the other two reactions) yielded goethite. Apparently, for longer reaction times and lower temperatures, such as those encountered in the troilite and pyrrhotite experiments, goethite becomes the dominant product at the expense of lepidocrocite and jarosite phases.

What then is the explanation for the presence of jarosite, lepidocrocite and hematite as final reaction products in the experiments? For the jarosite phases, they are probably stabilized by the highly acidic environment of the solutions as indicated in other studies [*Brown* 1971; *Music et al.* 1982]; also, the reaction of jarosite → goethite is sluggish and jarosite can persist outside of its stability field [*Brown* 1971]. The lepidocrocite probably represents a metastable intermediate phase that is being constantly formed and has not yet had time to further degrade into goethite, possibly due to sluggish reaction rates similar to those encountered with jarosite. The hematite, as mentioned earlier, could possibly form from the desiccation of goethite after removal from the aqueous environment. Hematite also is a product of dehydration and rearrangement of ferrihydrite aggregates in solution [*Schwertmann and Murad* 1983]. Since the presence of ferrihydrite is indicated by some of the 298K spectra (Figures 4a, 4d and 5c), it is reasonable to assume that hematite might have formed from it. It is likely though, that the amount produced relative to goethite is small and thus its peaks would be to weak to be observed during Mössbauer fitting procedures, which would account for it only appearing once.

Evidence for the slow kinetics of jarosite and lepidocrocite degrading to goethite is given by the 80°C reactions. Neither lepidocrocite nor jarosite is

found in those reactions done at 80°C for 14 days (samples T2N80, T2F80, P2N80 and P2F80; the 4.2K spectra for lepidocrocite and the 298K spectra for jarosite). At this higher temperature, the rate of goethite formation from either jarosite or lepidocrocite must exceed those rates which control the formation of jarosite and lepidocrocite. This explains the lack of these phases under the high temperature conditions.

The purpose behind the pH 4 reactions was to study the effects of a higher pH on the eventual reaction products. Jarosite is thought to be stable in an acidic (pH<3) and oxidizing environment [*Brown* 1971]. At higher pHs (greater than 3) goethite becomes the stable mineral. Thus, in theory, those reactions that started out at pH 2 should have favoured jarosite formation over those with a starting pH of 4. According to the results from the 4.2K spectra, goethite is present under all conditions, while the room temperature reactions indicate that jarosite is present in both acid environments (see Figures 5b, 5e and 5f). The explanation for this is either the slow kinetics of reaction which allows jarosite to coexist with goethite, an occurrence that is not uncommon in terrestrial gossans, or that the oxidation of pyrite and with it the production of sulfuric acid, has lowered the pH of all reaction solutions to something less than 3, where jarosite is stable. Unfortunately, the final pHs of the reaction solutions were not investigated and it is unknown whether or not this is true. But since there were no silicate minerals to react with the acid in these reactions, which is the usual acid-buffering mechanism in terrestrial weathering regimes, it is not unreasonable to assume the generation of a highly acidic solution regardless of the initial pH.

Coming full circle, we now discuss how these results might relate to

regolith formation on Mars. It is obvious that the basic weathering model proposed, that komatiitic hosted sulfide deposits have undergone acidic, oxidative weathering to produce gossaniferous goethite-jarosite-opal-clay silicate deposits, is supported by the experimental results described herein. The H_2SO_4-degraded FeS mineralization has undergone supergene enrichment reactions to form a secondary FeS_2 phase (pyrite and/or marcasite) which then degrades and leads to the deposition of goethite and jarosite. On Mars, such deposition of goethite and jarosite would take place in gossans above the main ore body and above the water table. It is this goethite ± jarosite mineral assemblage that accounts for the greater part of the ferric-bearing martian regolith, and probably for the reflectance spectra features described above and shown in Figure 1.

Even though the reactions are not necessarily Mars-like, particularly in the temperature ranges and water-rich environment used, this does not invalidate the conclusions drawn from them. In fact, in the analogous terrestrial processes to those proposed for Mars, the main reactions of interest, those being the hydrolysis reactions that take place above the water table, proceed in a drier environment than in our experimental conditions. Under these drier conditions, as hydrothermal fluids are circulated above the intruded magma and above the water table, any hydrolysis products that precipitate out might tend to get "left behind" in a non-aqueous environment where they become stable phases due to very slow kinetics. In a similar fashion, Mars' cold and dry environment would stabilize metastable minerals deposited above the water table (as jarosite, goethite and lepidocrocite would be). Thus, very slow reaction rates would encourage the persistence of thermodynamically unstable minerals in the martian regolith, such as jarosite, over long periods of time, up to and including the

present day.

In addition to the weathering of sulfide mineralization, the acidic solutions generated would also react to some extent with the silicate mineralization that either accompanies the intrusion of the magma or is part of the wall rock mineral assemblage. These dissolution reactions would release alkali metals (K^+, Na^+ and Ca^{2+}) into solution (reaction (17)) which would further promote the precipitation of jarosite type minerals in gossans on Mars. This was shown with reaction S2K80, in which the addition of K^+ cations to the reaction solution caused the formation of the more stable and less soluble, K-bearing jarosite (natural jarosite) rather than the hydronium jarosite.

The presence of Cl^- anions in the martian regolith, as indicated by the Viking XRF results (Table 1), also has an effect on the hydrolysis reactions, occurring above the water table, which could affect the ultimate composition of the fines. The presence of Cl^- during hydrolysis reactions, results in the formation of akaganeite (β-FeOOH) over that of goethite (α-FeOOH) [*Flynn* 1984; *Kauffman and Hazel* 1975], although for longer reaction periods a mixture of poorly crystalline hematite and goethite is formed [*Kauffman and Hazel* 1975]. Thus, the martian regolith may contain quantities of akaganeite that would not have shown up in our reactions since no Cl^- ions were present.

A final note about the composition of the martian regolith. The consistent formation of significant amounts of lepidocrocite in our reactions (see Figures 3a, 3e and 3f), suggests that maghemite could be present in the martian soils in reasonably significant quantities. Dehydration of lepidocrocite yields maghemite, and the dry martian environment would seem to promote this type of reaction, possibly during eolian transport [*Burns* 1987]. Thus, it is mag-

hemite, along with remnant pyrrhotite, that most likely accounts for the magnetic fraction of the martian fines that was discovered by the Viking landers.

Odds and Ends: Perhaps the least expected result from the set of experiments undertaken, was the production of pyrrhotite when troilite samples were reacted in the various aqueous solutions (Figure 4 shows the appearance of the inner pyrrhotite peaks). Pyrrhotite is the more stable of the two FeS mineral forms in an oxidizing environment (troilite is generally only found in more reducing environments, for example, the lunar surface and in meteorites). Apparently, the ferrous cation sites in troilite are susceptible to oxidation, with the result that ferric cations are released and the non-stoichiometric pyrrhotite structure is adopted to allow for charge balance (i.e. $Fe_2^{3+}Fe_5^{2+}S_8$). The following reaction is proposed,

$$32FeS + 3O_{2(aq)} + 2H_2O = 4FeOOH_{(s)} + 4Fe_7S_{8(s)} \qquad (20)$$

with the attendant formation of a FeOOH polymorph (goethite probably, considering the evidence of the Mössbauer spectra). It is unclear whether the troilite undergoes this reaction only, and that the pyrrhotite formed then undergoes oxidation to form the secondary FeS_2 mineralization, or whether troilite undergoes pyritization, similar to that of reaction (3) as pyrrhotite is postulated to do, as well as reaction (20).

The presence of ferric cations in solution seems to promote the "oxidation" of troilite to pyrrhotite (though a similar argument to that made about the effects of aqueous ferric cations on the pyritization of pyrrhotite may also be made, in which the ferric cations shift the equilibrium concentrations rather than increasing reaction rates). The ratio of the areas of the incoming pyrrhotite peaks to that of the troilite peaks increases with the addition of the

ferric sulfate solution (Table 5, last column). Thus, it seems that the troilite structure is also susceptible to oxidation by Fe^{3+} cations as well as dissolved oxygen.

For the most part, the hydrolysis products formed have shown superparamagnetic behavior in the Mössbauer studies. This indicates a nanophase (<10 nm) particle size. It is possible that on Mars, where these reactions may have taken place at a kinetically slower pace, that the phases formed would exhibit larger particle sizes than those obtained, with bulk crystalline properties. This affects the remote sensing spectra that would be obtained from sampling these products. Studies so far of such reflectance spectra are inconclusive in specifying any one general particle size. For instance compare the studies of *Morris et al.* (1989) and *Bell et al.* (1990) with the ideas of *Singer* (1982). Most likely, a broad range of particle sizes is present in the martian regolith, from nanophase to bulk crystalline, formed under numerous, slightly differing, weathering regimes. In fact, the presence of goethite sextets in the room temperature Mössbauer spectra of this study (Figures 8a and 8b), indicate, that even in the relatively simplistic and similar reactions undertaken, that a range of particle sizes is formed. This will complicate any reflectance spectroscopic study.

SUMMARY AND CONCLUSIONS

The experimental results for the sulfuric acid reacted pyrrhotites and troilites support the weathering model summarized earlier. Supergene oxidation and enrichment of FeS mineralization below the water table by acidic groundwater produces a secondary FeS_2 phase which, upon further oxidation at or near the table, produces a solution rich in Fe^{3+} and SO_4^{2-} ions. Above the water table, in less acidic environments, this solution undergoes hydrolysis reactions and precipitates out goethite and jarosite in gossans lying over the primary sulfide ore body.

This oxidative weathering model of sulfide mineralization (pyrrhotite-pentlandite) disseminated in komatiitic basalts, similar to that associated with terrestrial komatiites, is proposed for Mars, leading to a gossaniferous martian regolith. Evidence for the formation of these gossans on Mars comes from several sources. One, the study of the remote-sensed reflectance spectra of the bright and dark regions of Mars. Two, the possible presence of preterrestrial ferric-bearing phases (jarosite, for example) in SNC meteorites which are believed to originate from Mars. And three, data from the Viking Lander experiments (the XRF, magnetic and biology experiments all contributed pieces to the puzzle). Theoretical modelling based on the above evidence (see the ***Background*** section for a more detailed account of this evidence) lead to the oxidative weathering model investigated.

The reactions studied in this thesis suffered from being both too simple and too complex. Investigations of the hydrolysis reactions of ferric-containing

solutions indicate a great deal of complexity. The reactions undertaken did not fully take into account these complexities. Parameters, such as, ferric ion concentration and pH, should have been monitored more closely. This would have allowed one to address the identification of the reaction pathways with greater clarity, which hopefully, would have lead to an increased understanding of the final hydrolysis products obtained. As it was, the only data base was that obtained from the Mössbauer spectra, which yielded information only on the probable final products. Without a better understanding of pH and concentration effects, it is unclear just how applicable these lab-based experiments are to investigating the martian regolith. Greater control on individual parameters is needed in any further investigations undertaken.

On the other hand, the martian regolith (based on the Viking XRF data) is known to contain elements (for example, Cl and K), presumably from volcanic exhalates and dissolution of silicate rocks, that would even further complicate the already complicated hydrolysis reaction pathways. Possibly, the presence of these additional ions in solution would invalidate the conclusions drawn from the investigated reactions.

Nonetheless, several conclusions may be drawn from the experimental results. These are: (1) that secondary FeS_2 mineralization (pyrite and/or marcasite) is formed in the oxidation of primary sulfide ores (mostly pyrrhotite) to ferric oxide/oxyhydroxides; (2) that ferric cations seem to promote the formation of supergene FeS_2; (3) that troilite is unstable in an oxidizing environment and alters into pyrrhotite in the presence of either dissolved oxygen or aqueous ferric cations; (4) that the postulated gossaniferous martian regolith is predominantly formed of goethite and jarosite; (5) that the jarosite is

metastable, but that the conditions on present day Mars would tend to stabilize it, because of very slow reaction rates; (6) that the magnetic fraction, of the martian fines, discovered by the Viking landers, is most likely a combination of exposed, unoxidized pyrrhotite and a maghemite phase, and that the maghemite formed form dehydration of lepidocrocite; and (7) that an oxidizing, sulfuric acid solution can indeed induce the pyrrhotite $\rightarrow$ FeS_2 $\rightarrow$ FeOOH + jarosite reaction pathway that is postulated to occur on Mars.

APPENDIX: THE MÖSSBAUER EFFECT

Detailed discussions of the theory and applications of Mössbauer spectroscopy exist elsewhere [*Bancroft* 1973; *Burns* 1990; *Hawthorne* 1988; *Murad and Johnston* 1987]. Below is given a brief review of some of the more important points about the Mössbauer effect in view of this thesis.

The Mössbauer effect, originating from recoil-free fluorescent emission and nuclear gamma ray resonance absorption, yields three useful spectral parameters, namely, isomer shift, quadrupole splitting and magnetic hyperfine splitting. The values of these parameters depend on the interactions between the absorbing nucleus and the surrounding electric and magnetic fields induced by the orbiting electrons and by differences in the chemical environments of each nucleus.

Gamma rays, released from the radioactive decay of a ^{57}Co source by electron capture to stable ^{57}Fe, are used to excite nuclear transitions in ^{57}Fe (which has a natural isotopic abundance of 2.2%) in the material under investigation. Several gamma rays of differing energies are released in the process of the parent ^{57}Co decaying to the stable daughter ^{57}Fe. All are transmitted through the irradiated sample except for the 14.41 keV gamma ray associated with the nuclear transition from an excited state with nuclear spin quantum number $I = \pm 3/2$ to the ground-state with $I = \pm 1/2$. Resonant absorption of this energy by the target sample is possible only if the ^{57}Fe is in the same chemical environment as the ^{57}Co emitter. However, the nuclear energy levels of Fe in the target sample have slightly different energies due to differing

chemical environments, for example, differences in the coordination environment or differences in oxidation states. These differences destroy the conditions for resonance absorption. To restore resonance absorption, the source is vibrated such that the emitted gamma rays are doppler shifted into a continuum of differing energies. Those energies which correspond to transitions in the nuclear levels of the target sample, now undergo resonance absorption and appear as absorption peaks on a Mössbauer spectra associated with a specific velocity. For ^{57}Fe-bearing minerals all absorption peaks are in the range of 0 to ±10 mm/s. The placement and relation of these peaks yields the above mentioned spectral parameters used in characterizing mineral samples and are briefly discussed below.

The isomer shift, δ, arises from differences in the s-electron density, at the nuclei, between the radioactive source and the absorbing iron nuclei. The shift is, in general, controlled by subtle differences in the chemical environment of the absorbing nuclei which is, in turn, affected by the oxidation state, coordination number, spin state of the iron atom and ligand effects of the target iron nuclei. Isomer shifts are measured relative to an arbitrary midpoint (stated to be 0 mm/s) obtained from use of a standard, in this case a pure metallic iron foil. Use of other standards alters the midpoint reference, and thus, may affect the absolute values of the measured isomer shifts.

Quadrupole splitting, Δ, arises from the interaction of a non-spherical nucleus ($I \geq 1$) with any non-spherical component of an electric field gradient (EFG). This interaction causes the excited state of the 14.41 keV transition to be split into two levels (the ground state, with $I = 1/2$, is unaffected). Two factors contribute to the nature of the EFG and thus to the value of the

quadrupole splitting: one, an asymmetrical electronic structure for the Fe atom; and two, any distortions from perfect cubic symmetry of the Fe cation coordinating environment. This results in the splitting of a single absorption peak into two peaks of equal area in a Mössbauer spectrum, where the isomer shift is now measured from the midpoint of the doublet.

Magnetic hyperfine splitting, H_{int}, arises from the interaction of the magnetic dipole moment of the nucleus with the magnetic field at the nucleus. The magnetic field, originating from either an applied external field or unpaired electrons in the 3d-orbitals of the iron cation, removes the degeneracies of the nuclear spin states. Selection rules for magnetic dipole transitions allow only six transitions between the now split nuclear states. This leads to the formation of a sextet in a Mössbauer spectrum for crystalline phases. The parameter, H_{int}, used to quantify this magnetic splitting, is usually determined by the separation of peaks 1 and 6 and is measured in teslas. For a sextet to form, the magnetic field produced by unpaired d-electrons must exist for a longer period then the lifetime of the excited Fe nuclear state. This happens for paramagnetic minerals only when the samples are cooled to temperatures below their Curie (for ferromagnetic minerals) or Néel (for antiferromagnetic minerals) temperatures where magnetic coupling of electron spins on adjacent iron atoms takes place, which for most iron sulfides and ferric oxides and oxyhydroxides is above room temperature. Though certain ferric oxides and oxyhydroxides, when formed, may be poorly crystalline and display superparamagnetism (doublets) at room temperature. Superparamagnetism arises when thermal fluctuations of the coupled magnetic moments of microcrystals collapses the magnetic hyperfine field resulting in a non-magnetic Mössbauer spectrum. Superparamagnetic

effects can lower the onset of magnetic ordering for such nanophases (<10 nm) below their usual Curie or Néel temperatures associated with bulk crystalline samples. Non-stoichiometry and structural defects may also lower the Curie/Néel temperatures of an iron-bearing material. For example, goethite's Néel temperature can be lowered below room temperature by the substitution of Al for Fe in the crystal lattice. However, by 4.2K most iron-rich minerals give magnetically split spectra.

Particle size also affects the H_{int} parameter of a material. Nanophases usually exhibit smaller values of H_{int} than their more bulk crystalline counterparts. Thus, for a material that has a distribution of particle sizes, the H_{int} parameter will have a corresponding range. This may result in asymmetric peaks in a sextet of a Mössbauer spectrum.

It is important to note that the Mössbauer effect only works for crystalline materials. In order for resonant absorption to take place the 2.2% ^{57}Fe isotopes have to be held tightly in place, as is the case in a crystal lattice. By being so bound, the mass of the absorbing ^{57}Fe atom is effectively the whole lattice. This minimizes the recoil energy (the energy associated with the recoil of a nucleus upon emission of radiation) and improves the resonance absorption of the 14.41 keV gamma ray. If either the emitting nuclei or absorbing nuclei are in the fluid phase, the recoil energy is too high and prevents nuclear gamma resonance absorption from occurring. This leads to the recoil-free fraction, f, being defined as the probability of a recoilless emission and absorption occurring. The recoil-free fraction is dependent on the vibrational amplitude of the nucleus and this leads to an inverse relationship between the value for f and temperature. In general the value of f increases as temperature decreases. Thus, for the spectra

collected at 4.2K, increased nuclear gamma resonance absorption will be observed due to increases in the recoil-free fraction. Approximate values of f are: 0.8 for sulfides and 0.9-1.0 for silicates and oxides. Also there is a tendency to expect ferric iron to have higher f values than ferrous iron due to its higher valency which possibly leads to tighter bonding in the lattice (i.e. decreased vibrational amplitude).

Finally, a last parameter is mentioned which can yield useful information about an analysed product. The linewidth, Γ, of a recoilless event is limited by Heisenberg's Uncertainty Principle as applied to gamma-ray transitions. For ^{57}Fe, the 14.41 keV transition has a half-life of approximately 10^{-7} sec, this corresponds to an energy uncertainty of $5x10^{-9}$ eV or in terms of the usual Mössbauer scale, a linewidth of 0.19 mm/s. This is the theoretical minimum linewidth allowed for a transition and corresponds to the full width at half peak height of a Mössbauer absorption peak. In practical applications, this theoretical minimum is never reached and a more practical lower limit is obtained from the linewidths of the iron foil standard used for calibration. This experimentally determined lower-limit is approximately 0.23-0.24 mm/s (for ^{57}Co in a Rh matrix used as the source). Deviations (broadening of the peaks) from this minimum may result from, among others, poor quality of fit when overlapped peaks are involved, a range of particle sizes, next nearest neighbor effects or crystal defects.

Table 6 contains summarized data of several Mössbauer and magnetic parameters for some important iron oxides and sulfides. The combination of the above parameters measured at room temperature and at 4.2K enables us to readily distinguish between ferric iron (in oxides, oxyhydroxides and sulfates),

low-spin ferrous iron (in pyrite and marcasite) and high-spin ferrous iron (in troilite and pyrrhotite), even as coexisting phases in a single reaction product.

REFERENCES

Adams, J. B. and T. B. McCord. (1969) Mars: interpretation of spectral reflectivity of light and dark regions. *J. Geophys. Res.* **74**, 4851-4856.

Afanasev, A. M., V. D. Gorobchenko, D. S. Kulgawczuk and I. I. Lukashevich. (1974) Nuclear γ-resonance in iron sulfates of the jarosite group. *Phys. Status Solidi A* **26**, 697-701.

Arvidson, R. E., K. A. Goettel and C. M. Hohenberg. (1980) A post-Viking view of martian geologic evolution. *Revs. Geophys. and Space Phys.* **18**, 565-603.

Baird, A. K. and B. C. Clark. (1981) On the original igneous source of martian fines. *Icarus* **45**, 113-123.

Baird, A. K., P. Toulmin, B. C. Clark, H. J. Rose, K. Keil, R. P. Christian and J. L. Gooding. (1976) Mineralogic and petrologic implications of Viking geochemical results from Mars: interim report. *Science* **194**, 1288-1293.

Bancroft, G. M. (1973). Mössbauer Spectroscopy. An Introduction for Inorganic Chemists and Geochemists. New York, McGraw-Hill.

Banin, A., G. C. Carle, S. Chang, L. M. Coyne, J. B. Orenberg and T. W. Scattergood. (1988) Laboratory investigations of Mars: chemical and spectroscopic characteristics of a suite of clays as Mars soil analogs. *Origin of Life and the Evolution of the Biosphere* **18**, 239-265.

Banin, A., L. Margulies and Y. Chen. (1985) Iron montmorillonite: a spectral analog of martian soil. *Proc. 15th Lunar Planet. Sci. Conf., J. Geophys. Res.* **90**, C771-C774.

Becker, R. H. and R. O. Pepin. (1984) The case for a Martian origin of the shergottites: nitrogen and noble gases in EETA79001. *Earth Plan. Sci.* **69**, 225-242.

Bell, J. F., III, T. B. McCord and P. D. Owensby. (1990) Observational evidence of crystalline iron oxides on Mars. *J. Geophys. Res.* **in press**.

Bertka, A. K. and J. R. Holloway. (1988) Martian mantle primary melts: an experimental study of iron-rich garnet lherzolite minimum melt composition. *Proc. 19th Lunar Planet Sci. Conf.* 723-739.

Biemann, K., J. Oro, P. Toulmin III, L. E. Orgel, A. O. Nier, D. M. Anderson, P. G. Simmonds, D. Flory, A. V. Diaz, D. R. Rushneck, J. E. Biller and A. L. Lafleur. (1977) The search for organic substances and inorganic volatile compounds in the surface of Mars. *J. Geophys. Res.* **82**, 4641-4658.

Blain, C. F. and R. L. Andrew. (1977) Sulfide weathering and the evaluation of gossans in mineral exploration. *Minerals Sci. Engng.* **9**, 119-150.

Bogard, D. D. and P. Johnson. (1983) Martian gases in an Antarctic meteorite? *Science* **221**, 651-654.

Brown, J. B. (1971) Jarosite-Goethite stabilities at 25°C, 1 atm. *Mineral. Deposita (Berl.)* **6**, 245-252.

Bunch, T. E. and A. M. Reid. (1975) The Nakhlites, Part I: petrography and mineral chemistry. *Meteoritics* **10**, 303-315.

Burns, R. G. (1987) Ferric sulfates on Mars. *Proc. 17th Lunar Planet. Sci. Conf., J. Geophys. Res.* **92**, E570-E574.

Burns, R. G. (1988) Gossans on Mars. *Proc. 19th Lunar Planet Sci. Conf.* 713-721.

Burns, R. G. (1989) Spectral mineralogy of terrestrial planets: scanning their surfaces remotely. *Mineral. Mag.* **53**, 135-151.

Burns, R. G. (1990). Mössbauer Spectral Characterization of Planetary Surface Materials. In Remote Geochemical Analysis: Elemental and Mineralogical Composition. **in press**.

Burns, R. G. and D. S. Fisher. (1988) Weathering of sulfides on Mars, in: MEVTV Workshop on Nature and Composition of Surface Units on Mars (J. R. Zimbelman, S. C. Solomon and V. L. Sharpton, eds.). *Lunar Planet. Inst. Tech Rept.* **88-05**, 34-36.

Burns, R. G. and D. S. Fisher. (1990a) Iron-sulfur mineralogy of Mars: magmatic evolution and chemical weathering products. *J. Geophys. Res.* **in press**.

Burns, R. G. and D. S. Fisher. (1990b) Evolution of sulfide mineralization on Mars. *J. Geophys. Res.* **in press**.

Bussod, G. and T. R. McGetchin. (1979) Martian lavas - reconnaissance experiments on a model ferro-picrite composition. *Lunar Planet. Sci.* **X**, 172-174.

Caroll, M. R. and M. J. Rutherford. (1985) Sulfide and sulfate saturation in hydrous silicate melts. *Proc. 15th Lunar Planet. Sci. Conf., J. Geophys. Res.* **90**, C601-C612.

Carr, M. H. (1987) Water on Mars. *Nature* **326**, 30-35.

Carr, R. H., M. M. Grady, I. P. Wright and C. T. Pillinger. (1985) Martian atmospheric carbon dioxide and weathering products in SNC meteorites. *Nature* **314**, 248-250.

Clark, B. C. and A. K. Baird. (1979) Is the martian lithosphere sulfur rich? *J. Geophys. Res.* **84**, 8395-8403.

Clark, B. C., A. K. Baird, H. J. Rose Jr., K. Keil, A. J. Castro, W. C. Kelliher, C. D. Rowe and P. H. Evans. (1976) Inorganic analyses of the Martian surface samples at the Viking landing sites. *Science* **194**, 1283-1288.

Clark, B. C., A. K. Baird, R. J. Weldon, D. M. Tsusaki, L. Schnabel and M. P. Candelaria. (1982) Chemical compositions of martian fines. *J. Geophys. Res.* **87**, 10059-10067.

Clark, B. C. and D. C. Van Hart. (1981) The salts of Mars. *Icarus* **45**, 370-378.

Delano, J. W. and R. J. Arculus. (1980) Nakhla: oxidation state and other constraints. *Lunar Planet. Sci.* **XI**, 219-222.

Dousma, J., D. den Ottelander and P. L. de Bruyn. (1979) The influence of sulfate ions on the formation of iron(III) oxides. *J. Inorg. Nucl. Chem.* **41**, 1565-1068.

Driebus, G. and H. Wanke. (1987) Volatiles on Earth and Mars: a comparison. *Icarus* **71**, 225-240.

Dyar, M. D. (1984) Precision and interlaboratory reproducibility of measurements of the Mössbauer effect in minerals. *Am. Mineral.* **69**, 1127-1144.

Floran, R. J., M. Prinz, P. F. Hlava, K. Keil, C. E. Nehru and J. R. Hinthorne. (1978) The Chassigny meteorite: a cumulate dunite with hydrous amphibole-bearing melt inclusions. *Geochim. Cosmochim. Acta* **42**, 1213-1229.

Flynn, C. H., Jr. (1984) Hydrolysis of inorganic iron(III) salts. *Chem. Rev.* **84**, 31-41.

Garrels, R. M. and M. E. Thompson. (1960) Oxidation of pyrite by iron sulfate solutions. *Amer. J. Sci.* **258-A**, 57-67.

Gibson, E. K., S. J. Wentworth and D. S. McKay. (1983) Chemical weathering and diagenesis of a cold desert soil from Wright Valley, Antarctica: an analog of martian weathering processes. *Proc. 13th Lunar Planet. Sci. Conf. in J. Geophys. Res.* **88**, A912-A928.

Goettel, K. A. (1981) Density of the mantle of Mars. *Geophys. Res. Lett.* **8**, 497-500.

Gooding, J. L. (1978) Chemical weathering on Mars: thermodynamic stabilities of primary minerals (and their alteration products) from mafic igneous rocks. *Icarus* **33**, 483-513.

Gooding, J. L. and K. Keil. (1978) Alteration of glass as a possible source of clay minerals on Mars. *Geophys. Res. Lett.* **5**, 727-730.

Gooding, J. L. and D. W. Muenow. (1986) Martian volatiles in shergottite EETA 79001: new evidence from oxidized sulfur and sulfur-rich aluminosilicates. *Geochim. Cosmochim. Acta* **50**, 1049-1059.

Gooding, J. L., S. J. Wentworth and M. E. Zolensky. (1988) Calcium carbonate and sulfate of possible extraterrestrial origin in the EETA79001 meteorite. *Geochim. Cosmochim. Acta* **52**, 909-915.

Green, D. H. (1975) Genesis of Archean peridotitic magmas and constraints on Archean geothermal gradients and tectonics. *Geology* **3**, 15-18.

Green, D. H. (1981). Petrogenesis of Archean ultramafic magmas and implications for Archean tectonics (Chap. 19). Precambrian Plate Tectonics. Amsterdam, Elsevier Sci. Publ. Co.

Green, D. H., I. A. Nicholls, M. Viljoen and R. Viljoen. (1975) Experimental demonstration of the existence of peridotitic liquids in earliest Archean magmatism. *Geology* **3**, 11-14.

Hargraves, R. B., D. W. Collinson, R. E. Arvidson and C. R. Spitzer. (1977) The Viking magnetic properties experiment: primary mission results. *J. Geophys. Res.* **82**, 4547-4558.

Haughton, D. R., P. L. Roeder and B. J. Skinner. (1974) Solubility of sulfur in mafic magmas. *Econ. Geol.* **69**, 451-462.

Hawthorne, F. C. (1988). Mössbauer spectroscopy (Chap. 8). Spectroscopic Methods in Mineralogy and Geology. Mineralogical Society of America.

Huguenin, R. L. (1982) Chemical weathering and the Viking biology experiments on Mars. *J. Geophys. Res.* **87**, 10069-10082.

Johnston, J. H. (1977) Jarosite and akaganeite from White Island volcano, New Zealand: an X-ray and Mössbauer study. *Geochim. Cosmochim. Acta* **41**, 539-544.

Kauffman, K. and F. Hazel. (1975) Infrared and Mössbauer spectroscopy, electron microscopy and chemical reactivity of ferric chloride hydrolysis products. *J. Inorg. Nucl. Chem>* **37**, 1139-1148.

Leclerc, A. (1980) Room temperature Mössbauer analysis of jarosite-type compounds. *Phys. Chem. Minerals* **6**, 327-334.

Matijevic, E., R. S. Sapieszko and J. B. Melville. (1975) Ferric hydrous. oxide sols. I. Mono-dispersed basic iron (III) sulfate particles. *J. Colloid. Interface. Sci.* **50**, 567-581.

McGetchin, T. R. and J. R. Smyth. (1978) The mantle of Mars: some possible geological implications of its high density. *Icarus* **34**, 512-536.

McSween, H. Y., Jr. and E. Jarosewich. (1983) Petrogenesis of the Elephant Moraine A79001 meteorite: multiple magma pulses on the shergottite parent body. *Geochim. Cosmochim. Acta* **47**, 1501-1513.

Morris, R. V., H. V. Lauer Jr., C. A. Lawson, R. K. Gibson Jr., G. A. Nace and C. Stewart. (1985) Spectral and other physicochemical properties of submicron powders of hematite (α-Fe_2O_3), maghemite (γ-Fe_2O_3), magnetite (Fe_3O_4), goethite (α-FeOOH) and lepidocrocite (γ-FeOOH). *J. Geophys. Res.* **90**, 3126-3144.

Morris, R. V., D. G. Agresti, H. V. Lauer Jr., J. A. Newcomb, T. D. Shelfer and A. V. Murali. (1989) Evidence for pigmentary hematite on Mars based on optical, magnetic and Mössbauer studies of superparamagnetic (nanocrystalline) hematite. *J. Geophys. Res.* **94**, 2760-2778.

Moses, C. O., D. K. Nordstrom, J. S. Herman and A. L. Mills. (1987) Aqueous pyrite oxidation by dissolved oxygen and by ferric iron. *Geochim. Cosmochim. Acta* **51**, 1561-1571.

Murad, E. (1982) The characterization of goethite by Mössbauer spectroscopy. *Amer. Mineral.* **67**, 1007-1011.

Murad, E., L. H. Bowen, G. J. Long and T. G. Quin. (1988) The influence of crystallinity on magnetic ordering in natural ferrihydrites. *Clay Minerals* **23**, 161-173.

Murad, E. and J. H. Johnston. (1987). Iron oxides and oxyhydroxides (Chap. 12). Mössbauer Spectroscopy Applied to Inorganic Chemistry. New York, Plenum.

Murad, E. and U. Schwertmann. (1980) The Mössbauer spectrum of ferrihydrite and its relation to those of other iron oxides. *Amer. Mineral.* **65**, 1044-1049.

Murphy, P. J., A. M. Posner and J. P. Quirk. (1975) Chemistry of iron in soils. Ferric hydrolysis products. *Aust. J. Soil Res.* **13**, 189-201.

Music, S., A. Vertes, G. W. Simmons, I. Czako-Nagy and H. Leidhesier Jr. (1982) Mössbauer spectroscopic study of the formation of Fe(III) oxyhydroxides and oxides by hydrolysis of aqueous Fe(III) solutions. *J. Colloid. Interface Sci.* **85**, 256-266.

O'Keefe, J. D. and T. J. Ahrens. (1986) Oblique impact: a process for obtaining meteorite samples from other planets. *Science* **234**, 346.

Reid, A. M. and T. E. Bunch. (1975) The Nakhlites, Part II: where, when and how. *Meteoritics* **10**, 317-324.

Ruby, S. L. (1973). Why MISFIT when you already have chi-squared? In, Mössbauer Effect Methodology. New York, Plenum Press.

Sapieszko, R. S., R. C. Patel and E. Matijevic. (1977) Ferric hydrous oxide sols. 2. Thermodynamics of aqueous hydroxo and sulfato ferric complexes. *J. Phys. Chem.* **81**, 1061-1068.

Sato, M. (1960) Oxidation of sulfide ore bodies. II. Oxidation mechanisms of sulfide minerals at 25°C. *Econ. Geol.* **55**, 1202-1231.

Schwertmann, U. and E. Murad. (1983) Effect of pH on the formation of goethite and hematite from ferrihydrite. *Clays and Clay Minerals* **31**, 277-284.

Sherman, D. M., R. G. Burns and V. M. Burns. (1982) Spectral characteristics of the iron oxides with application to the martian bright region mineralogy. *J. Geophys. Res.* **87**, 10169-10180.

Siever, R. and N. Woodford. (1979) Dissolution kinetics and the weathering of mafic minerals. *Geochim. Cosmochim. Acta* **43**, 717-724.

Singer, R. B. (1982) Spectral evidence for the mineralogy of high-albedo soils and dust on Mars. *J. Geophys. Res.* **87**, 10159-10168.

Singer, R. B. (1985) Spectroscopic observation of Mars. *Adv. Space Res.* **5**, 59-68.

Smith, J. V., I. M. Steele and C. A. Leitch. (1983) Mineral chemistry of the shergottites, nakhlites, Chassigny, Brachina, pallasites and ureilites. *Proc. 14th Lunar Planet. Sci. Conf., J. Geophys. Res.* **88**, B229-B236.

Solberg, T. C. and R. G. Burns. (1989) Iron Mössbauer spectral study of weathered antarctic and SNC meteorites. *Proc. 19th Lunar Planet. Sci. Conf.* 313-322.

Steele, I. M. and J. V. Smith. (1982) Petrography and mineralogy of two basalts and olivine-pyroxene-spinel fragments in achondrite EETA79001. *Proc. 13th Lunar Planet. Sci. Conf., J. Geophys. Res.* **87**, A375-A384.

Stolper, E. M. and H. Y. McSween Jr. (1979) Petrology and origin of the SNC meteorites. *Geochim. Cosmochim. Acta* **43**, 1475-1498.

Stone, A. J., K. M. Parkin and M. D. Dyar. (1984). STONE: a program for resolving Mössbauer spectra. Marlboro, Massachusetts, DEC Users's Society Program Library.

Takano, M., T. Shinjo, M. Kiyama and T. Takada. (1968) Magnetic properties of jarosites, $RFe_3(OH)_6(SO_4)_2$ ($R=NH_4$, Na or K). *J. Phys. Soc. Japan* **25**, 902.

Thornber, M. R. (1975) Supergene alteration of sulfides. I. A chemical model based on massive nickel sulfide deposits at Kambalda, Western Australia. *Chem. Geol.* **15**, 1-14.

Toulmin, P. A., III, A. K. Baird, B. C. Clark, K. Keil, H. J. Rose Jr., R. P. Christian, P. H. Evans and W. C. Keliher. (1977) Geochemical and mineralogical interpretation of the Viking inorganic chemical results. *J. Geophys. Res.* **82**, 4625-4634.

Treiman, A. H. (1986) The parental magma of the Nakhla achondrite: ultrabasic volcanism on the shergottite parent body. *Geochim. Cosmochim. Acta* **50**, 1061-1070.

Treiman, A. H. (1988) Crystal fractionation in the SNC meteorites: implications for surface units on Mars, in: MEVTV Workshop on Nature and Composition of Surface Units on Mars (J. R. Zimbelman, S. C. Solomon and V. L. Sharpton, eds.). *Lunar Planet. Inst. Tech Rept.* **88-05**, 127-128.

Vaughan, D. J. and J. Craig. (1978). Mineral Chemistry of Metal Sulfides. Cambridge Earth Science Series. Cambridge, Cambridge University Press.

Wood, C. A. and L. D. Ashwal. (1981) SNC meteorites: igneous rocks from Mars? *Proc. 12th Lunar Planet. Sci. Conf.* 1359-1375.

TABLE 1

COMPOSITION OF MARTIAN SAMPLES FROM VIKING I LANDING SITE (C) AND THE VIKING II LANDING SITE (U) BASED ON XRF DATA

	C1	C2	C3	U1
Oxides (wt.%):				
SiO_2	44.7	44.5	43.9	42.8
Al_2O_3	5.7	—	5.5	—
Fe_2O_3	18.2	18.0	18.7	20.3
MgO	8.3	—	8.6	—
CaO	5.6	5.3	5.6	5.0
K_2O	<0.3	<0.3	<0.3	<0.3
TiO_2	0.9	0.9	0.9	1.0
SO_3	7.7	9.5	9.5	6.5
Cl	0.7	0.8	0.9	0.6
Trace Elements (ppm):				
Rb	≤30			≤30
Sr	60±30			100±40
Y	70±30			50±30
Zr	≤30			30±20

SOURCE: *Toulmin et al.* (1977).

TABLE 2

EXPERIMENTAL CONDITIONS

Code [a]	Starting Material	Aqueous Solution [b] pH	Aqueous Solution [b] Fe^{3+}?	Temperature (°C)	Time (days)
T2N60	Troilite	2	No	60	35
T2F60	Troilite	2	Yes	60	35
T2N80	Troilite	2	No	80	14
T2F80	Troilite	2	Yes	80	14
T4N60	Troilite	4	No	60	7
T4F60	Troilite	4	Yes	60	7
P2N60	Pyrrhotite	2	No	60	35
P2F60	Pyrrhotite	2	Yes	60	35
P2N80	Pyrrhotite	2	No	80	14
P2F80	Pyrrhotite	2	Yes	80	14
P4N60	Pyrrhotite	4	No	60	7
P4F60	Pyrrhotite	4	Yes	60	7
S2N80	None	2	Yes	80	1
S2N60	None	2	Yes	60	35
S2K80	(K_2SO_4)	2	Yes	80	2
S7N80	None	7	Yes	80	2

[a] The code is used to refer to these reactions later on and for labelling the spectra. The first character refers to the starting material (T=troilite, P=pyrrhotite, S=ferric sulfate solution only), the second character is the pH, the third character indicates whether or not the aqueous environment was a sulfuric acid solution only (N), a ferric sulfate and sulfuric acid solution (F) or a ferric and potassium sulfate solution (K). The last two characters are the reaction temperature.

[b] The columns refer to the pH of the reaction solution due to the presence of sulfuric acid and whether or not a 10^{-2} M ferric sulfate solution was also present.

TABLE 3

MÖSSBAUER PARAMETERS FROM THE 4.2K SPECTRA [a,b]

Sample [c]	Cation [d]	δ (mm/s)	Δ (mm/s)	H_{int} (T)	Area (%)[e]
		Troilite Samples			
T2N60	l.s. Fe^{2+}	0.34	0.51	—	2.0
	h.s. Fe^{3+}	0.65	–0.15	50.4	8.8
	h.s. Fe^{3+}	—	—	44.3 [f]	—
T2F60	l.s. Fe^{2+}	0.39	0.62	—	2.4
	h.s. Fe^{3+}	0.65	–0.10	50.8	13.6
	h.s. Fe^{3+}	—	—	45.0 [f]	—
T2N80	l.s. Fe^{2+}	0.40	0.58	—	1.7
	h.s. Fe^{3+}	0.66	0.08	51.6	7.8
T2F80	l.s. Fe^{2+}	0.39	0.56	—	3.3
	h.s. Fe^{3+}	0.64	0.13	50.8	10.0
T4N60	l.s. Fe^{2+}	0.35	0.53	—	3.9
	h.s. Fe^{3+}	0.62	–0.14	51.0	6.3
T4F60	l.s. Fe^{2+}	0.39	0.61	—	3.0
	h.s. Fe^{3+}	0.66	–0.28	50.4	16.0
	h.s. Fe^{3+}	—	—	45.1 [f]	—
		Pyrrhotite Samples			
P2N60	l.s. Fe^{2+}	0.38	0.63	—	14.9
	h.s. Fe^{3+}	—	—	49.2	26.0
P2F60	l.s. Fe^{2+}	0.41	0.61	—	30.8
	h.s. Fe^{3+}	—	—	45.5	4.4
	h.s. Fe^{3+}	—	—	50.8	21.0

TABLE 3 – Continued...

Sample [c]	Cation [d]	δ (mm/s)	Δ (mm/s)	H_{int} (T)	Area (%)[e]
P2N80	l.s. Fe^{2+}	0.42	0.58	—	25.4
	h.s. Fe^{3+}	—	—	50.9	10.1
	h.s. Fe^{3+}	—	—	53.7	1.8
P2F80	l.s. Fe^{2+}	0.40	0.57	—	38.0
	h.s. Fe^{3+}	—	—	50.8	6.1
P4N60	l.s. Fe^{2+}	0.44	0.67	—	13.1
	h.s. Fe^{3+}	—	—	44.6	11.1
	h.s. Fe^{3+}	—	—	50.8	23.2
P4F60	l.s. Fe^{2+}	0.43	0.62	—	26.5
	h.s. Fe^{3+}	—	—	45.5	6.4
	h.s. Fe^{3+}	—	—	50.5	23.6
		Ferric Sulfate Hydrolysis Samples			
S2N80	h.s. Fe^{3+}	0.50	0.34	47.4	—
	h.s. Fe^{3+}	0.43	0.57	44.4	—
S2N60	h.s. Fe^{3+}	—	—	49.9 [f]	—
S2K80	h.s. Fe^{3+}	0.49	0.19	47.6	—
S7N80	h.s. Fe^{3+}	0.50	0.35	46.9	—

[a] Errors are: (1) for isomer shifts, ≥0.02 mm/s; (2) for quadrupole splitting, ≥0.06 mm/s; (3) for peak areas, ≥1.5%; and (4) for H_{int}, ≥0.5T.

[b] Only the data for new phases appearing is included. The parameters for troilite and pyrrhotite peaks are not included.

[c] See footnote (a) of Table 2 for an explanation of this code.

[d] Refers to the nature of the iron cation responsible for the measured peaks (h.s.=high spin, l.s.=low spin and s.p.=superparamagnetic).

[e] For the troilite spectra this area is based on the total peak area of a sextet (for the h.s. Fe^{3+} cation)or doublet (for the l.s. Fe^{2+} cation). For the pyrrhotite spectra only the outermost peaks of a the sextet were fitted (with a doublet) and thus the areas for the h.s. Fe^{3+} cations is only the total of the areas of these doublets.

[f] These parameters were not obtained through fitting with STONE but were calculated from the spectra themselves. This explains the lack of area % for the troilite samples; though in each case the area for these peaks is less than for the other h.s. Fe^{3+} fitted sextet.

TABLE 4

MÖSSBAUER PARAMETERS FROM THE RT SPECTRA [a,b]

Sample [c]	Cation [d]	δ (mm/s)	Δ (mm/s)	Area (%)[e]
		Troilite Samples		
T2N60	s.p. Fe^{3+}	0.34	0.58	42.7
	h.s. Fe^{2+}	0.61	1.39	8.2
T2F60	s.p. Fe^{3+}	0.20	0.77	31.6
	h.s. Fe^{2+}	0.61	1.33	22.3
T2N80	s.p. Fe^{3+}	0.30	0.53	22.7
	h.s. Fe^{2+}	0.64	1.39	24.9
T2F80	s.p. Fe^{3+}	0.17	0.76	30.4
	h.s. Fe^{2+}	0.64	1.38	41.7
T4N60	s.p. Fe^{3+}	0.33	0.52	27.7
T4F60	s.p. Fe^{3+}	0.35	0.59	31.6
	h.s. Fe^{2+}	0.64	1.37	13.1
		Pyrrhotite Samples		
P2N60	s.p. Fe^{3+}	0.33	0.62	47.7
P2F60	s.p. Fe^{3+}	0.32	0.55	61.8
	s.p. Fe^{3+}	0.35	0.97	9.2
P2N80	s.p. Fe^{3+}	0.18	0.73	33.3
P2F80	s.p. Fe^{3+}	0.36	0.55	53.3
P4N60	s.p. Fe^{3+}	0.35	0.55	48.9
	s.p. Fe^{3+}	0.38	0.99	15.2

TABLE 4 – Continued...

Sample [c]	Cation [d]	δ (mm/s)	Δ (mm/s)	Area (%)[e]
P4F60	s.p. Fe^{3+}	0.36	0.56	70.8
	s.p. Fe^{3+}	0.42	1.07	6.7
	Ferric Sulfate Hydrolysis Samples			
S2N80	s.p. Fe^{3+}	0.35	0.99	——
S2N60	s.p. Fe^{3+}	0.36	0.58	——
S2K80	s.p. Fe^{3+}	0.35	1.09	——
S7N80	s.p. Fe^{3+}	0.48	0.97	——

[a] Errors are: (1) for isomer shifts, ≥0.02 mm/s; (2) for quadrupole splitting, ≥0.06 mm/s; and (3) for peak areas, ≥1.5%.

[b] Only the data for new phases appearing is included. The parameters for troilite and pyrrhotite peaks are not included.

[c] See footnote (a) of Table 2 for an explanation of this code.

[d] Refers to the nature of the iron cation responsible for the measured peaks (h.s.=high spin, l.s.=low spin and s.p.=superparamagnetic).

[e] These areas are based on the areas of doublets only as either all the phases are superparamagnetic or have their sextets cut off by the velocity range used.

TABLE 5

FERRIC/FERROUS RATIOS FOR VARIOUS EXPERIMENTAL CONDITIONS BASED ON THE PEAKS AREAS OF THE MÖSSBAUER SPECTRA

Sample [a]	Fe^{3+}/h.s. Fe^{2+} (b)	l.s.Fe^{2+}/h.s.Fe^{2+} (c)	Po/Tro [d]
T2N60	0.099	0.022	0.167
T2F60	0.162	0.029	0.484
T2N80	0.086	0.019	0.475
T2F80	0.115	0.038	1.495
T4N60	0.070	0.043	n/a
T4F60	0.198	0.037	0.237
P2N60	0.474	0.271	——
P2F60	0.688	0.835	——
P2N80	0.202	0.431	——
P2F80	0.113	0.705	——
P4N60	0.751	0.287	——
P4F60	0.836	0.738	——

[a] See footnote (a) of Table 2 for an explanation of this code.

[b] Derived from the 4.2K spectra. It is the ratio of the total areas of any sextets compared to the total area of the starting material (either troilite or pyrrhotite). For the pyrrhotite spectra the areas are based only on the fitted outermost sextet peaks.

[c] Derived from the 4.2K spectra. It is the ratio of the total areas of any doublets due to a low-spin ferrous phase (either marcasite or pyrite) compared to the total area of the starting material (either troilite or pyrrhotite).

[d] Derived from the RT spectra. It is the ratio of pyrrhotite as measured by the area of a fitted doublet to that of the starting material, troilite, also fitted as a doublet. This ratio exists only for the troilite reactions.

TABLE 6

MÖSSBAUER PARAMETERS FOR STANDARDS [a]

Mineral (Formula)	T (K)	δ (mm/s)	Δ (mm/s)	H_{int} (T)	T_n or T_c
Pyrite (FeS_2)	298	0.31	0.62	.... diamagnetic	
	4.2	0.41	0.62		
Marcasite (FeS_2)	298	0.27	0.51	.... diamagnetic	
	4.2	0.37	0.52		
Troilite (FeS)	298	0.86	–0.28	31.0	T_n=588K
	4.2	0.91	0.14	33.3	
Pyrrhotite (Fe_7S_8) [b]	298	0.69	0.16	30.7	T_c=578K
		0.64	0.31	35.5	
		0.64	0.30	22.5	
	77	0.81	–0.36	34.5	
		0.79	0.60	31.1	
		0.79	0.12	26.7	
		0.77	0.32	22.9	
		0.39	0.25	——	
Jarosite (natural, $K(Fe,Al)_3(SO_4)_2(OH)_6$)	298	0.38	1.24	——	T_n=60K[f]
	4.2	0.49	0.09	49.7	
Jarosite (H_30^+ var.) [c]	298	0.39	1.01	——	T_n~17K[h]
Hematite (xtalline, α–Fe_2O_3) [d]	298	0.37	–0.20	51.7	T_c=955K
	4.2	0.49	–0.40	54.4	
Hematite (s.p.) [e]	298	0.34	0.89	——	T_c=955K
Maghemite [d] (γ–Fe_2O_3)	298	0.32	0.02	49.9	T_c~900K
	4.2	0.44	-0.01	53.0	

TABLE 6 – Continued...

Mineral (Formula)	T (K)	δ (mm/s)	Δ (mm/s)	H_{int} (T)	T_n or T_c
Goethite [d]	298	0.37	–0.26	38.2	T_n=400K
(α–FeOOH)	4.2	0.50	0.25	50.9	
Goethite (s.p.) [e]	298	0.37	0.52	——	T_n=400K
Lepidocrocite [d]	298	0.37	0.53	——	T_n=77K
(γ–FeOOH)	4.2	0.47	0.02	45.5	
Ferrihydrite [g]	298	0.35	0.54-0.90	——	——
($Fe_5HO_8 \cdot 4H_2O$)	4.2	0.48	0.03	46.5-50.0	

[a] Data is from this study unless otherwise noted. Metallic Fe foil used for calibration.

[b] Source: *Vaughan and Craig* (1978).

[c] Source: *Leclerc* (1980).

[d] Source: *Murad and Johnston* (1987).

[e] Source: *Morris et al.* (1985).

[f] Source: *Takano et al.* (1968).

[g] Sources: *Murad et al.* (1988); *Murad and Schwertmann* (1980).

[h] Sources: *Afanasev et al.* (1974).

FIGURE CAPTIONS

Figure 1: Composite reflectance spectra of typical bright and dark regions of Mars obtained from Earth-based observation. The data in the figure are relative reflectances, scaled to unity at 1.02 μm [from *Singer* 1985]. The broad band, in the bright-region spectrum, at 0.86 - 0.87 μm and slope changes near 0.5 μm and 0.6 μm are diagnostic of Fe^{3+}. The dark-region spectrum exhibits diagnostic Fe^{2+} absorptions in the 1 μm region, in addition to the Fe^{3+} features above.

Figures 2 – 7: Fitted Mössbauer spectra of the reactions detailed in Table 2. The numbers in the parentheses after the sample code (see Table 2 for an explanation), refer to the number of peaks used in the fit and to the number of constraints used to fit those peaks. The figures are grouped as follows: **2a-f** are 4.2K spectra of the troilite reactions; **3a-f** are 4.2K spectra of the pyrrhotite reactions; **4a-f** are 298K spectra of the same troilite reactions in Figures 2a-f; **5a-f** are 298K spectra of the same pyrrhotite reactions in Figures 3a-f; **6a-f** are 4.2K spectra of the hydrolysis reactions and **7a-f** are their 298K spectra counterparts. The 4.2K spectra have a velocity range of ±10.0 mm/s while that of the 298K spectra is ±2.5 mm/s (except some of the 298K spectra of the hydrolysis reactions which have a velocity range of ±5.0 mm/s). An explanation of the labels used is as follows: T# indicates troilite peaks, P# pyrrhotite, G# goethite, L# lepidocrocite, H# hematite, J# jarosite, Fh# ferrihydrite, F2 and F2' indicate peaks attributed to FeS_2, Fe^{3+}(IV) and Fe^{3+}(IV)' to phases containing tetrahedrally coordinated ferric cations,

"s.p. Fe^{3+} & l.s. Fe^{2+}" and "s.p. $Fe^{3+'}$ & l.s. $Fe^{2+'}$" indicate peaks which are attributed to a combination of nanophase hydrated ferric oxides and diamagnetic FeS_2 phases.

Figure 8: Unfitted Mössbauer spectra measured at 298K with a velocity scale range of ±10 mm/s. **8a** shows sample T2F60, **8b** is of sample P2F60 and **8c** is a room temperature spectra of unreacted pyrrhotite. Figure 8a shows the appearance of pyrrhotite forming from the reaction of troilite in an acidic environment (the pyrrhotite peaks are labelled P1 through P6, compare with the peak positions of pyrrhotite in Figure 8c; the troilite peaks are labelled T1 through T6). Also, the appearance of a sextet in Figures 8a and 8b, due to a ferric oxide/oxyhydroxide phase, is shown at this velocity range (labelled h.s. Fe^{3+} and h.s. $Fe^{3+'}$), indicating its crystalline nature.

Figure 9: Shows the correlations of isomer shifts versus quadrupole splittings of the various reaction products. They have been plotted using the cation labels given to them in Tables 3 and 4 (i.e. h.s. Fe^{2+} or s.p. Fe^{3+}) and have then been grouped according to their composition based on their Mössbauer parameters and labelled thus. The plot shows quite well the division of the reaction products into distinct phases.

Figure 1: Reflectance spectra of Mars

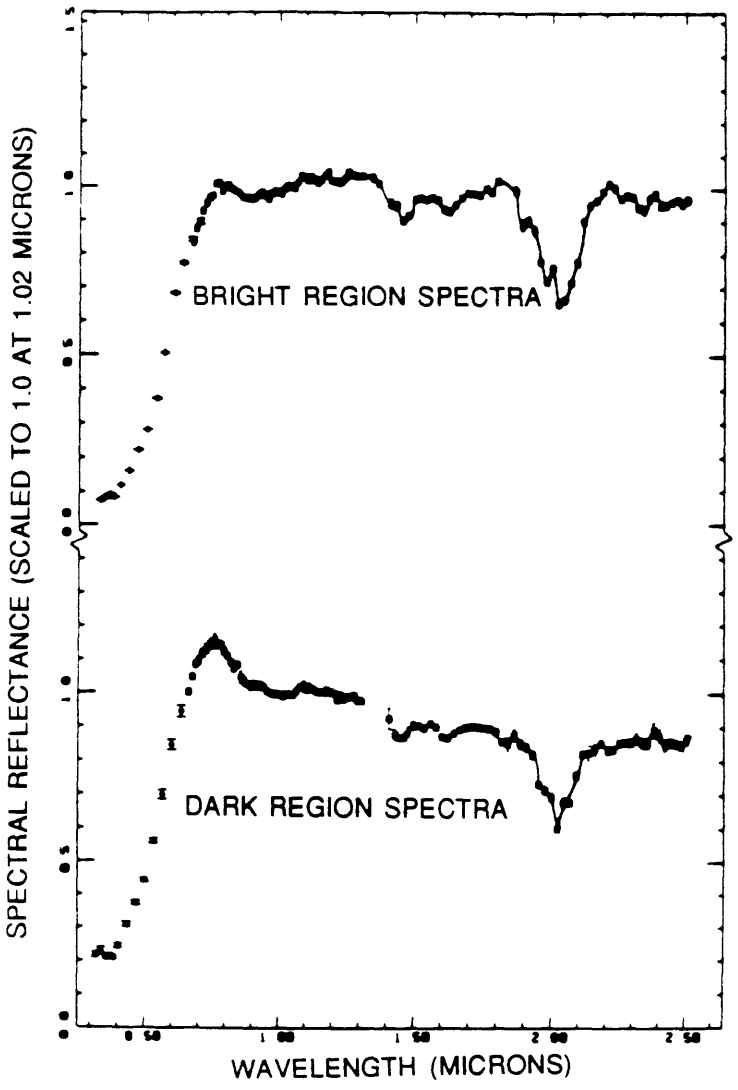

Figure 2a: T2N60 (13P/32C)

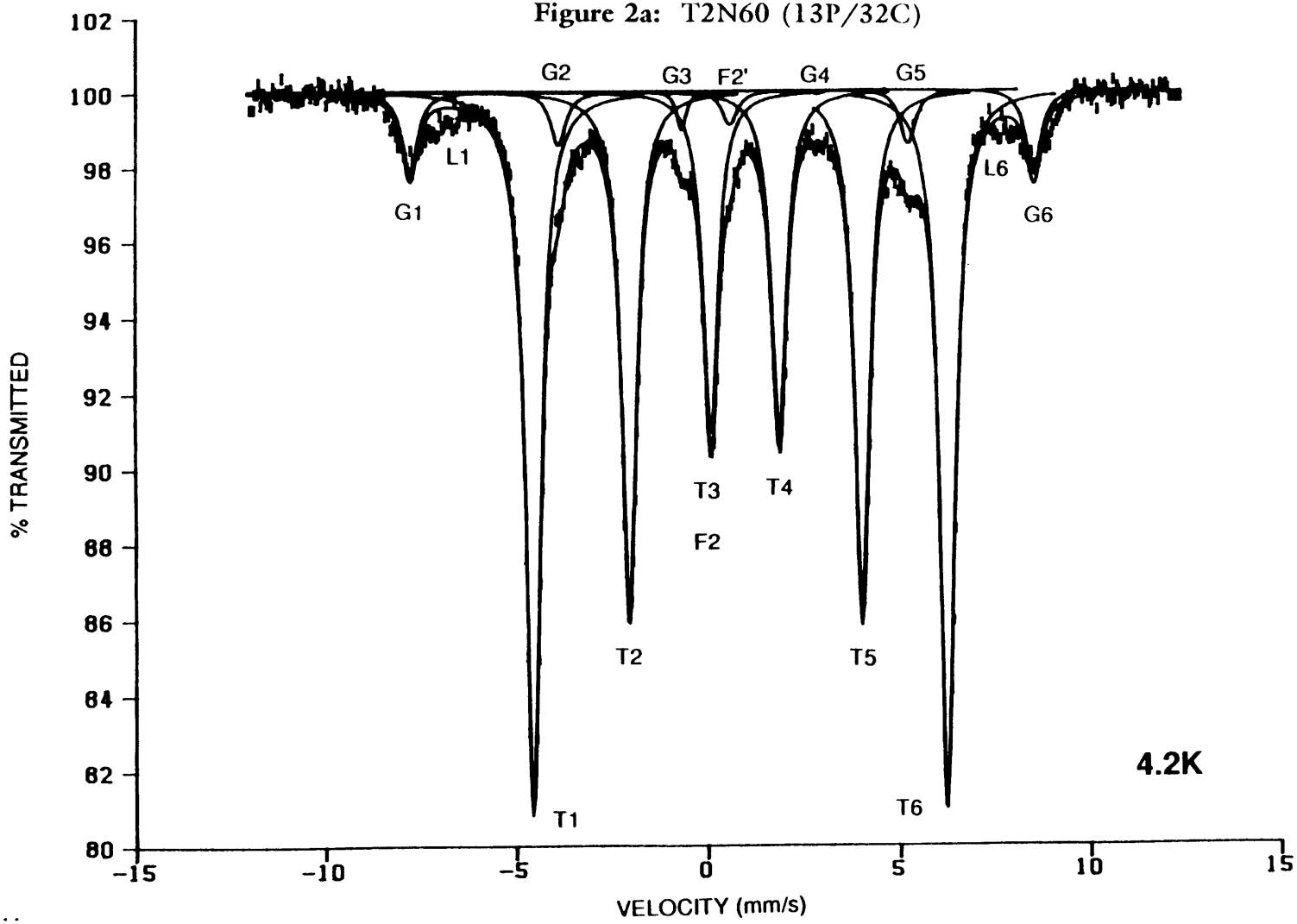

Figure 2b: T2F60 (13P/33C)

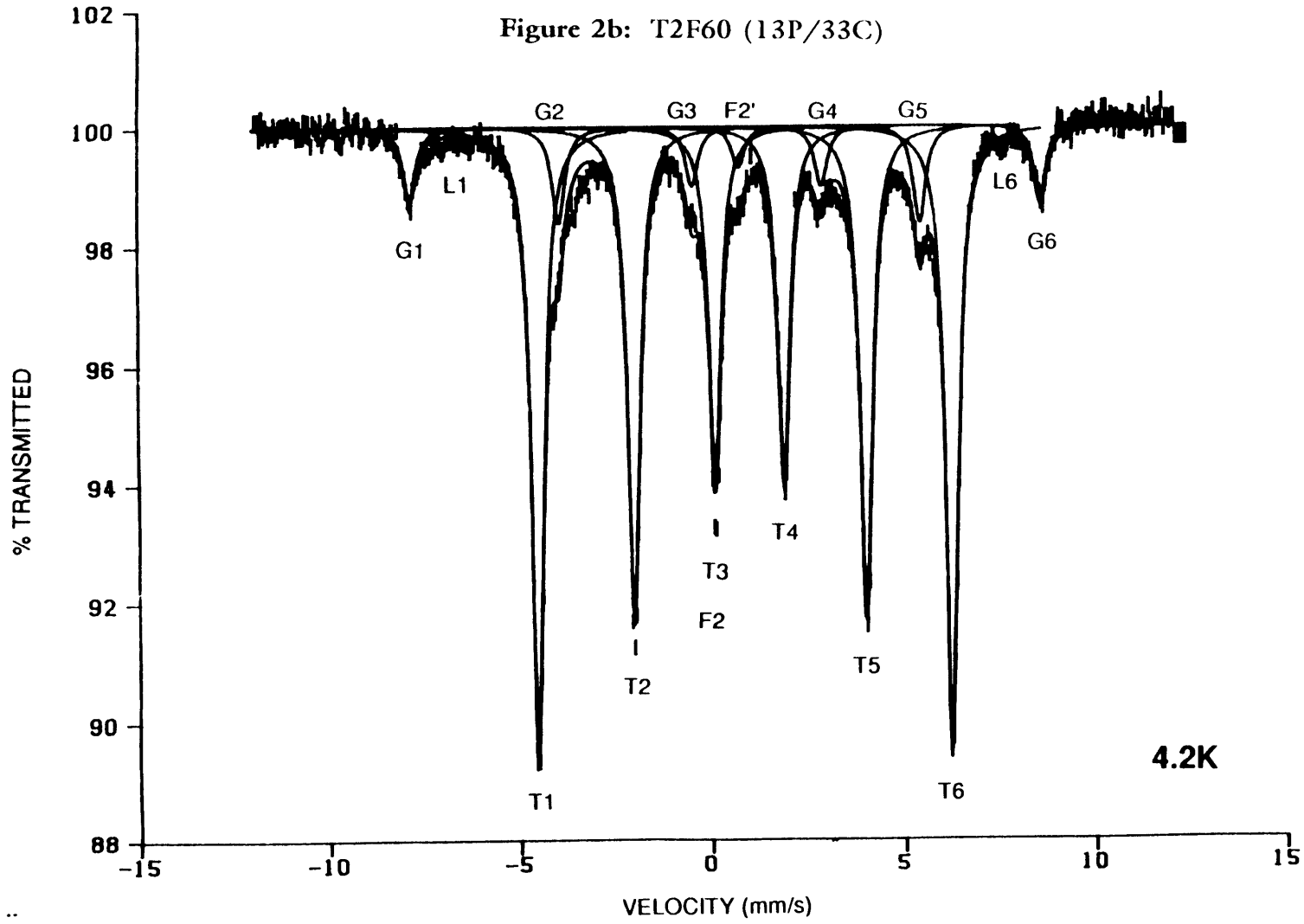

Figure 2c: T2N80 (13P/34C)

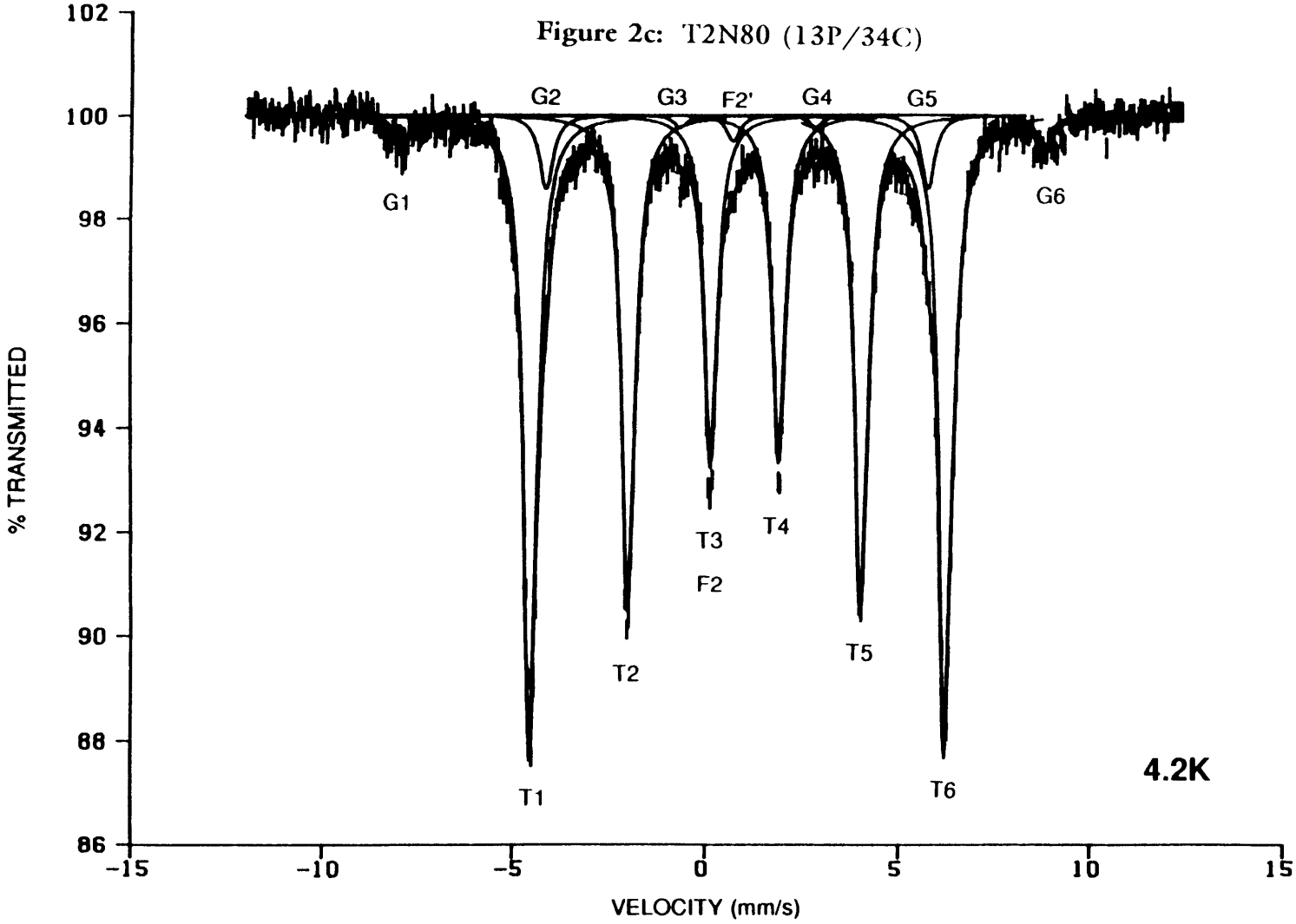

Figure 2d: T2F80 (13P/34C)

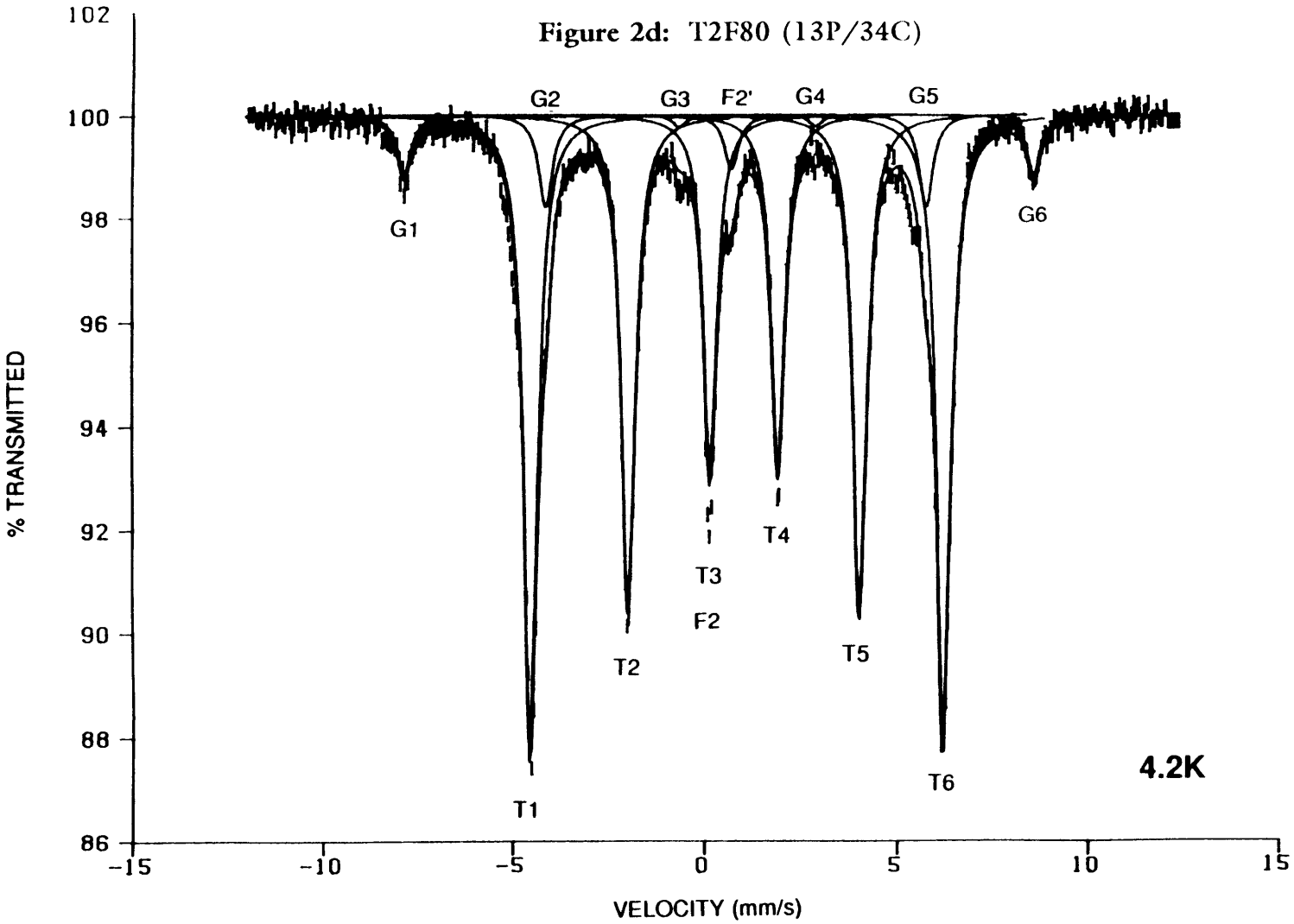

Figure 2e: T4N60 (13P/34C)

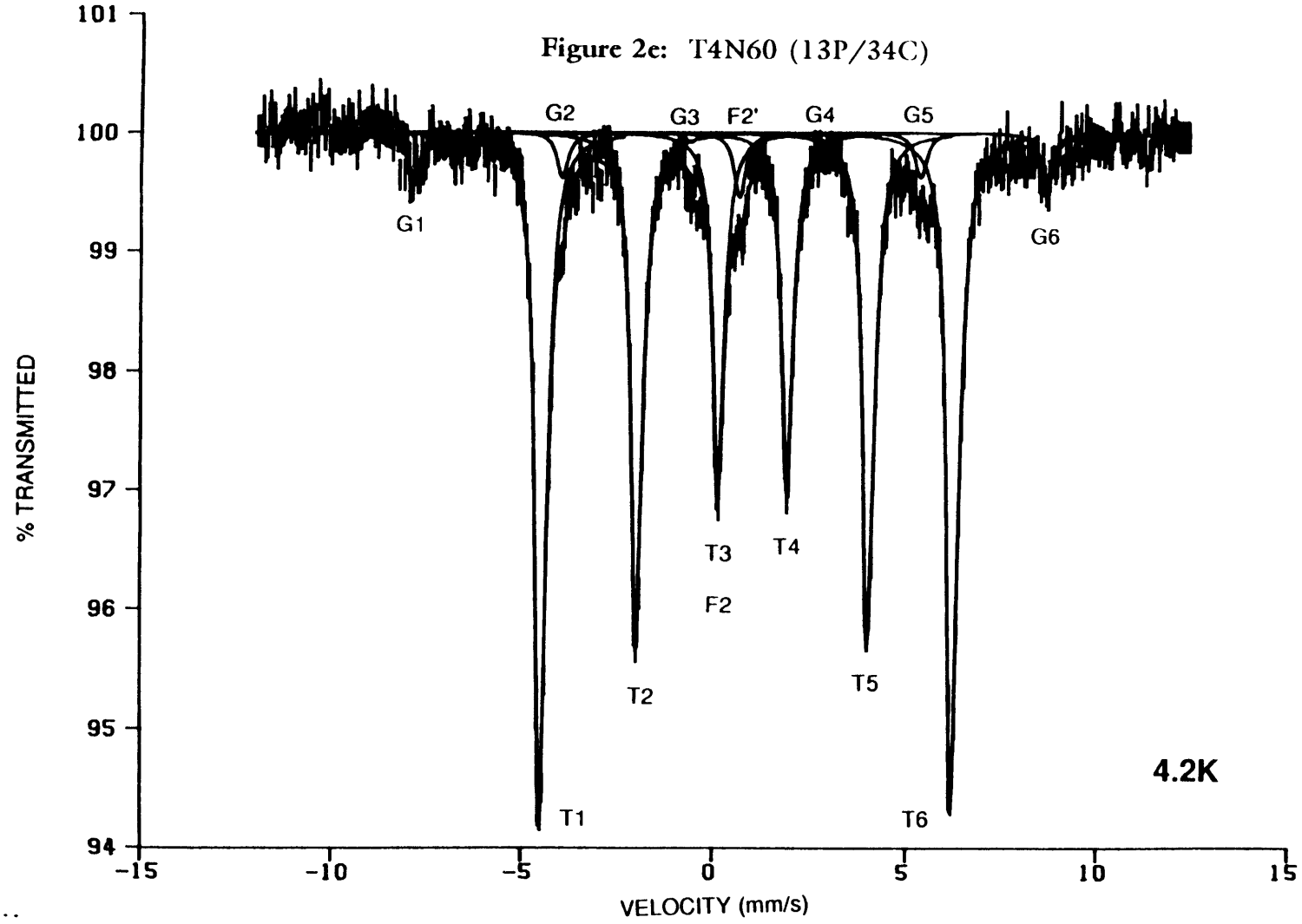

Figure 2f: T4F60 (13P/34C)

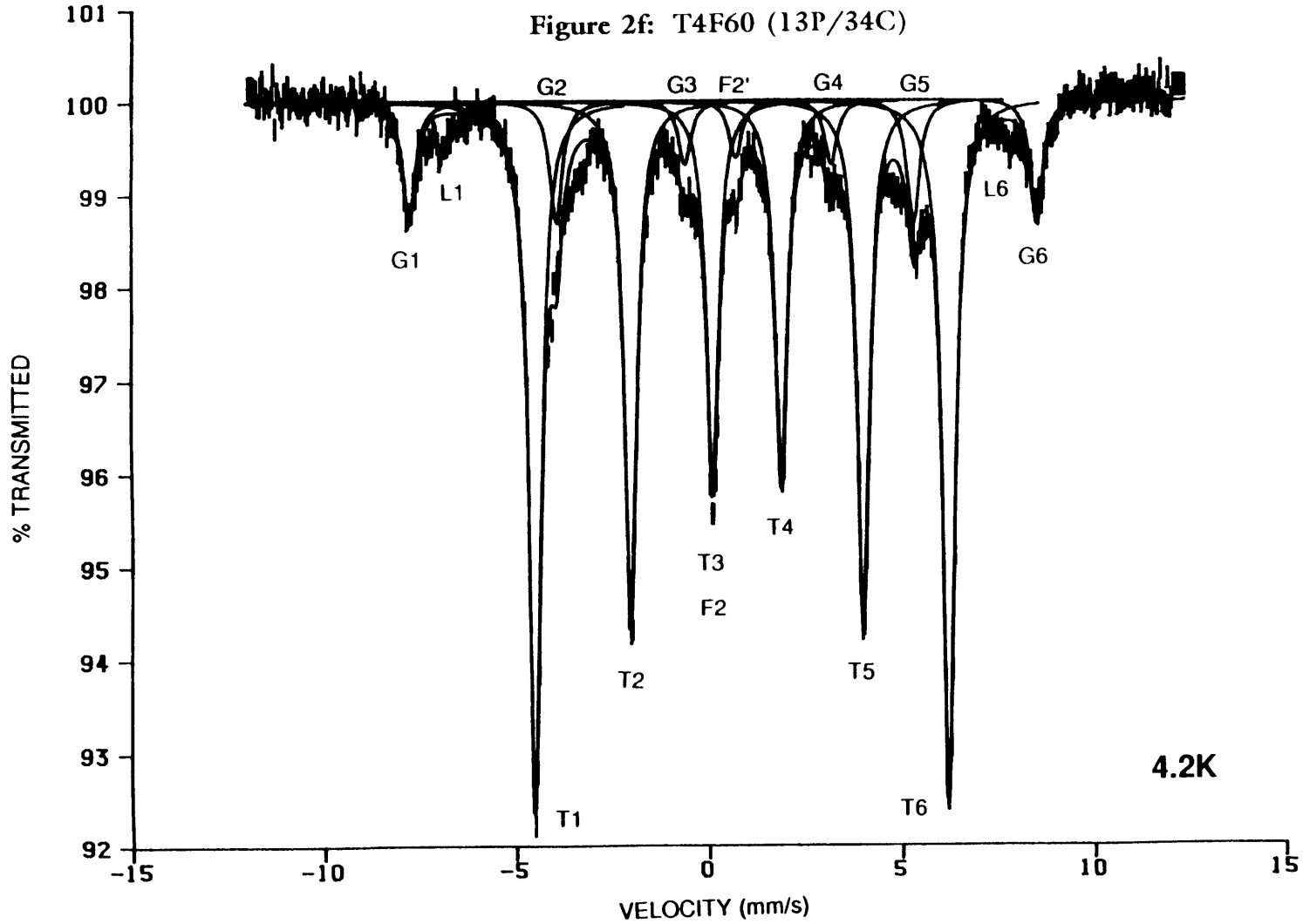

Figure 3a: P2N60 (7P/18C)

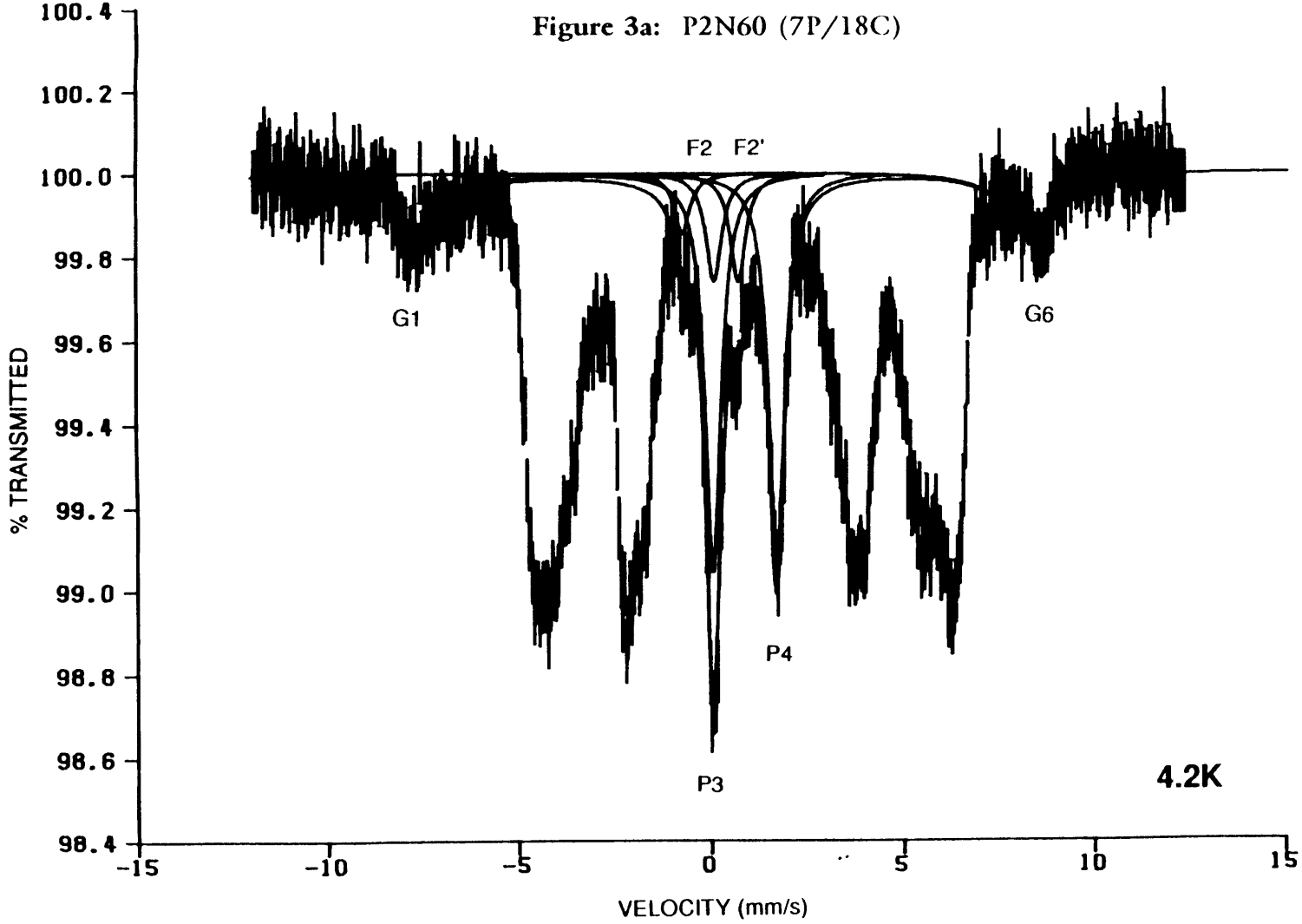

Figure 3b: P2F60 (9P/23C)

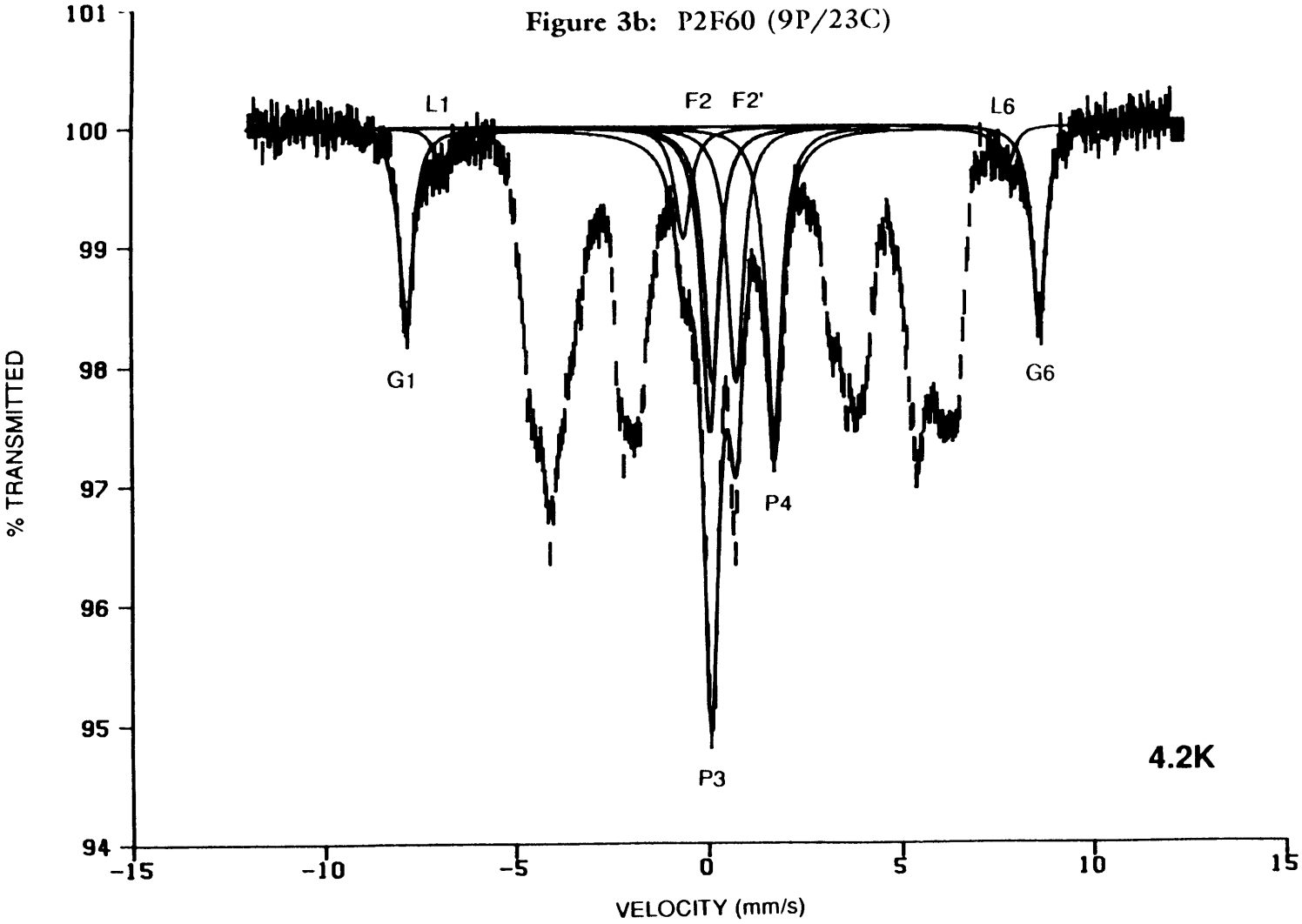

Figure 3c: P2N80 (9P/23C)

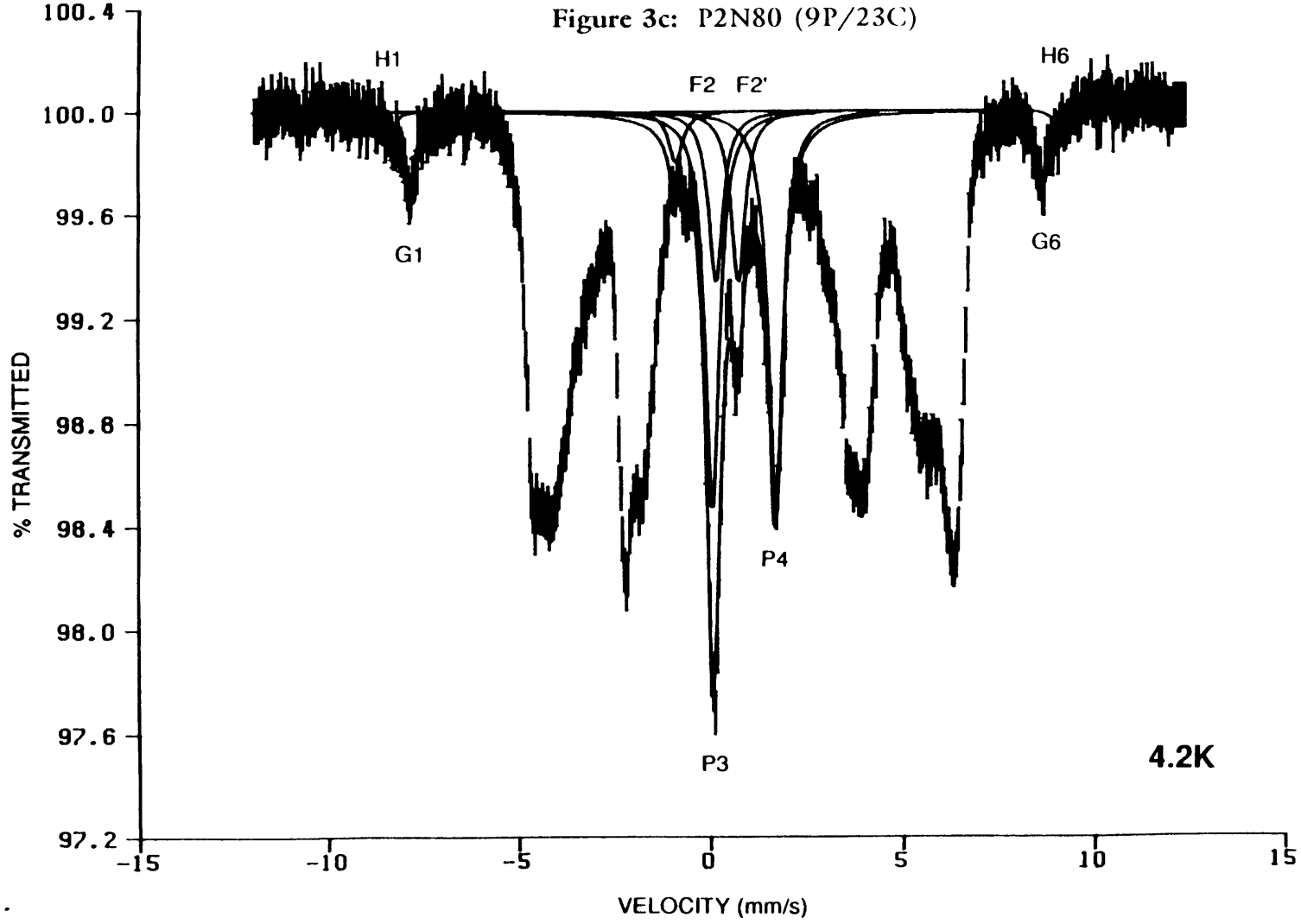

Figure 3d: P2F80 (7P/19C)

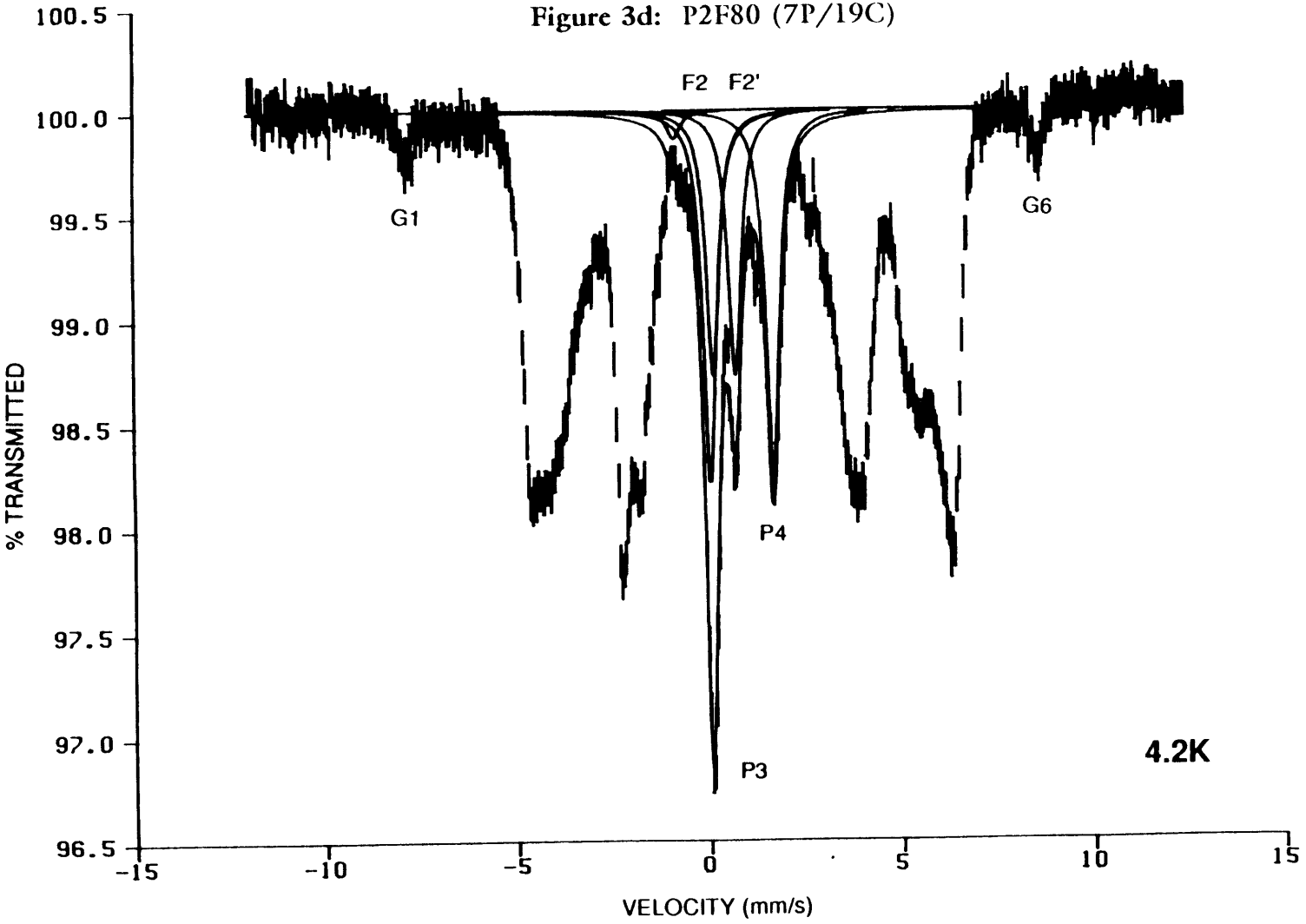

Figure 3e: P4N60 (9P/23C)

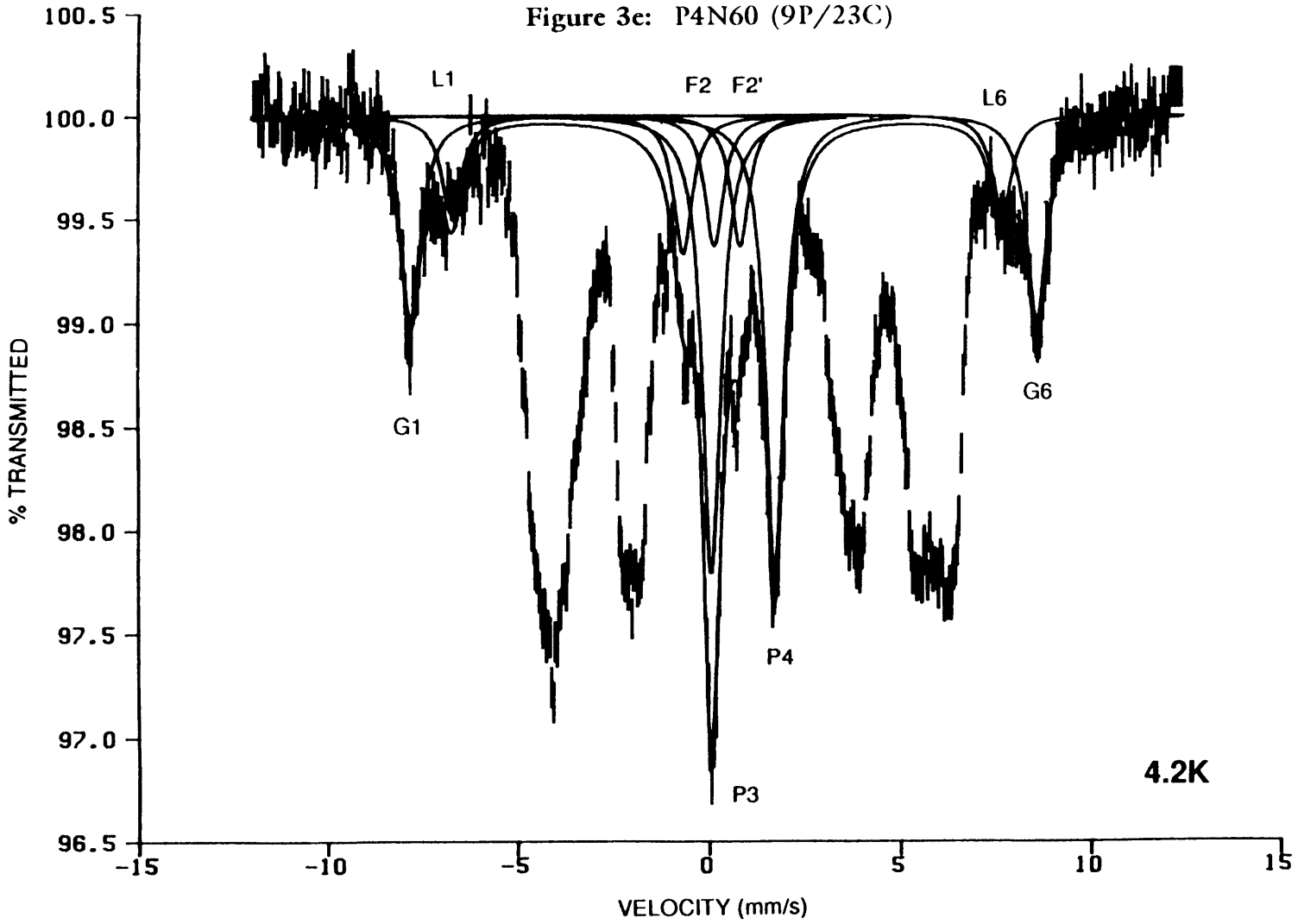

Figure 3f: P4F60 (9P/23C)

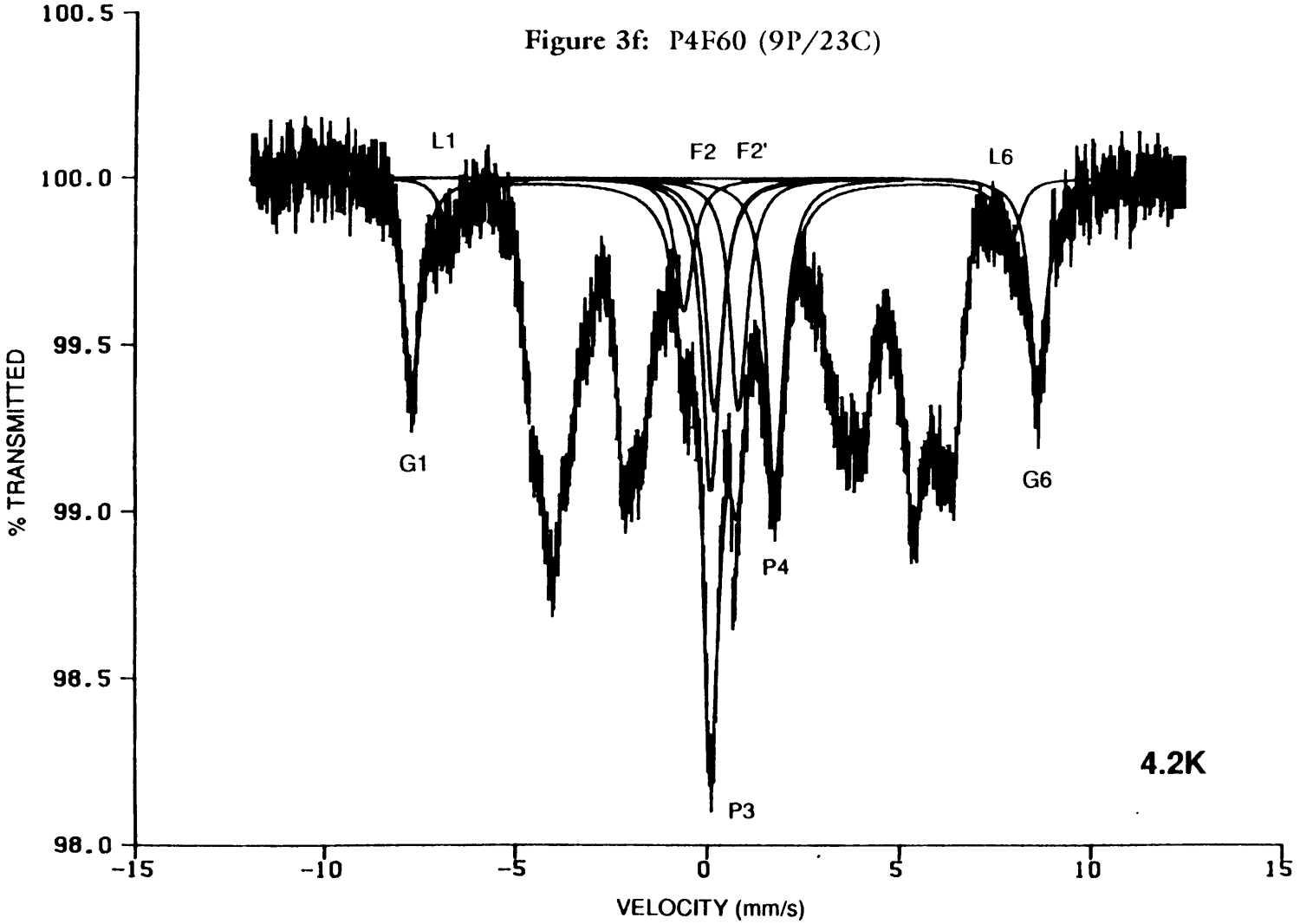

Figure 4a: T2N60 (6P/14C)

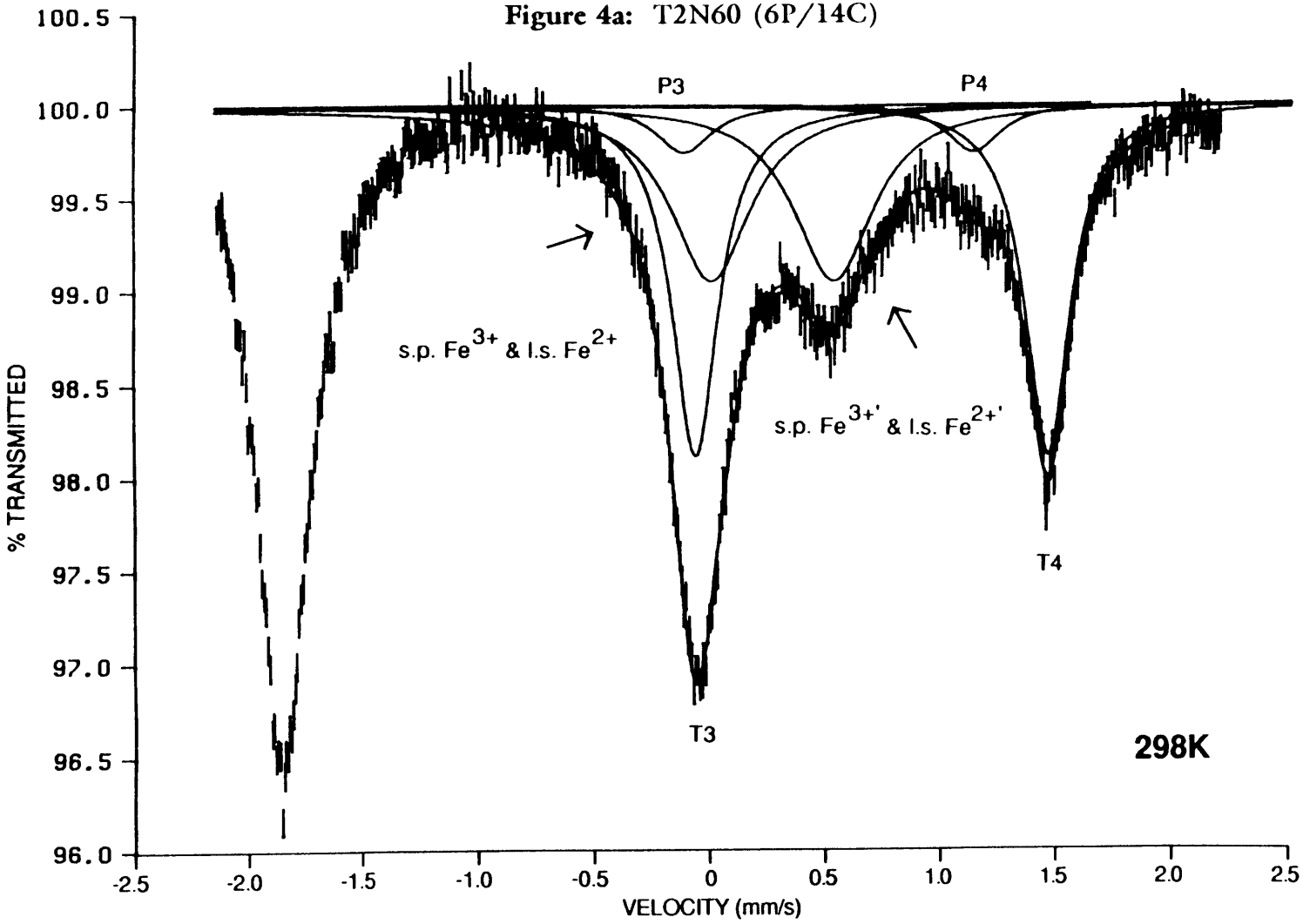

Figure 4b: T2F60 (6P/16C)

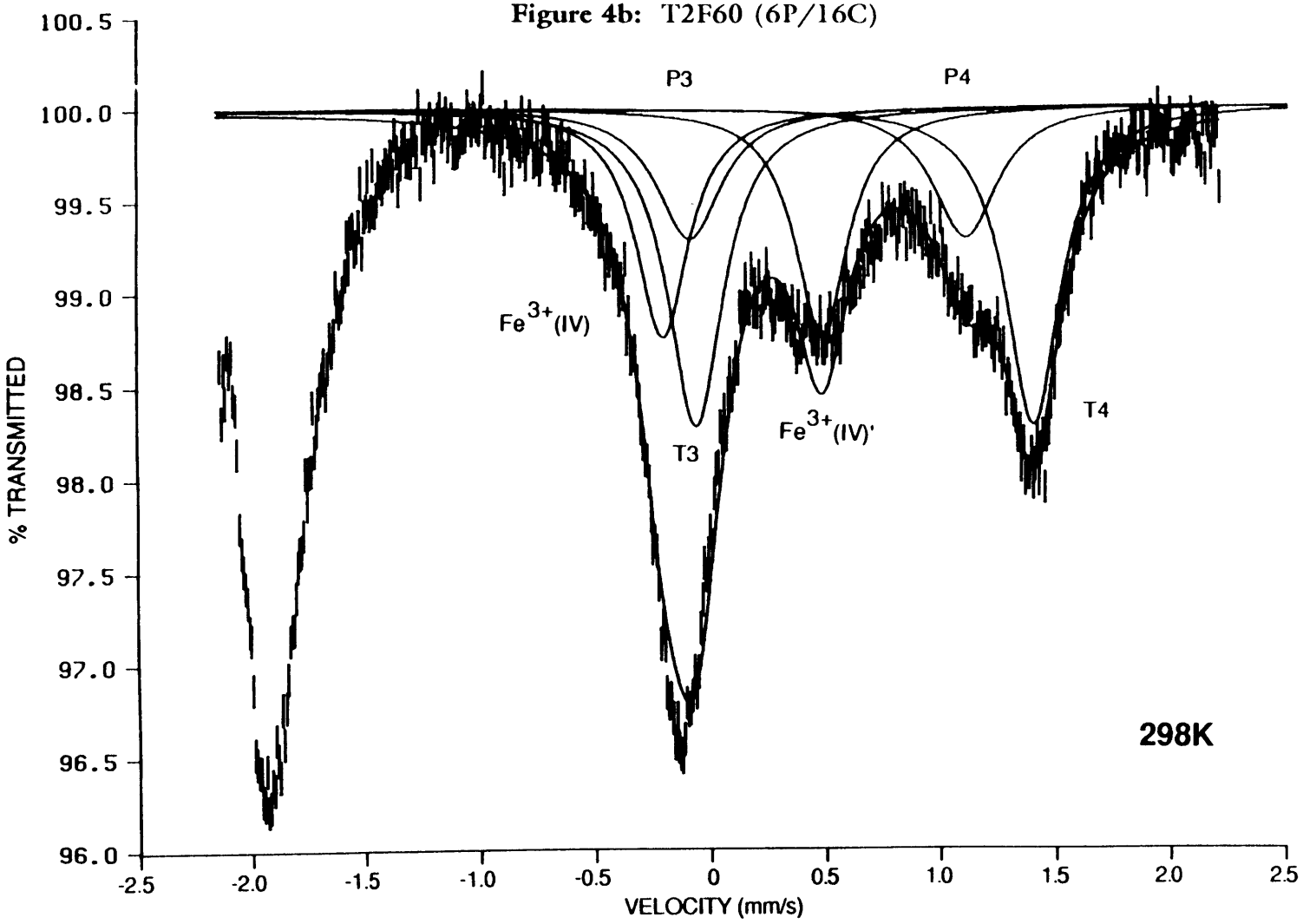

Figure 4c: T2N80 (6P/16C)

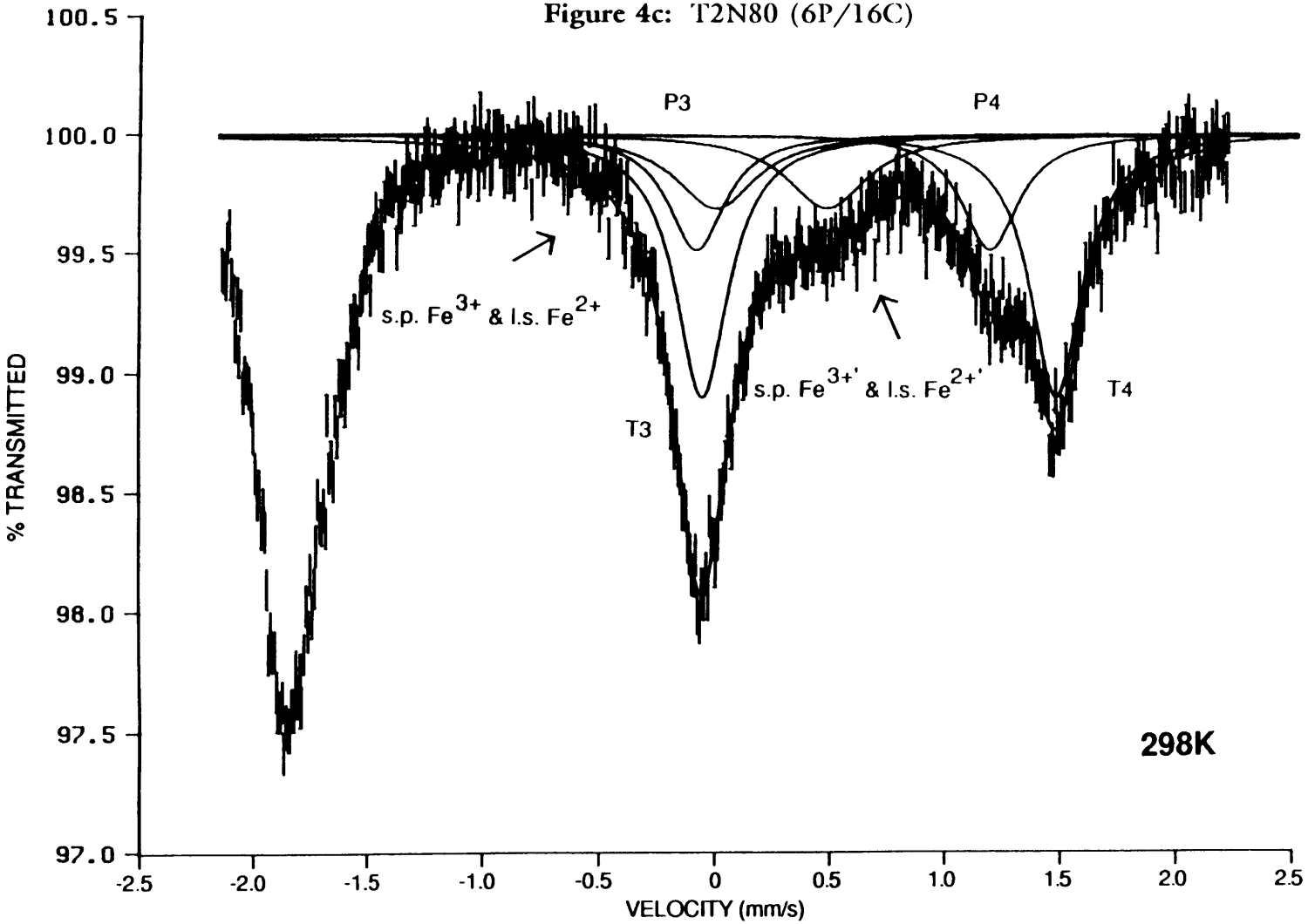

Figure 4d: T2F80 (6P/16C)

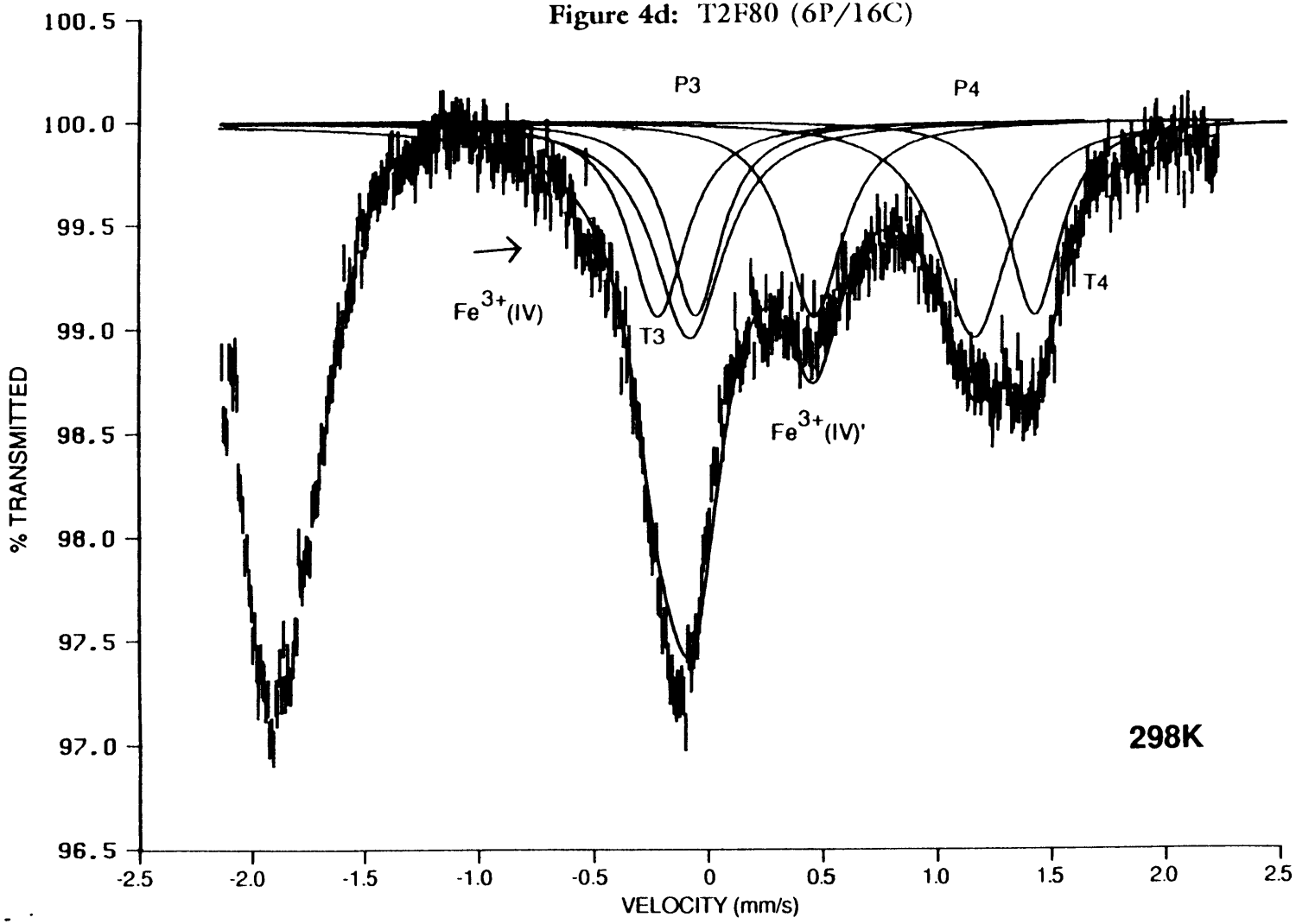

Figure 4e: T4N60 (4P/10C)

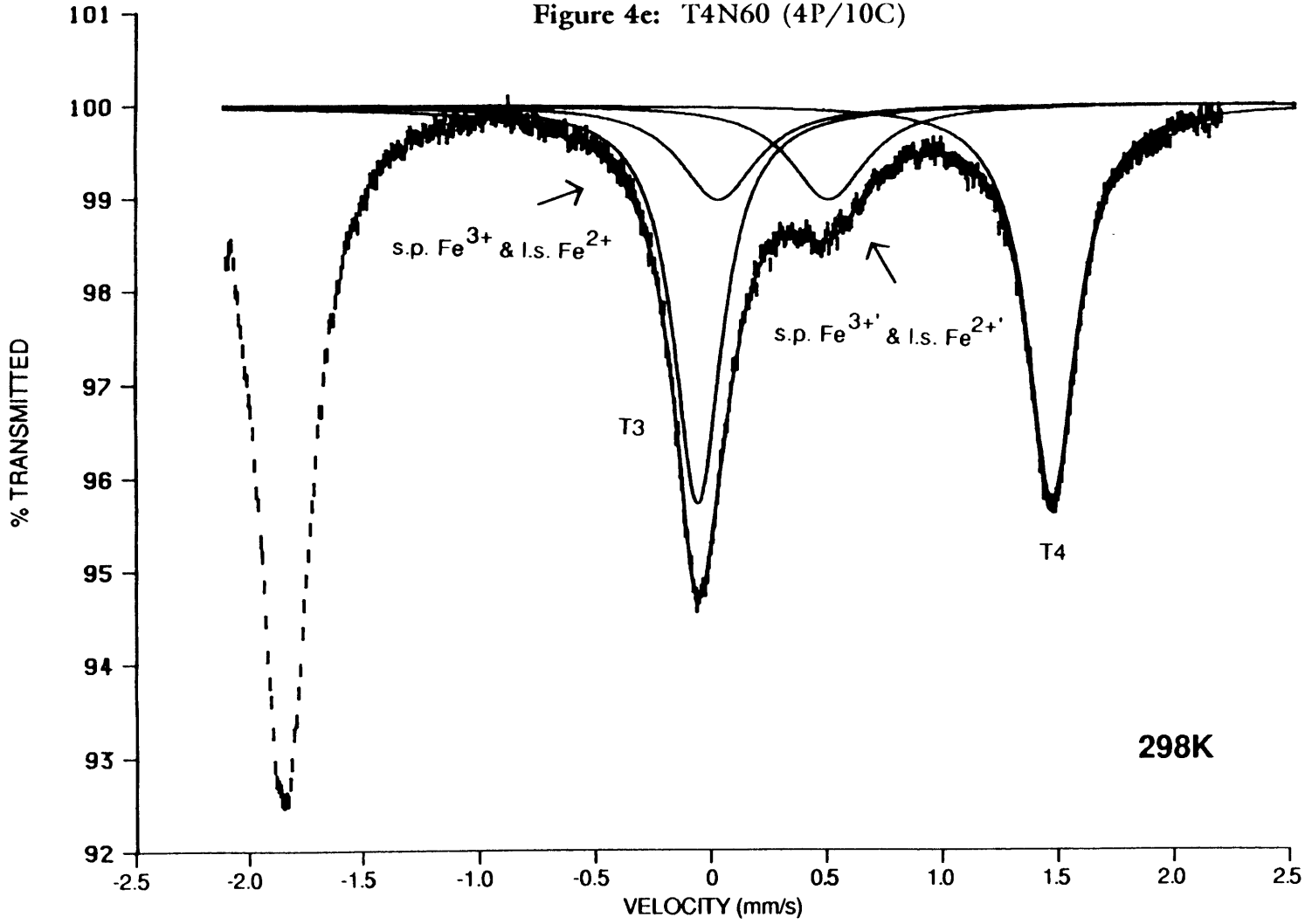

Figure 4f: T4F60 (6P/16C)

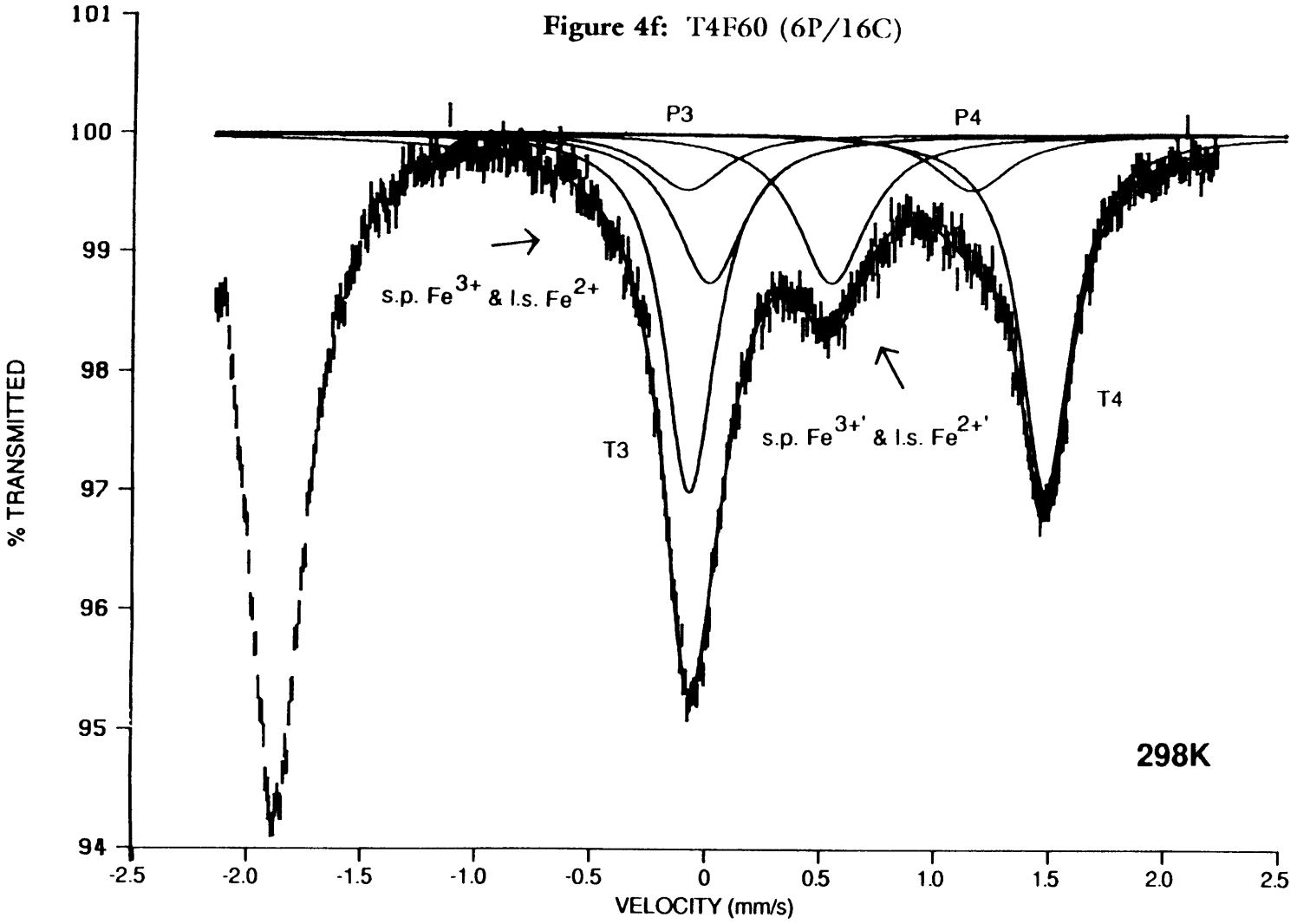

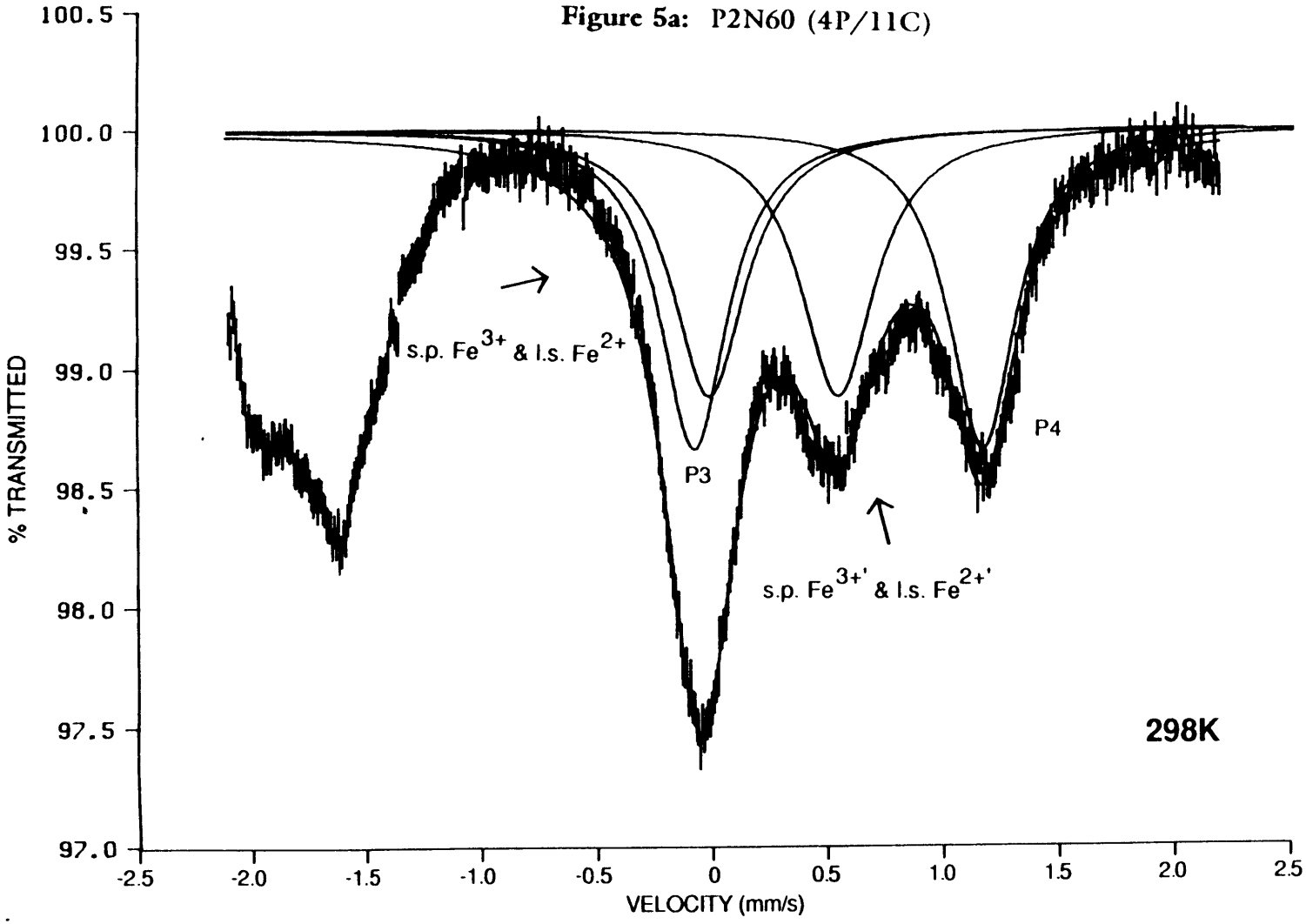

Figure 5a: P2N60 (4P/11C)

Figure 5b: P2F60 (6P/15C)

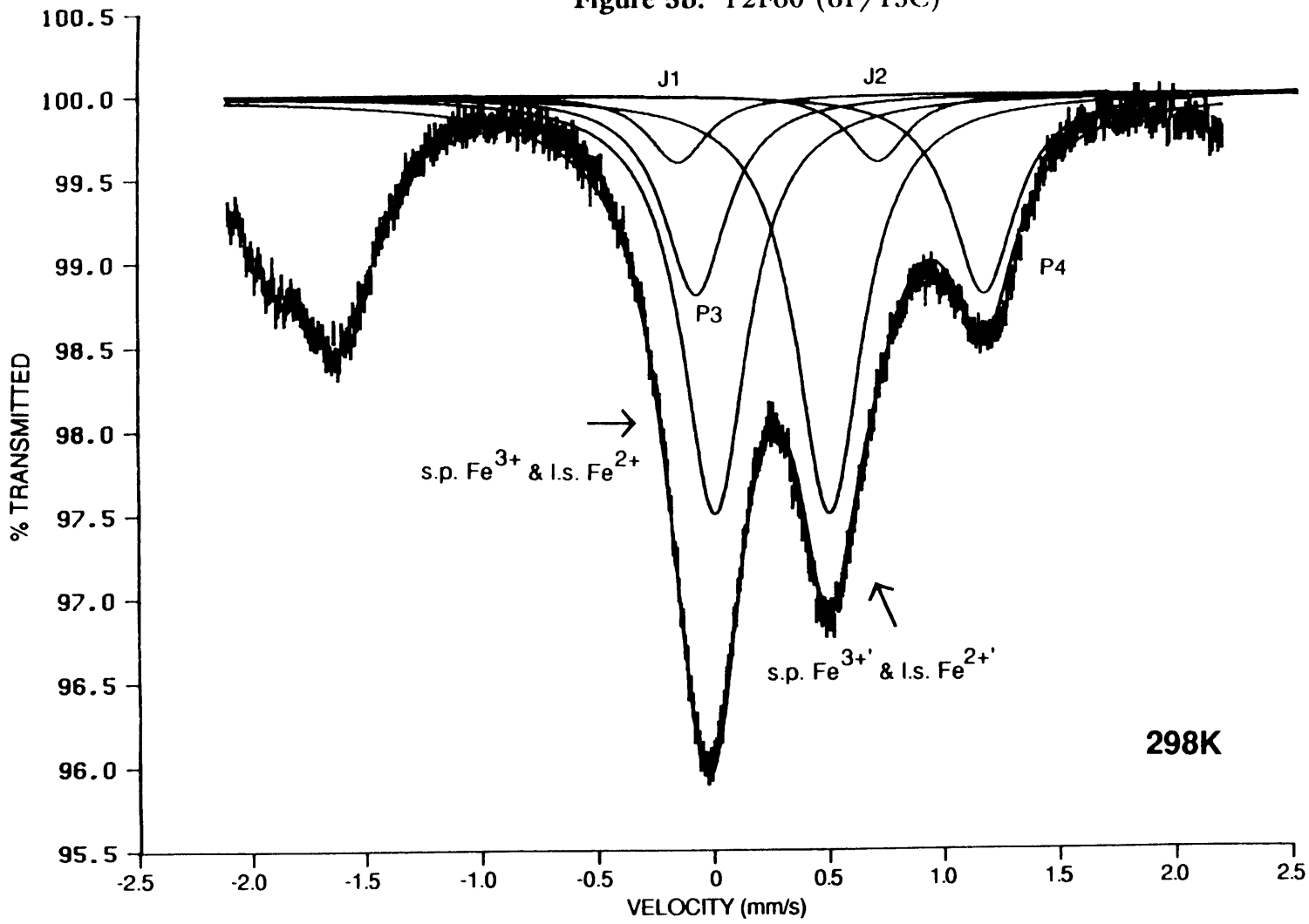

Figure 5c: P2N80 (4P/11C)

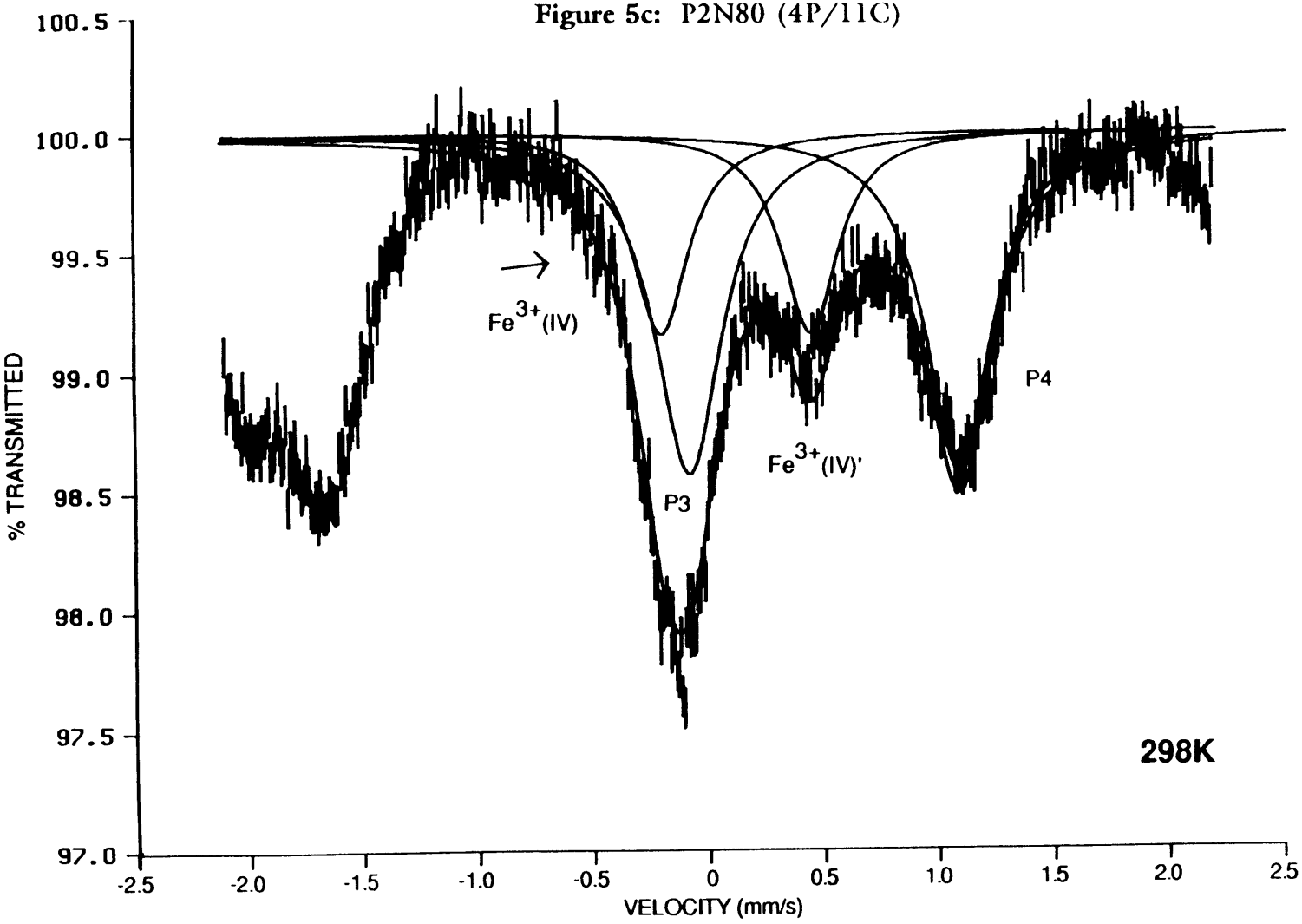

Figure 5d: P2F80 (4P/11C)

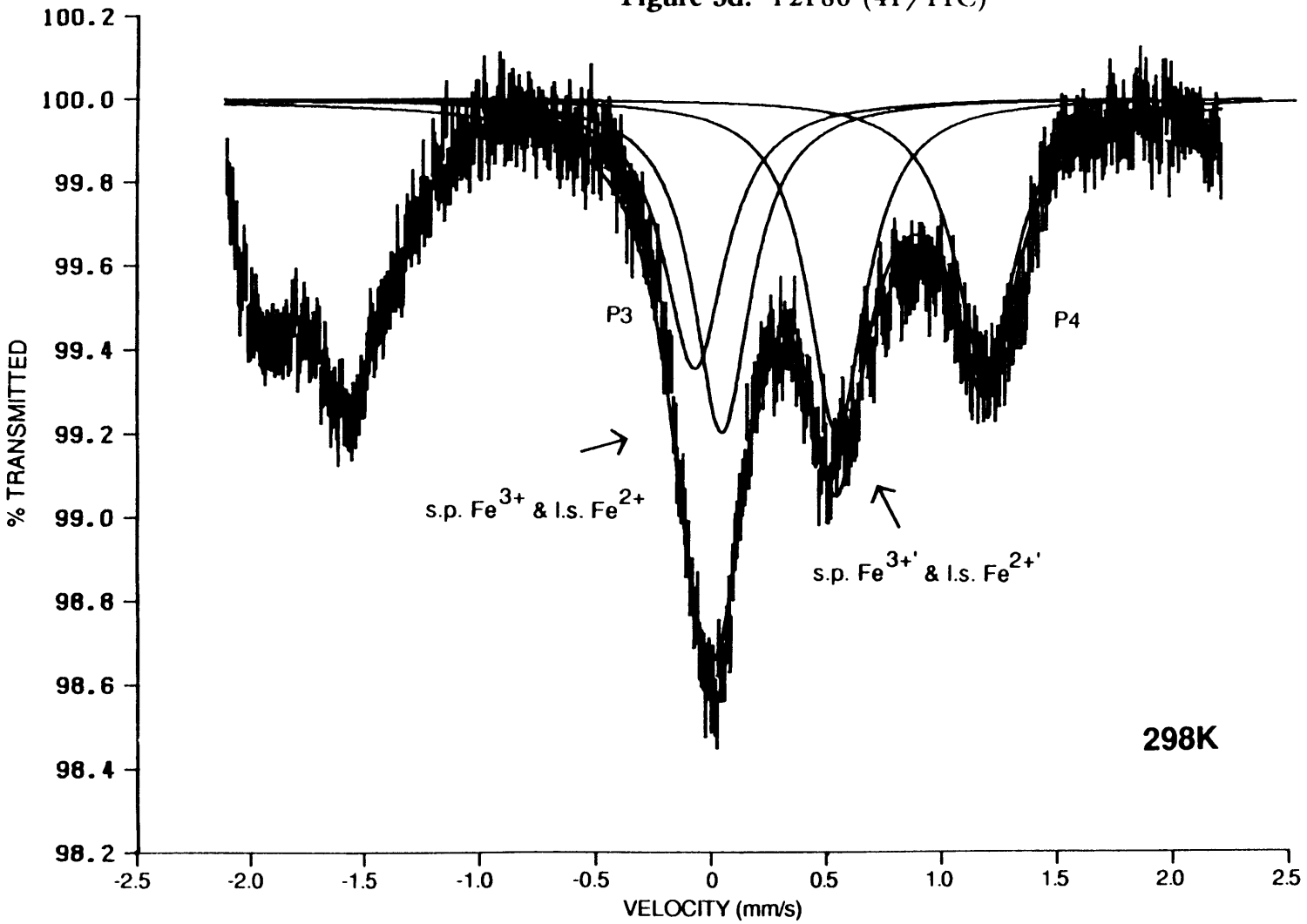

Figure 5e: P4N60 (6P/17C)

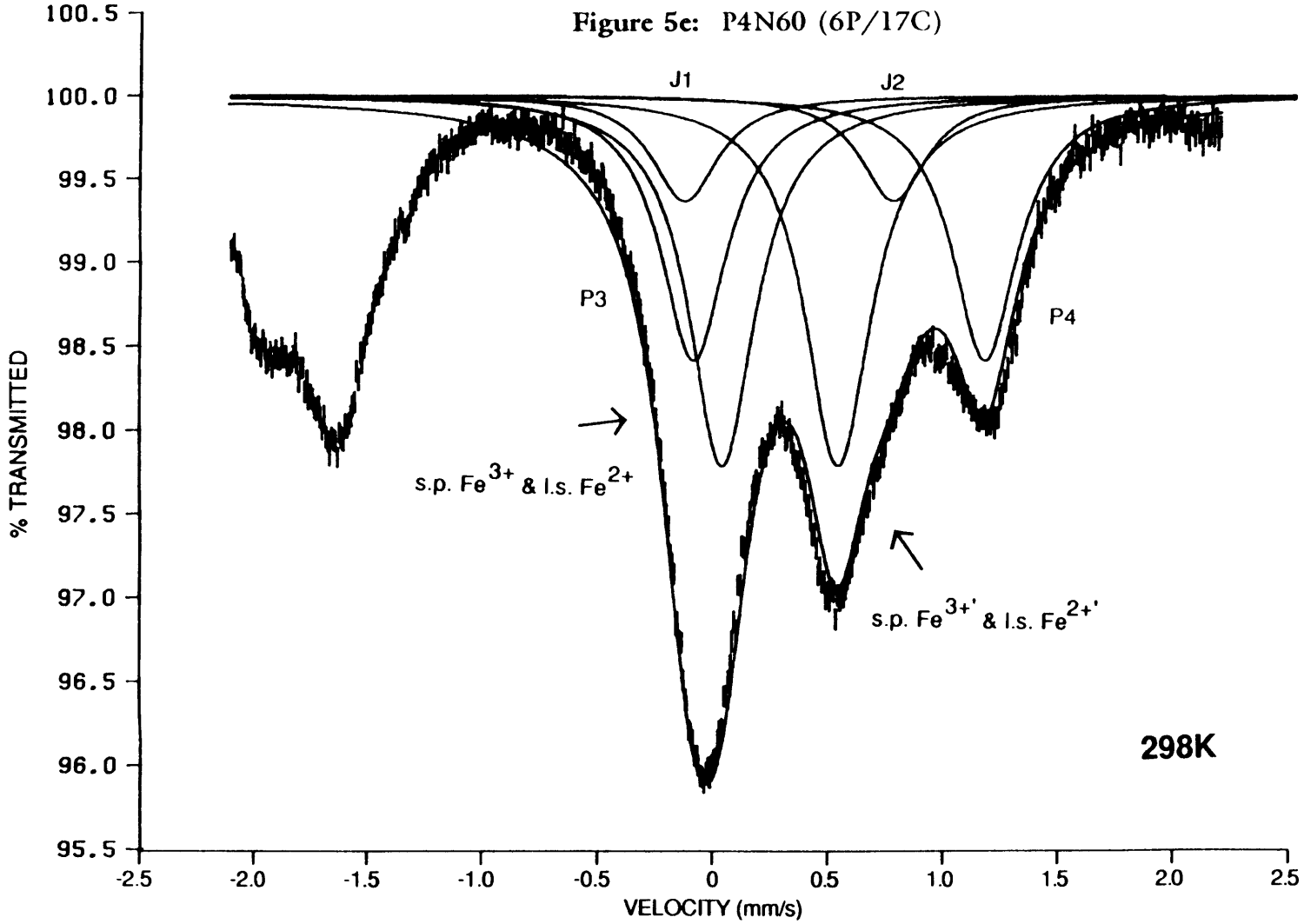

Figure 5f: P4F60 (6P/16C)

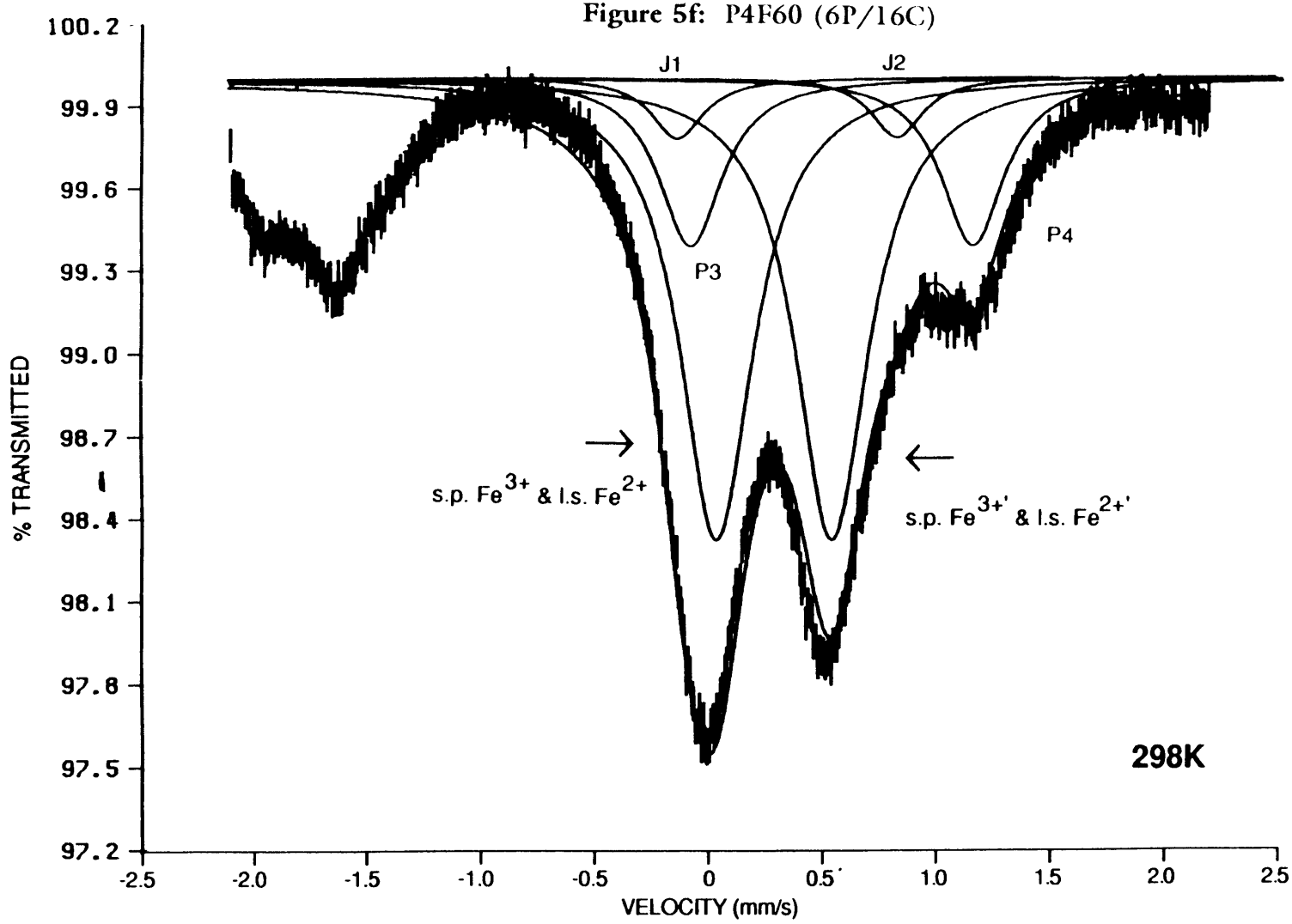

Figure 6a: S2N80 (10P/22C)

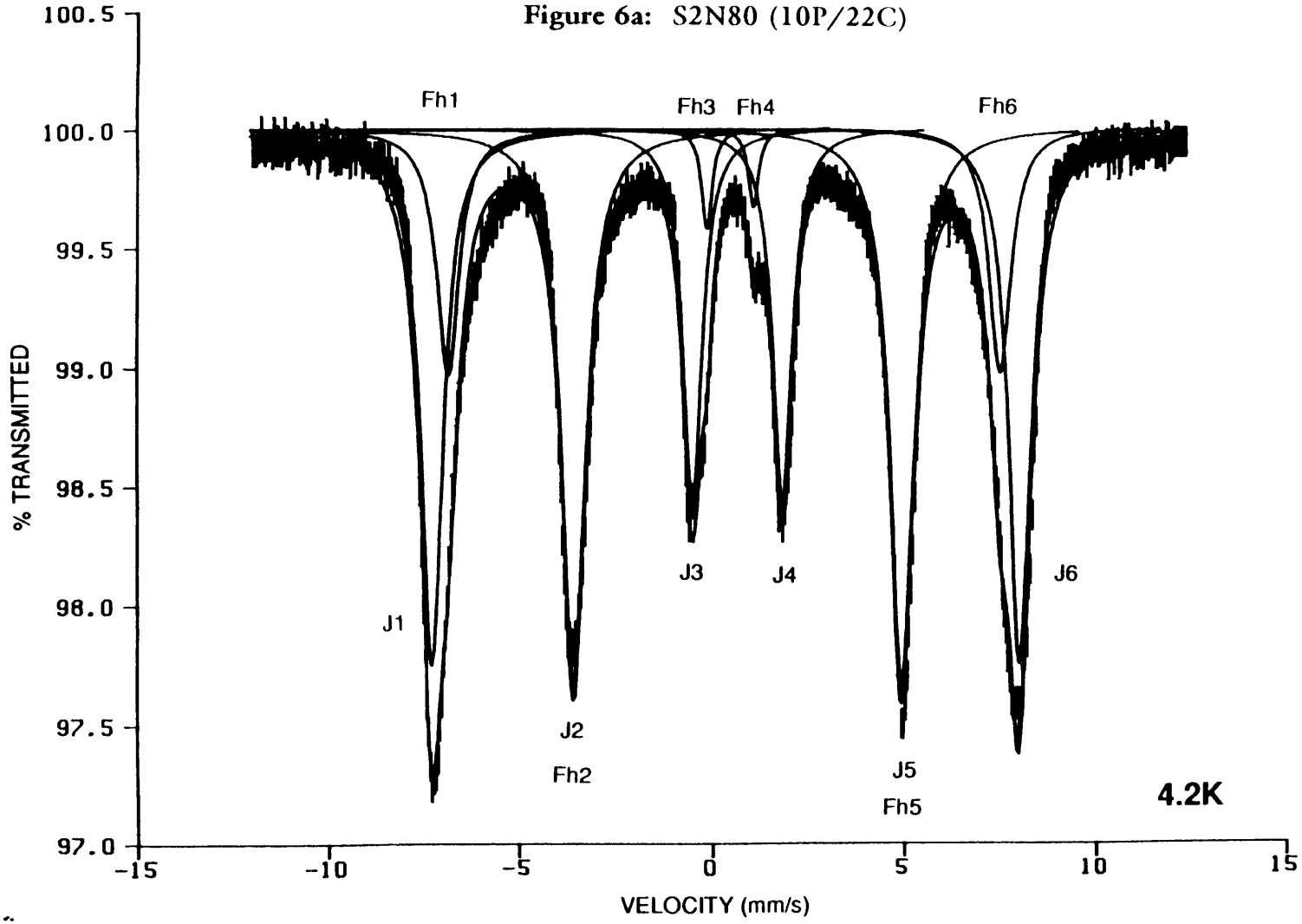

Figure 6b: S2N60 (unfitted)

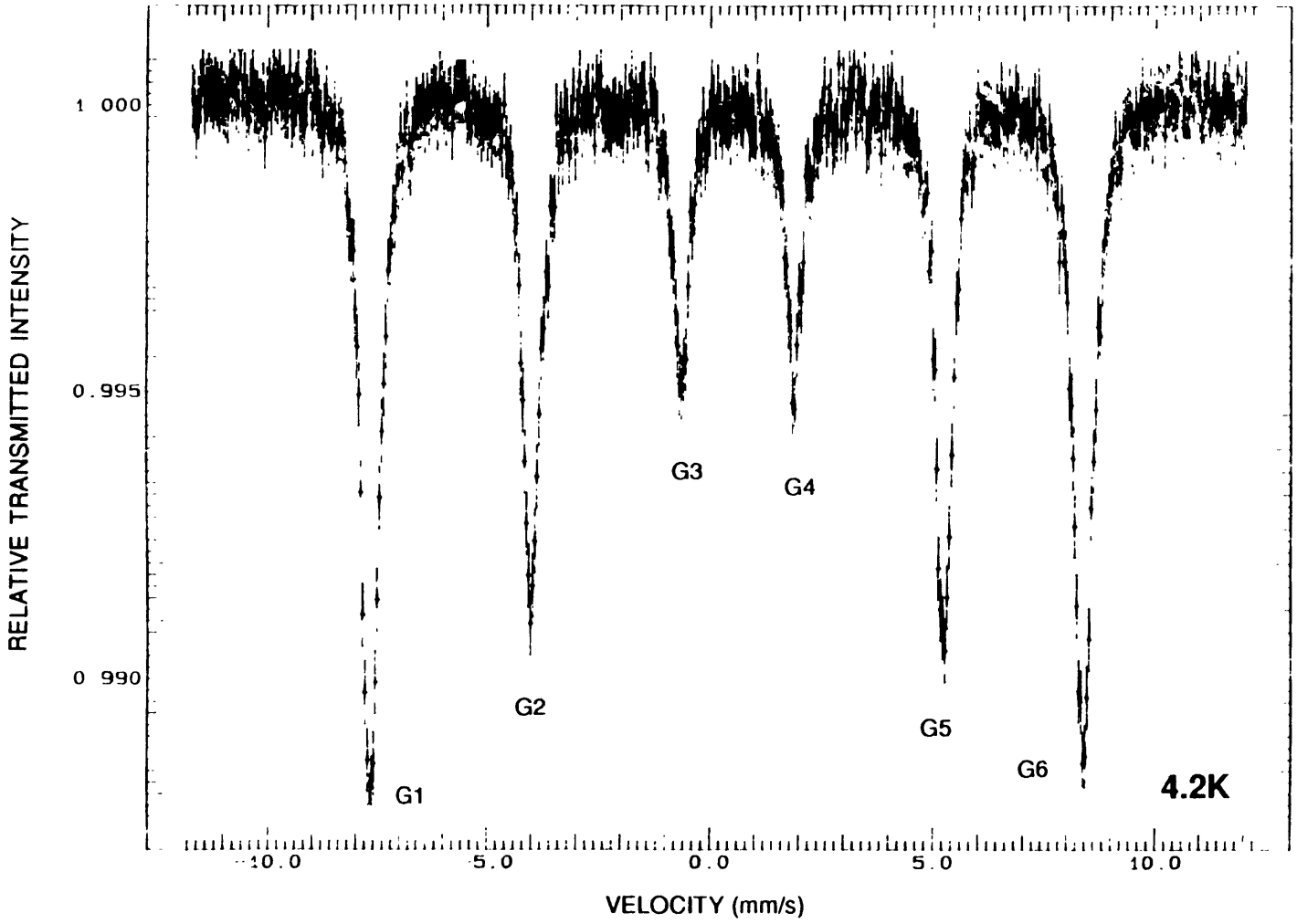

Figure 6c: S2K80 (6P/8C)

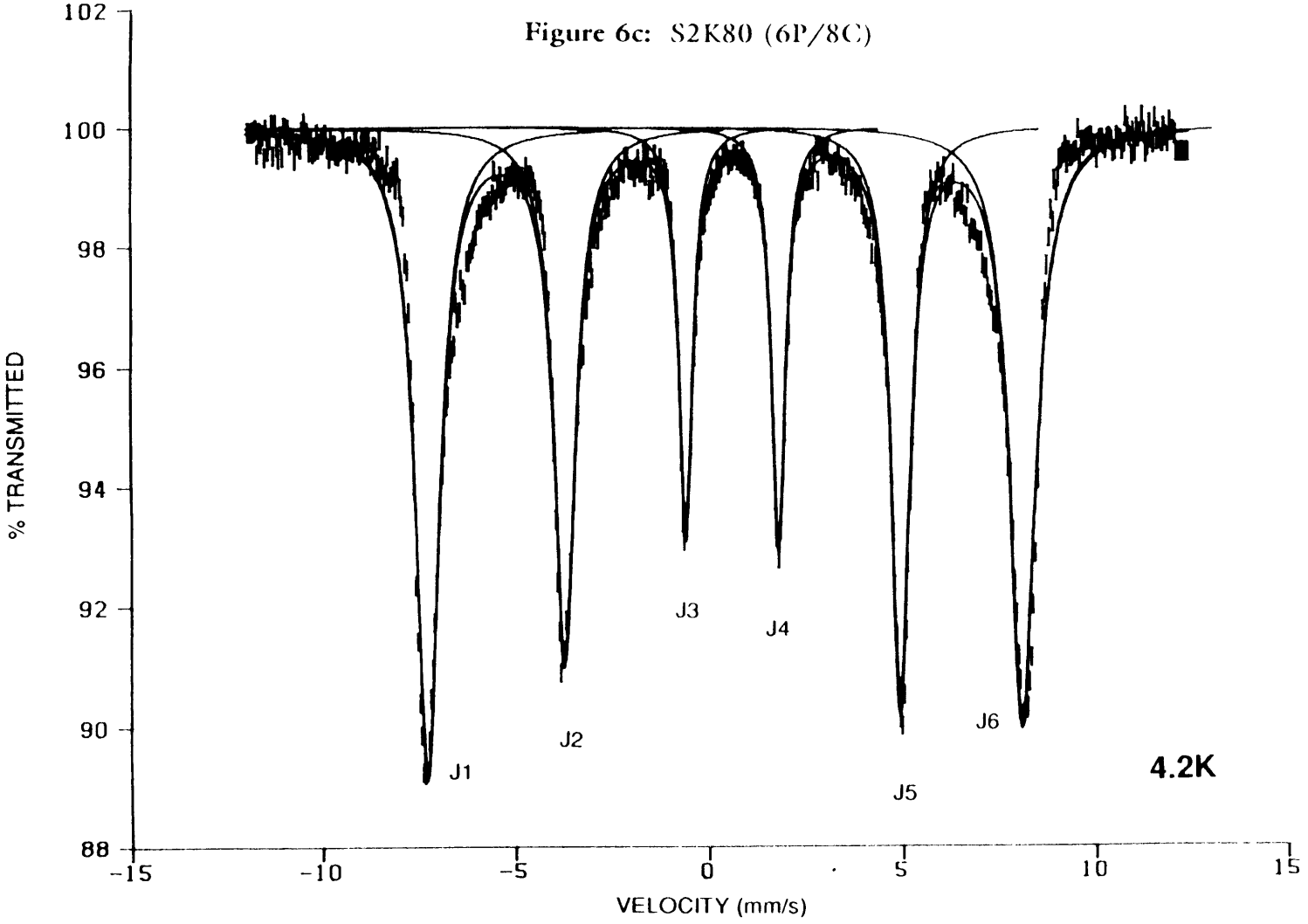

Figure 6d: S7N80 (6P/8C)

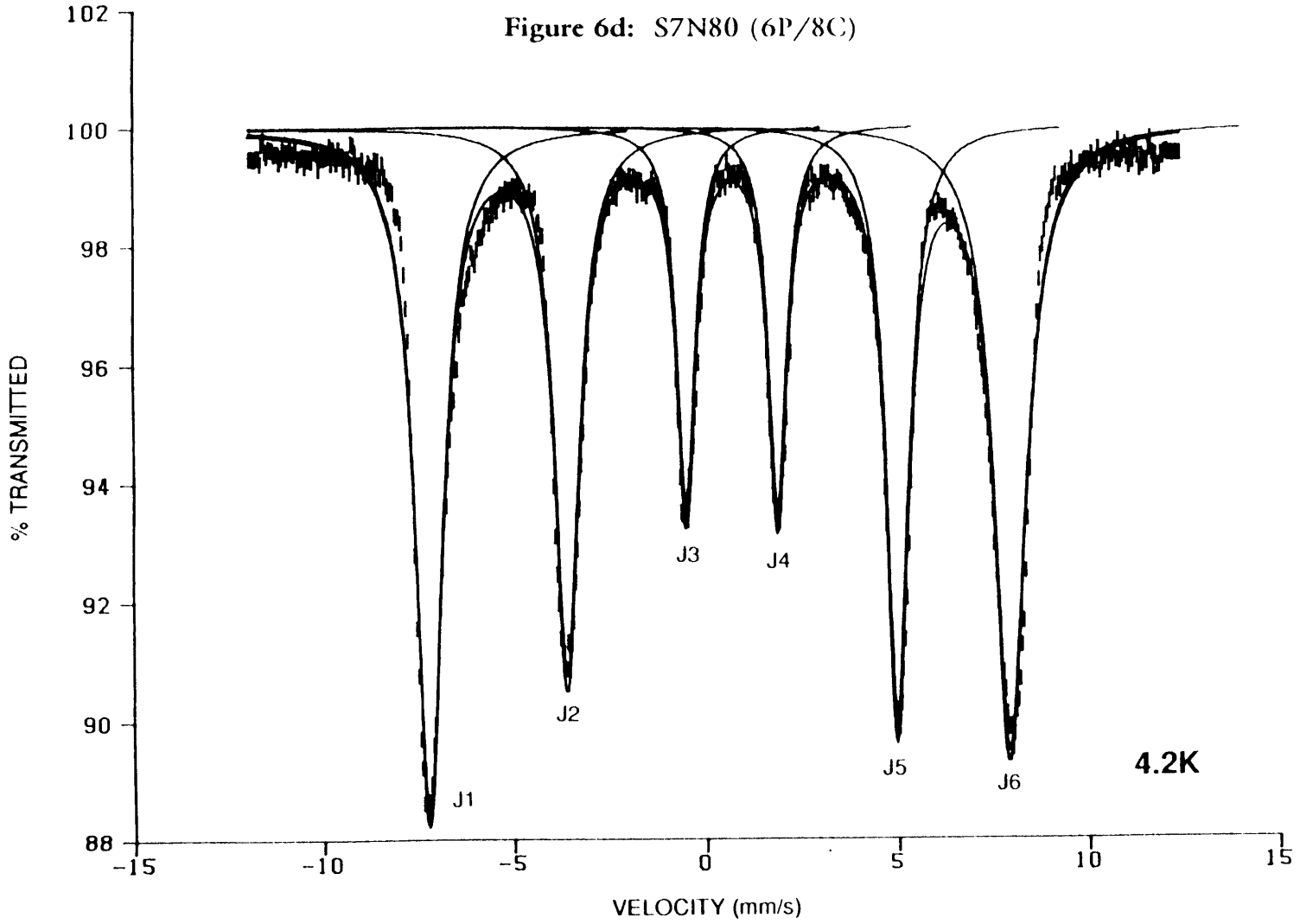

Figure 7a: S2N80 (2P/4C)

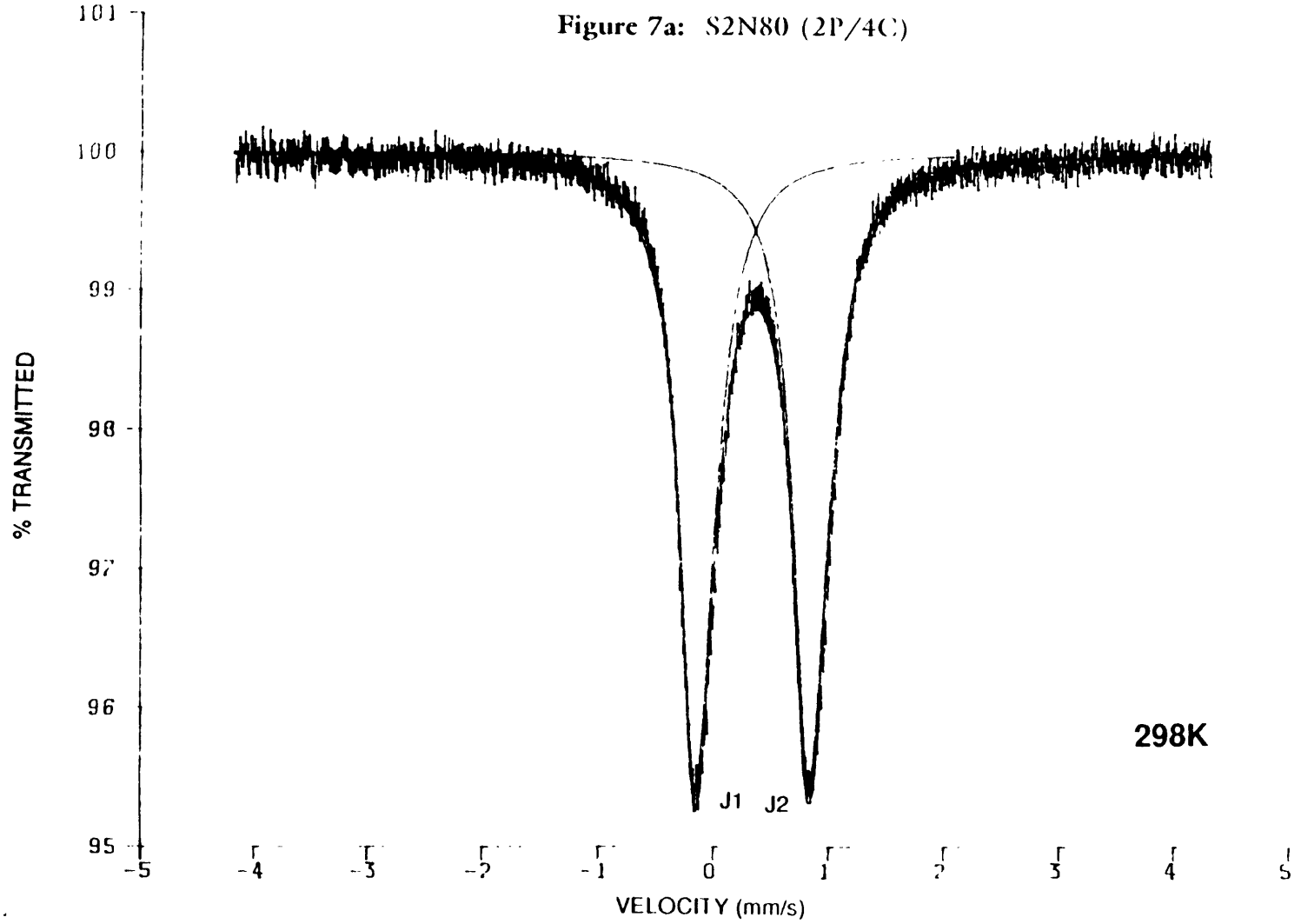

Figure 7b: S2N60 (2P/4C)

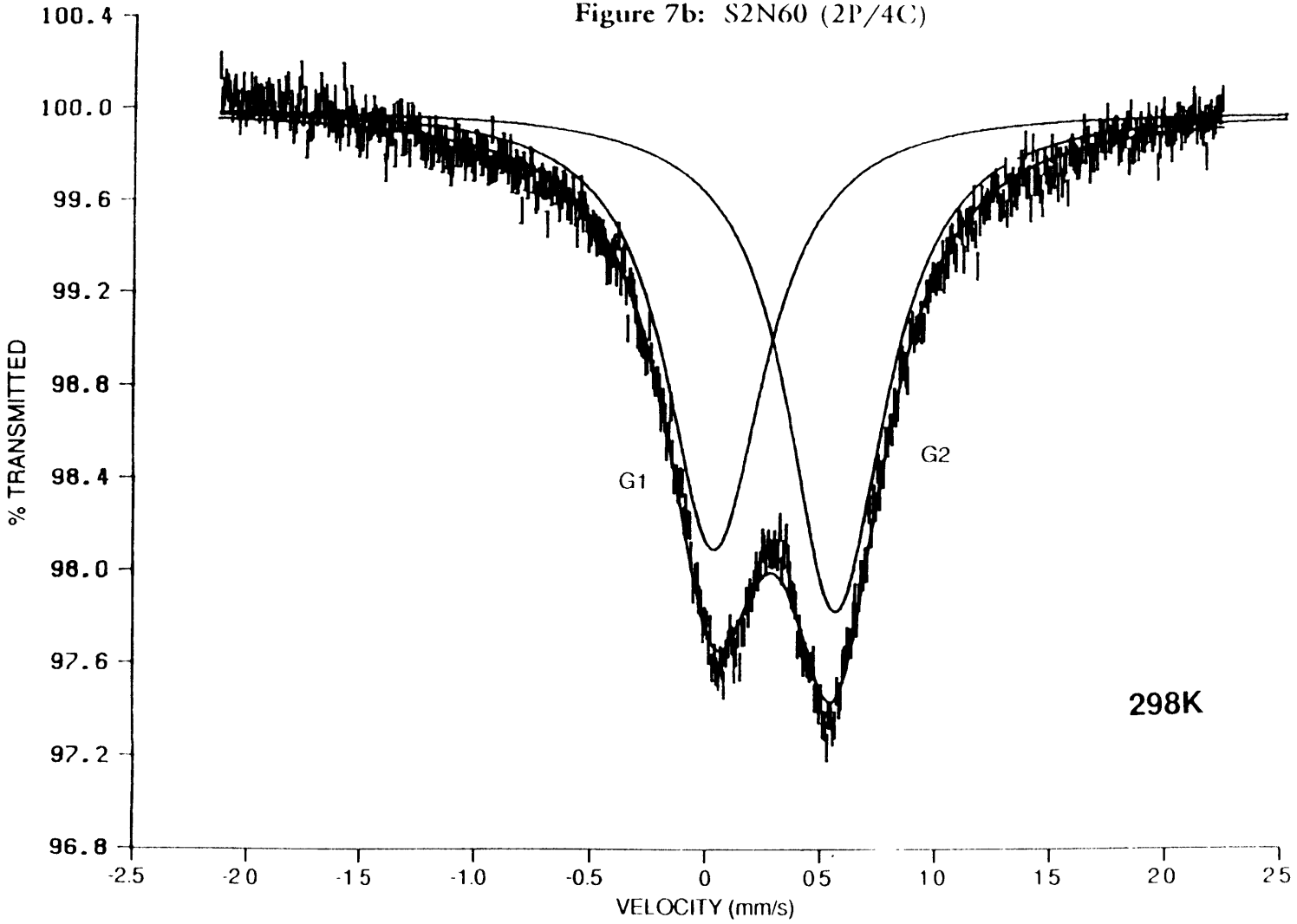

Figure 7c: S2K80 (2P/4C)

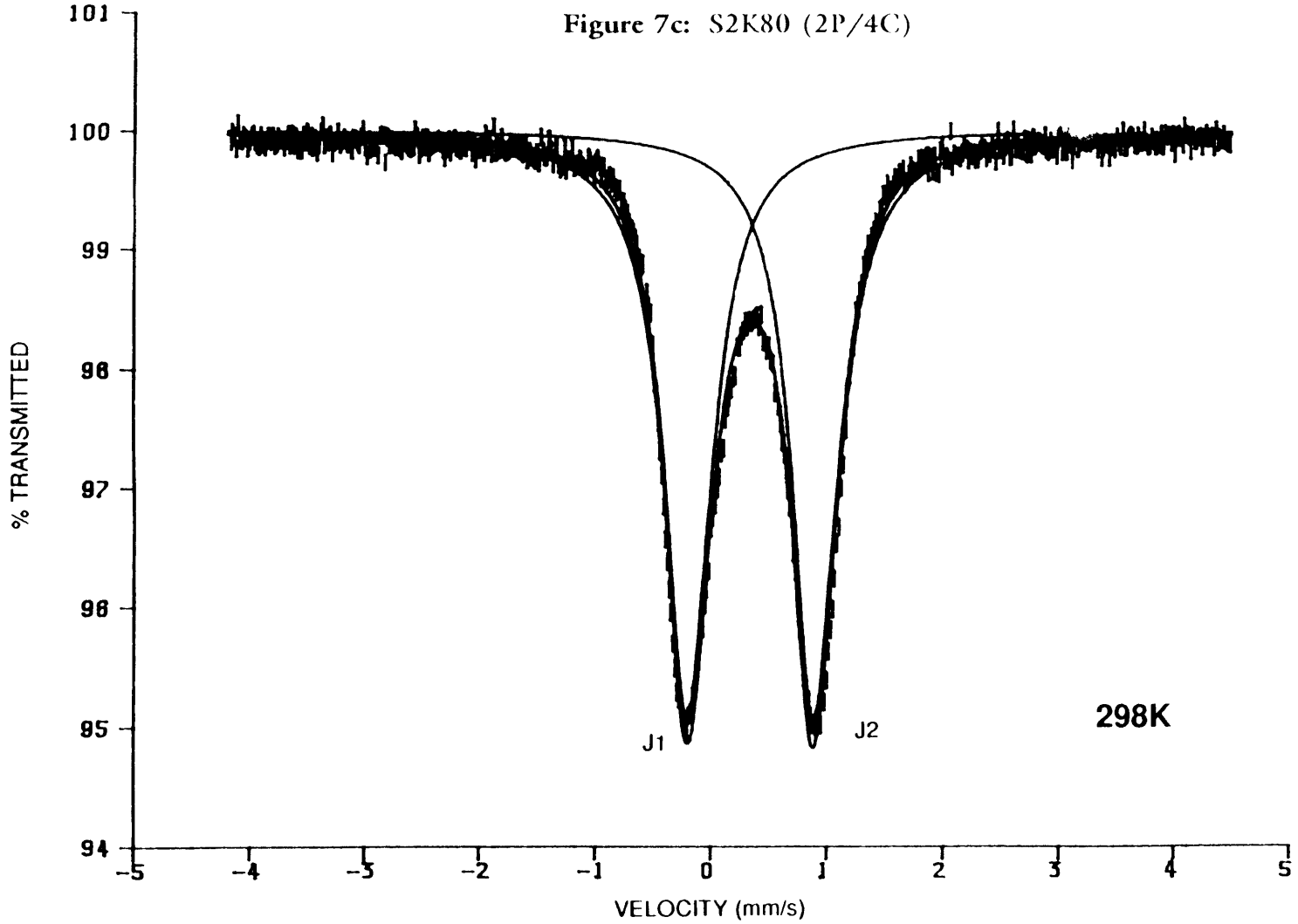

Figure 7d: S7N80 (2P/4C)

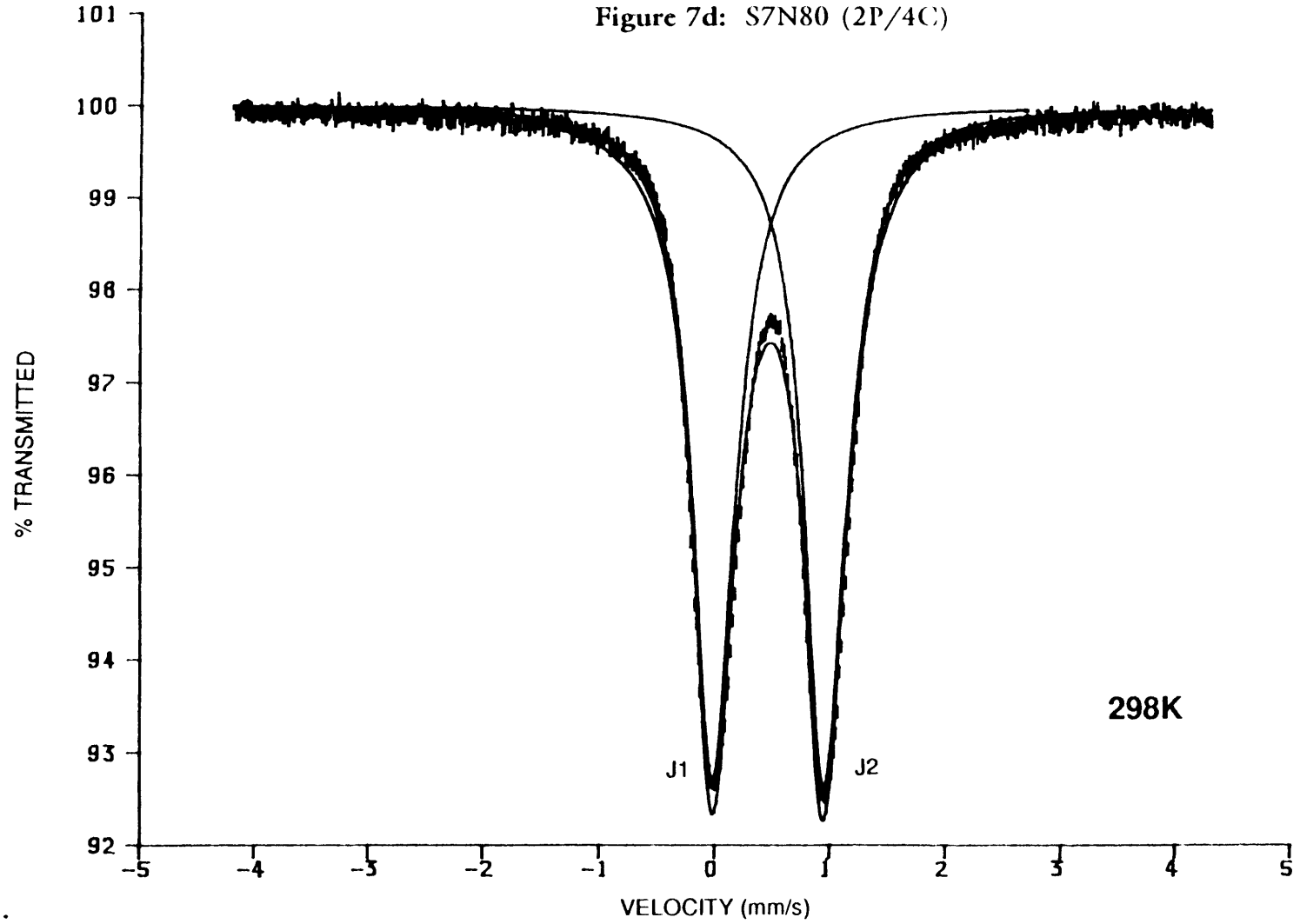

Figure 8a: T2F60 (unfitted) — Expanded Scale (±10 mm/s)

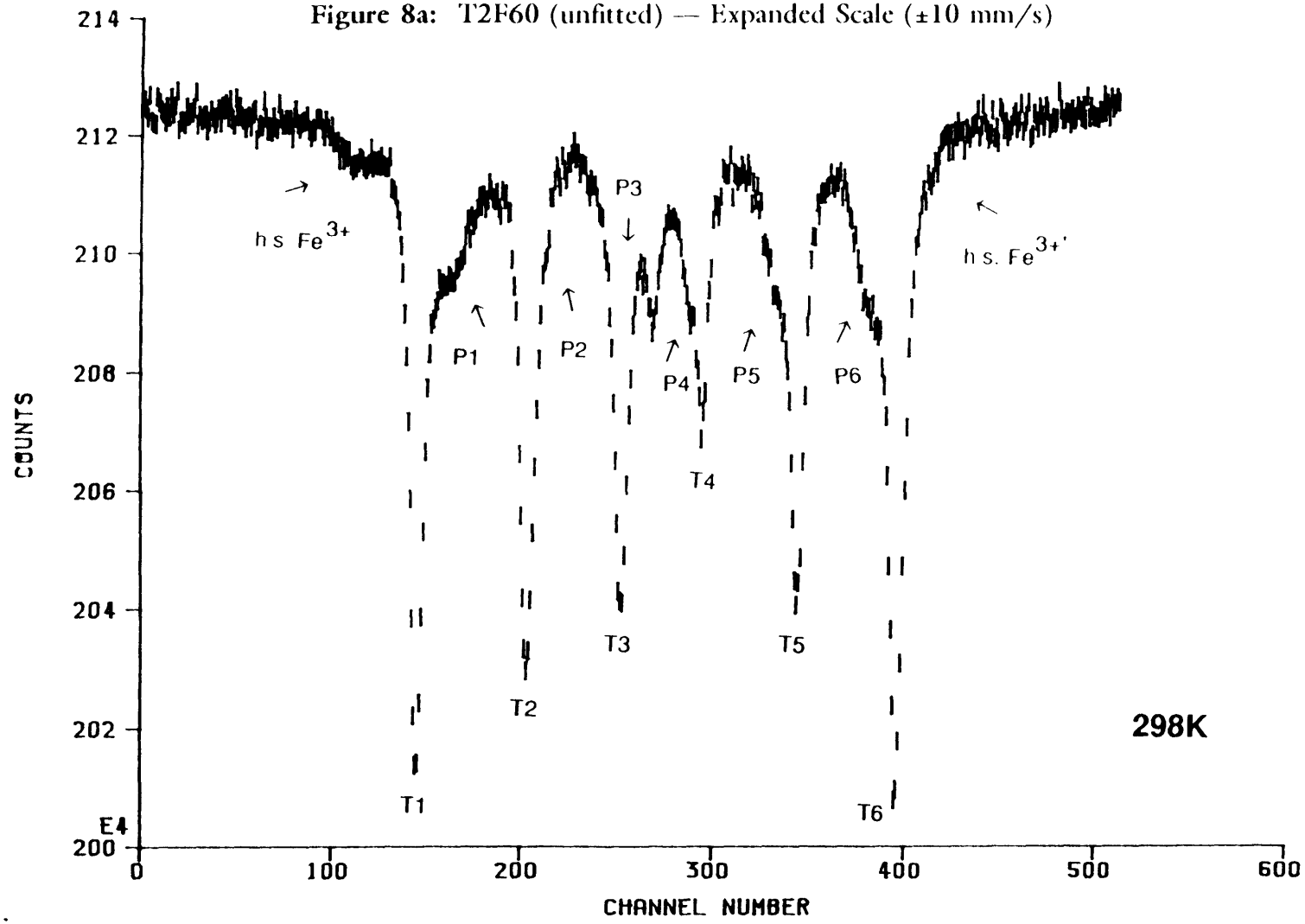

Figure 8b: P2F60 (unfitted) — Expanded Scale (±10 mm/s)

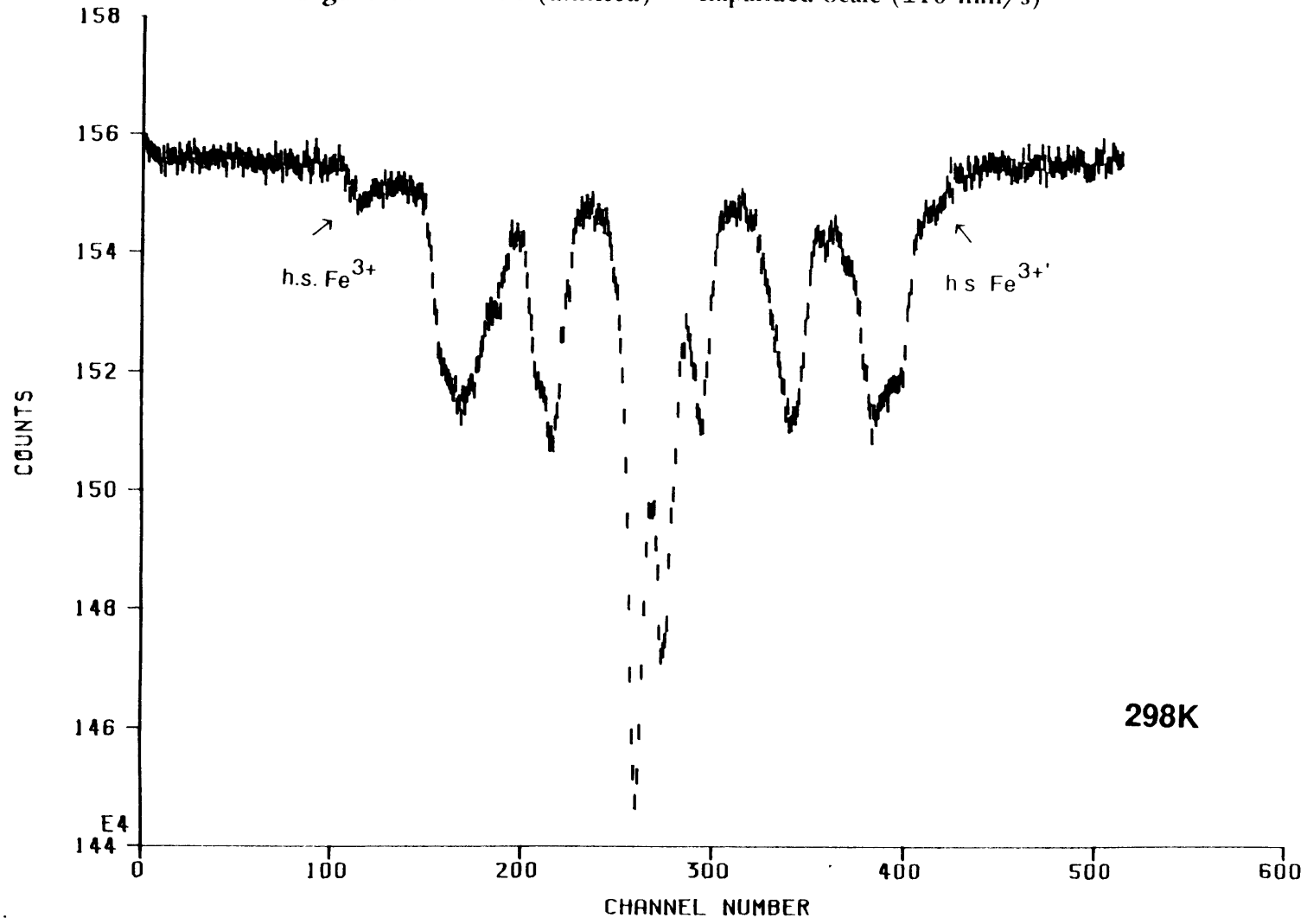

Figure 8c: Unreacted Pyrrhotite (unfitted) — Expanded Scale (±10 mm/s)

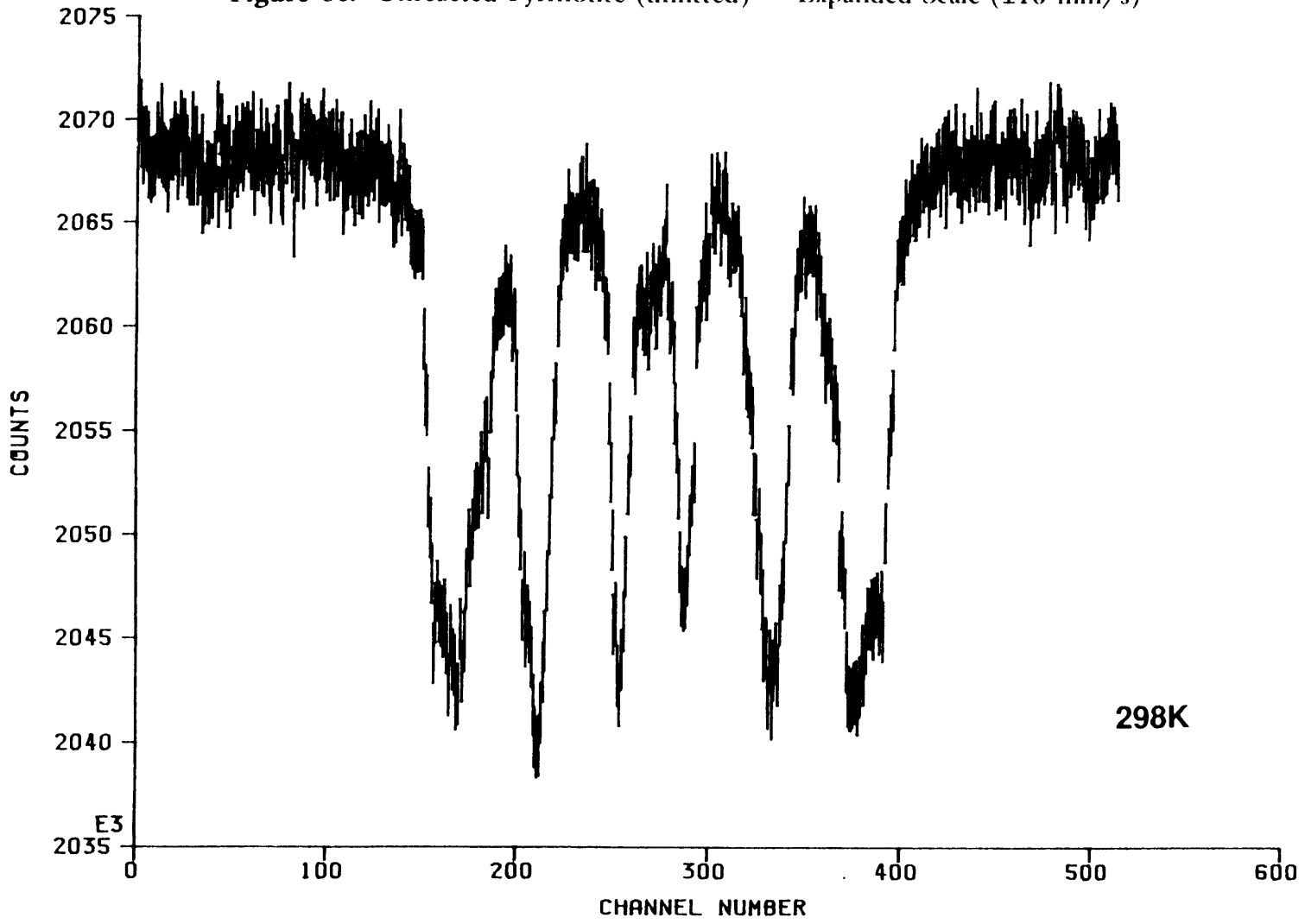

Figure 9: Isomer Shift vs. Quadrupole Splitting

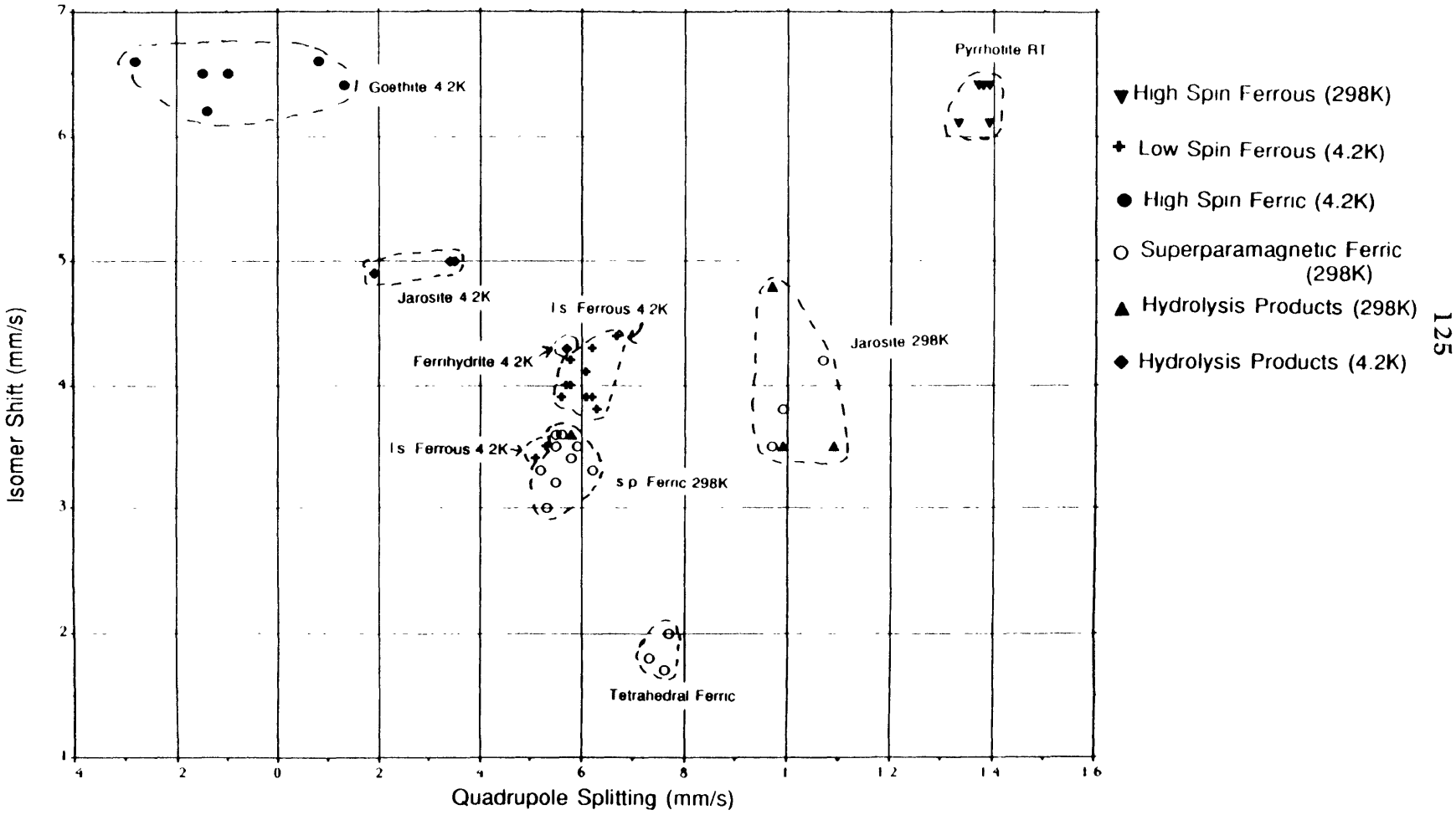

ACKNOWLEDGMENTS

(and Dedication)

First off and most importantly, I would like to thank Roger Burns. The patience, generosity and kindness he showed me was far more than I deserved. In the give and take of the supervisor/grad student relationship, I got, by far, the better half of the deal. I would also like to thank D'Arcy Straub for both helpful comments on this thesis and for the conversations dealing with topics other then Science. Things would have been a lot worse off without either of them. Though they would probably be surprised to find themselves mentioned here, Carolyn Ruppel and Cecily Wolfe, more than anyone else, have shown me what I do and do not want to do for the next part of my life, for which I am most grateful. I hope they won't take this in the wrong way. Thanks too, to everyone involved with the MIT Aikido Club. My present level of sanity owes much to them.

Thanks are due to Dr. G. Papaefthymiou and Vincent Diorio, who provided invaluable assistance with the 4.2K Mössbauer spectral measurements made at the National Magnet Lab at MIT.

Finally, I would like to thank my parents for providing for and supporting my education. I dedicate this thesis to my father, Gordon Fisher, who will never know.